

**DIVERSIFYING CATALYSTS, MONOMERS, CROSS-COUPLING STRATEGIES AND  
FUNCTIONAL GROUPS IN THE CONTROLLED SYNTHESIS OF  
CONJUGATED POLYMERS**

A Dissertation Presented

by

YUNYAN QIU

Submitted to the Faculty of  
Carnegie Mellon University  
In Partial Fulfillment of the  
Requirements for the Degree of

DOCTOR OF PHILOSOPHY

September 2016

Department of Chemistry

© Copyright by Yunyan Qiu 2016

All Rights Reserved

For my parents and wife

## ACKNOWLEDGMENTS

I would like to give my endless appreciation to my advisors, Professor Kevin Noonan and Professor Tomek Kowalewski. They have been great supervisors and mentors to me in the last five years. They have taught me through the most important five years of my life and made me the person I am now, a dedicated chemist. Thank you to Kevin for allowing me to explore my own curiosity sometimes in the lab. It means a lot to me and probably is the reason why I want to pursue an academic career.

Thank you to Professor Rongchao Jin and Professor Krzysztof Matyjaszewski for serving on my committee and all the helpful advices during my time in CMU. I appreciate the discussion with Professor Jin about career choices. Thank you to Professor Geoffrey Hutchison for serving as my guest examiner.

Thanks to all the collaborators I have worked with here in CMU, especially Dr. Stefan Bernhard, Dr. Roberto Gil, Dr. David Yaron, Dr. Hunaid Nulwala, Dr. Tomislav Pintauer and Dr. Stephanie Tristram-Nagle. Thanks to their students Danielle Chirdon, Aman Kaur, Andrew Maurer, Samuel Amsterdam and Christopher Collins for their valuable work. Thanks to Dr. Chakicherla Gayathri for creating a neat environment using NMR and the help with all my NMR problems.

I would like to also thank all the Noonan's group member Josh, Tyler, Chia-Hua and Matt for all sorts of interesting discussions and helpful suggestions. Thanks to all the undergraduate students in Noonan's lab that I have worked with: Jamie, Xinyi, Clare, Grace, Danny, Kevin, Hannah and many others. We made a good team working together. Special thanks to Josh for spending five years with me in the lab and teaching me weird English words and American culture. Many thanks to Tomek's group members Jake, Andria and Eric for all the help with my research. Special thanks to Andria for making most of my work possible.

I would like to express my sincere appreciation for Drs. John and Nancy Harrison's generosity in funding the John and Nancy Harrison Legacy Graduate Fellowship in Chemistry and Biochemistry.

## ABSTRACT

Diversifying Catalysts, Monomers, Cross-Coupling Strategies and Functional Groups

in the Controlled Synthesis of Conjugated Polymers

September 2016

Yunyan Qiu, B.S., Peking University

Ph.D., Carnegie Mellon University

Supervised by: Professor Kevin Noonan and Professor Tomasz Kowalewski

The ability to precisely incorporate monomers into polymeric materials grants polymer chemists access to a variety of complex architectures. These materials are commonly prepared by living chain-growth polymerization techniques which have revolutionized the field of polymer synthesis. Catalyst-transfer polycondensation (CTP) is one of those chain-growth methods to afford well-defined conjugated polymers. Serving as active components in most of optoelectronic devices, conjugated polymers prepared by CTP exhibit improved device performance due to uniform polymeric structures. Some promising features CTP can provide include control over size and microstructure, good chain end fidelity and the construction of sophisticated polymeric frameworks with functionality.

The frontier of CTP research now focuses on (a) understanding the exact mechanism, (b) monomer scope expansion by rational design of catalysts and conjugated monomers, and (c) obtaining conjugated materials with structural diversity. This dissertation details some of our endeavor towards diversifying the choice of catalysts, monomers, cross-coupling reactions and functional groups available in CTP process.

## TABLE OF CONTENTS

	Page
ACKNOWLEDGMENTS .....	iv
ABSTRACT.....	v
LIST OF TABLES.....	vii
LIST OF FIGURES .....	viii
LIST OF SCHEMES.....	xi
CHAPTER	
1. Controlled Synthesis of Conjugated Polymers .....	1
2. Synthesis of Polyfuran and Thiophene-Furan Alternating Copolymers Using Catalyst-Transfer Polycondensation .....	21
3. Stille Catalyst-Transfer Polycondensation using Pd-PEPPSI-IPr for High Molecular Weight Regioregular Poly(3-hexylthiophene).....	49
4. Nickel-Catalyzed Suzuki Polycondensation for Controlled Synthesis of Ester- Functionalized Conjugated Polymers .....	66
5. Synthesizing Electron-Rich and Electron-Deficient Conjugated Polymers by Direct Catalytic Cross-Coupling of Organolithium AB-Type Monomers.....	97
6. Conclusions and Outlook.....	115

## LIST OF TABLES

Table	Page
2.1. Comparison of furan-containing polymers .....	23
2.2. Data used to construct $M_n$ versus total monomer conversion plot .....	42
2.3. Summary of optical and electrochemical properties of HT-P3HF, HH-P3HF and P3HF- $\alpha$ -P3HT .....	44
3.1. Comparison of P3HT samples prepared by adjusting [monomer]/[catalyst] ratio.....	51
3.2. Detailed comparison of P3HT samples prepared by adjusting [monomer]/[catalyst] ratio.....	61
3.3. Data used to construct monomer conversion versus $M_n$ from first monomer feed .....	62
3.4. Data used to construct monomer conversion versus $M_n$ from second monomer feed.....	62
4.1. Model Compound Reactions with Methyl 2,5-Dibromothiophene-3-carboxylate .....	68
4.2. Polymerization Studies for Monomers 4.1, 4.2, and 4.3.....	72
4.3. Synthesis of P3HEF .....	77
4.4. Optimization of water content in P3HT synthesis from monomer 4.2 .....	91
4.5. Synthesis of P3HET- $\alpha$ -P3HT from monomer 4.3.....	92
5.1. Polymerization Studies for Monomer 5.1 .....	100
5.2. Polymerization Studies for Monomer 5.2.....	100
5.3. Polymerization Studies for Monomer 5.3.....	101
5.4. Polymerization Studies for Monomer 5.4.....	101

## LIST OF FIGURES

Figure	Page
1.1. Graphic Illustration of a Typical Step-Growth Polycondensation Reaction.....	2
1.2. Graphic Illustration of a Typical Chain-Growth Polycondensation Reaction .....	2
1.3. General Pd-Catalyzed Cross-Coupling Mechanism .....	3
1.4. Selected Nickel and Palladium Precatalysts .....	5
1.5. Electronic Influences of Ligands in Promoting Chain-Growth .....	6
1.6. Selected Electron-Rich Polymers Synthesized using CTP .....	7
1.7. Selected Electron-Deficient Polymers Synthesized by CTP.....	9
1.8. Selected All Conjugated Polymers .....	12
1.9. Selected Conjugated/Nonconjugated Polymers .....	13
2.1. Plot of $M_n$ versus conversion for polymerization of P3HF- <i>a</i> -P3HT using 1.25 mol % Ni(dppp)Cl <sub>2</sub> .....	26
2.2. <sup>1</sup> H NMR spectra of HT-P3HF, HH-P3HF and P3HF- <i>a</i> -P3HT collected at 22 °C in CDCl <sub>3</sub> , the * indicates H <sub>2</sub> O .....	27
2.3. Top Left - UV-Vis absorption spectra in THF for HT-P3HF, HH-P3HF and P3HF- <i>a</i> -P3HT compared with <i>rr</i> -P3HT. Top Right - Solid-state UV-Vis of the 3 polymer samples compared with <i>rr</i> -P3HT. Bottom - Tapping-mode AFM phase images showing nanofibrillar structures of HT-P3HF, HH-P3HF and P3HF- <i>a</i> -P3HT.....	29
2.4. P3HF- <i>a</i> -P3HT NMR spectra before and after exposure to light and oxygen (top – before exposure. Bottom – after exposure.) .....	31
2.5. P3HF- <i>a</i> -P3HT GPC spectra before and after exposure to light and oxygen .....	32
2.6. P3HF- <i>a</i> -P3HT UV-Vis spectra before and after exposure to light and oxygen .....	32
2.7. Stack Plot of GC-MS Traces from the $M_n$ versus conversion plot. The signal at ~13 min corresponds to nonadecane which was used to determine conversion. The two isomers correspond to H-terminated monomer and are observed near 19 min. The dibromo starting material 2.3 is observed at ~21 min.....	43
3.1. GPC traces of P3HT samples obtained by varying the [monomer]/[catalyst] ratio.....	52

3.2.	MALDI-TOF mass spectrum of SnHTBr polymerization using 4 mol % catalyst.....	52
3.3.	<sup>1</sup> H NMR Spectrum of P3HT <sub>33</sub> . Insets highlight the end-groups of the polymer chain. * represents the solvent signal (CHCl <sub>3</sub> at 7.26 ppm) and H <sub>2</sub> O (1.53 ppm). The # sign indicates a <sup>13</sup> C satellite of the CHCl <sub>3</sub> solvent.....	54
3.4.	Left - Plot of <i>M<sub>n</sub></i> versus conversion for polymerization of SnHTBr using 2 mol % Pd-PEPSSI-IPr. Right – after refeeding the SnHTBr monomer.....	54
3.5.	a) and b) Azimuthally-averaged profiles of X-ray scattering patterns (insets) showing lamellar and π-stacking crystalline order peaks. c) and d) Tapping-mode AFM phase images of extended nanofibrillar structures corresponding to π-stacked P3HT chains. Images in a) and c) were obtained for P3HT <sub>33</sub> and images in b) and d) were obtained for P3HT <sub>400</sub> .....	56
4.1.	Cross-coupling methods used in catalyst-transfer polycondensation .....	66
4.2.	MALDI-TOF mass spectrum of P3HET prepared using Ni(PPh <sub>3</sub> )IPrCl <sub>2</sub> .....	70
4.3.	GPC chromatograms for the P3HT homopolymer and P3HT- <i>b</i> -P3HET copolymer synthesized using Ni(PPh <sub>3</sub> )IPrCl <sub>2</sub> .....	74
4.4.	Solution (CHCl <sub>3</sub> ) and solid-state UV-vis spectra for all polymers with P3HT included for reference.....	74
4.5.	<sup>1</sup> H NMR spectrum and end group analysis of P3HET. The star symbols (*) correspond to <sup>13</sup> C satellites for the aromatic signal of the polymer and the solvent .....	75
4.6.	Top – <sup>1</sup> H NMR Spectrum of P3HET. Bottom – P3HET treated with Ni(COD) <sub>2</sub> and HCl illustrating the loss of the Br-terminated end group.....	76
4.7.	MALDI-TOF spectrum for low molecular weight P3HEF.....	77
4.8.	Representative crude <sup>1</sup> H NMR Spectrum (500 MHz, CDCl <sub>3</sub> ) for model compound Suzuki-Miyaura coupling at 50 °C using methyl-2,5-dibromothiophene-3-carboxylate and Ni(PPh <sub>3</sub> )IPrCl <sub>2</sub> (1 mol %). The star symbols correspond to the terthiophene product.....	89
5.1.	Summarized Cross-Coupling Reactions used in Chain-Growth Polymerizations.....	98
5.2.	Compound <b>5.A</b> <sup>1</sup> H NMR Spectrum – 500 MHz, CDCl <sub>3</sub> .....	104
5.3.	Compound <b>5.A</b> <sup>13</sup> C NMR Spectrum – 126 MHz, CDCl <sub>3</sub> .....	104
5.4.	Compound <b>5.4</b> <sup>1</sup> H NMR Spectrum – 500 MHz, CDCl <sub>3</sub> .....	105
5.5.	Compound <b>5.4</b> <sup>13</sup> C NMR Spectrum – 126 MHz, CDCl <sub>3</sub> . .....	106

5.6.	Polyfluorenes <sup>1</sup> H NMR Spectrum – 500 MHz, CDCl <sub>3</sub> .....	107
5.7.	Polyfluorenes <sup>13</sup> C NMR Spectrum – 126 MHz, CDCl <sub>3</sub> .....	107
5.8.	Polycarbazoles <sup>1</sup> H NMR Spectrum – 500 MHz, CDCl <sub>3</sub> .....	108
5.9.	Polyfluorenes <sup>13</sup> C NMR Spectrum – 126 MHz, CDCl <sub>3</sub> .....	109
5.10.	Polybenzotriazoles <sup>1</sup> H NMR Spectrum – 500 MHz, CDCl <sub>3</sub> .....	110
5.11.	Polybenzotriazoles <sup>13</sup> C NMR Spectrum – 126 MHz, CDCl <sub>3</sub> .....	110
5.12.	Donor-acceptor copolymer <sup>1</sup> H NMR Spectrum – 500 MHz, CDCl <sub>3</sub> .....	111
5.13.	Donor-acceptor copolymer <sup>13</sup> C NMR Spectrum – 126 MHz, CDCl <sub>3</sub> .....	112
5.14.	Crude <sup>1</sup> H NMR Spectrum (500 MHz, CDCl <sub>3</sub> ) for monomer conversion experiments. Top – reaction mixture before adding <i>n</i> -BuLi. Middle – reaction mixture after adding 1 equiv. of <i>n</i> -BuLi. Bottom – reaction mixture after adding 2 equiv. of <i>n</i> -BuLi for comparison.....	112
6.1.	Selected Examples of Imide Containing Conjugated Building Blocks .....	116
6.2.	Functional Groups Expansion and Side Chain Sequence Defined Conjugated Polymers.....	116
6.3.	Proposed Controlled Synthesis of Imide Functionalized Conjugated Polymers .....	117

## LIST OF SCHEMES

Scheme	Page
1.1. Proposed Mechanism for Chain-Growth Kumada CTP .....	4
1.2. Small Molecule Competition Reactions .....	4
1.3. Electronic Influences of Substituents on Polymerization Initiation Rates.....	6
1.4. Representative Suzuki CTP to Synthesize Polyfluorenes.....	8
1.5. Alternating Donor-Acceptor Copolymers by Kumada CTP.....	10
1.6. Alternating Donor-Acceptor Copolymers by Suzuki CTP .....	11
1.7. One-Pot Synthesis of the Block Copolymer Consisting Polystyrenes and P3HT .....	14
1.8. Representations of CTP using Different Cross-Coupling Reactions.....	14
2.1. Synthesis of HT-P3HF, HH-P3HF and P3HF- <i>a</i> -P3HT .....	22
2.2. Preferential double substitution with furan, the percent yields are relative to Ph-MgBr. ....	24
2.3. Synthesis of Monomer 2.1 .....	36
2.4. Synthesis of Monomer 2.3 .....	38
3.1. Synthesis of poly(3-hexylthiophene) using a Pd-NHC catalyst.....	50
3.2. Investigation of preferential double substitution using the PEPPSI catalyst system. The percent yields listed for 3.3 and 3.4 are reported with respect to compound 3.2.....	50
4.1. Polymers Prepared using Nickel-Catalyzed Suzuki CTP .....	69
4.2. Synthesis of Monomer 4.1 .....	81
4.3. Synthesis of Monomer 4.3 .....	83
4.4. Synthesis of Monomer 4.4 .....	86
5.1. Synthesis of Monomer 5.4 .....	103

## CHAPTER 1

### Controlled Synthesis of Conjugated Polymers

#### 1.1 Introduction

Precision polymer synthesis enables chemists to prepare novel materials with control over composition, topology and functionality.<sup>1</sup> Thanks to the rapid development of living chain-growth polymerization techniques, multiblock copolymers with specific sequences and functionalities are constructed and have been found as promising materials in applications ranging from thin-film patterning to biomimetic engineering.<sup>2</sup> While living anionic polymerization,<sup>3</sup> controlled radical polymerization<sup>4</sup> (CRP) and ring-opening metathesis polymerization<sup>5</sup> (ROMP) protocols are well-established to make these kinds of functional materials, the controlled synthesis of conjugated polymers remains relatively underdeveloped.

The high conductivity of polyacetylenes upon doping with iodine, discovered by Shirakawa, MacDiarmid, and Heeger, started the field of conjugated polymers.<sup>6</sup> For this achievement, these three researchers were awarded the Nobel Prize in 2000. Since their initial discovery, conjugated polymers have been explored extensively in organic electronic devices, where performance largely depends on structure, molecular weight, dispersity and thin film morphology.<sup>7</sup> Consequently, readily available synthetic tools to afford well-defined conjugated materials are needed to improve their device performance.<sup>8</sup>

Conjugated polymers are commonly prepared using metal-catalyzed step-growth polymerization (AA/BB-type route) with prolonged reaction times and high temperatures. In a typical step-growth polycondensation reaction, the growing polymer chain and monomer have nearly identical reactivity, producing materials with limited control over the molecular weight and dispersity (Figure 1.1).<sup>9</sup> High molecular weight polymers can be only generated with strict control over stoichiometry and high monomer conversion using a robust condensation reaction. This is challenging to achieve with these metal catalyzed reactions, particularly when exotic

monomers are used. This shortcoming leads to significant batch-to-batch variations of semiconducting polymer materials and makes comparisons from different research teams difficult.

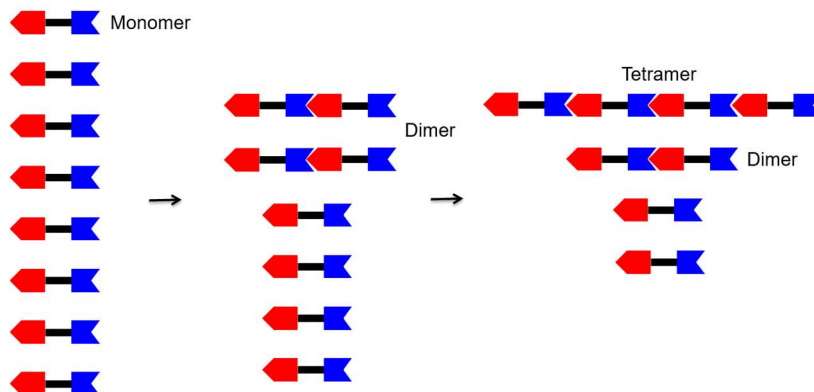


**Figure 1.1.** Graphic Illustration of a Typical Step-Growth Polycondensation Reaction.

Converting a step-growth polycondensation reaction into a chain-growth process relies on differentiating the reactivity between the growing polymer chain and the monomer (Figure 1.2).<sup>10</sup> This was first observed in conjugated polymer synthesis by McCullough<sup>11</sup> and Yokozawa<sup>12</sup> who independently reported a controlled chain-growth polymerization (catalyst-transfer polycondensation, CTP) when synthesizing poly(3-hexylthiophene) (P3HT). Following this discovery, researchers have focused on (a) understanding the exact mechanism behind this controlled process, (b) monomer scope expansion using this method, and (c) obtaining conjugated materials with structural diversity (e.g., block copolymers).<sup>8,10,13</sup>

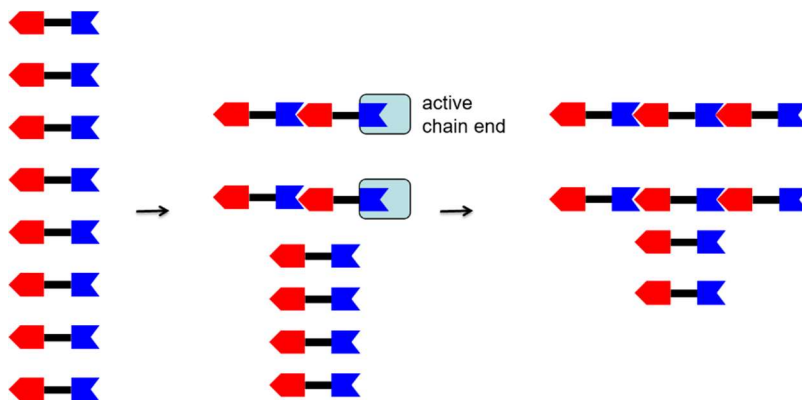


**Figure 1.2.** Graphic Illustration of a Typical Chain-Growth Polycondensation Reaction.

## 1.2 Mechanism

A typical catalytic cycle for metal catalyzed cross-coupling reactions is shown below (Figure 1.3, with Pd as an example). It involves oxidative addition, transmetallation, and reductive elimination to generate biaryl products. When using difunctional starting materials (X-Ar-X, M-Ar'-M), step-growth polymers will be obtained.

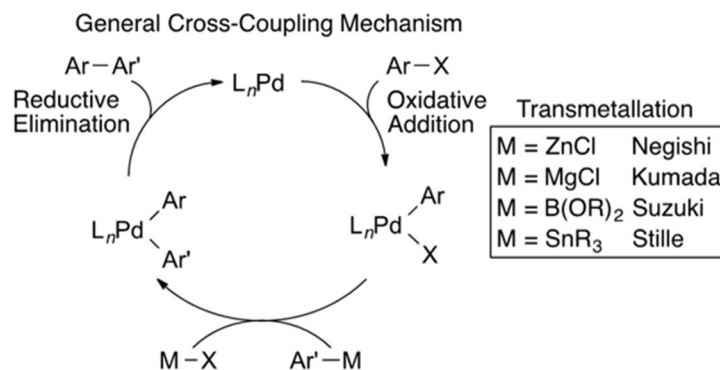
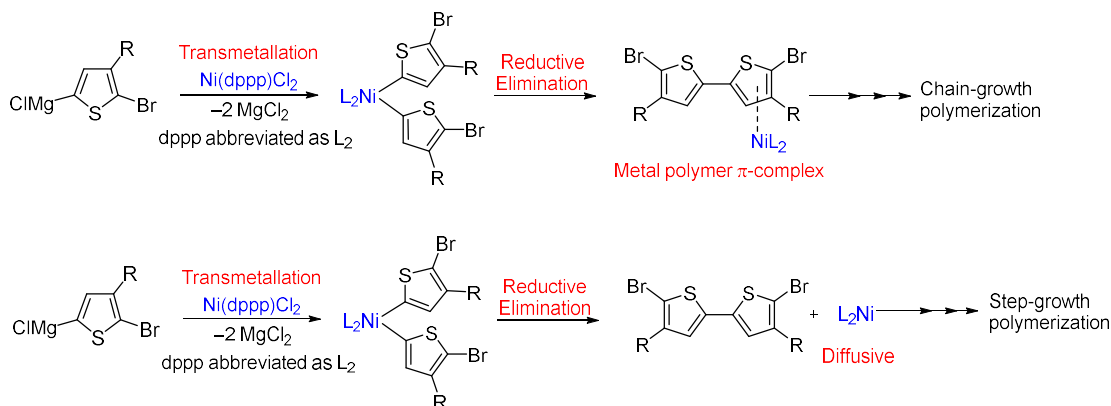


**Figure 1.3.** General Pd-Catalyzed Cross-Coupling Mechanism.

In a chain-growth polycondensation reaction, the major difference from the aforementioned step-growth polymerizations is the formation of a metal polymer  $\pi$ -complex. The metal remains bound to the polymer chain after each reductive elimination and the catalyst undergoes intramolecular oxidative addition at the polymer chain end, leading to uniform well-defined materials (Scheme 1.1). This enables the metal to not only serve as a catalyst but also as an initiator. Consequently, early reports by McCullough<sup>11</sup> and Yokozawa<sup>12</sup> exploring Kumada polymerization reactions for P3HT showed linear increase of molecular weights ( $M_n$ ) with monomer consumption, controlled molecular weights with various monomer/catalyst ratios and ability to form complex structures such as block copolymers by simple monomer additions.

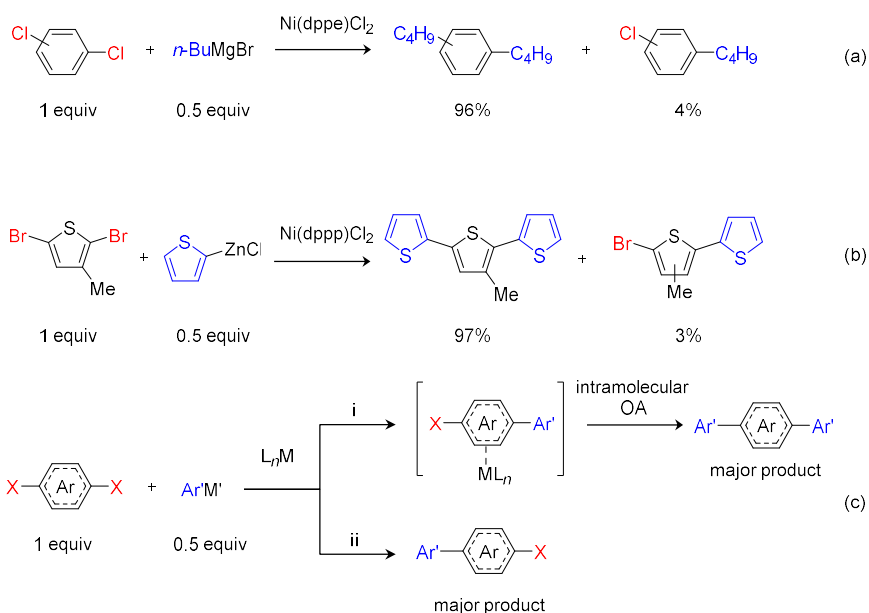
Metal catalysts such as Pd or Ni can form  $\pi$ -complex with arene- or alkene-based conjugated molecules.<sup>14</sup> However, direct evidence of a metal polymer  $\pi$ -complex has not been identified during the polymerization period for P3HT. Indirect evidence using a small molecule competition reaction generally provides guidance for selection of suitable catalysts to achieve a controlled polymerization process.

### Scheme 1.1. Proposed Mechanism for Chain-Growth Kumada CTP.



In 1976, Kumada and coworkers already indicated the presence of a possible associative  $\pi$ -complex where they found double-substituted product (dibutylbenzene) formation even using an excess amount of dihalogenated starting materials (dichlorobenzene) in a Kumada coupling reaction (Scheme 1.2, a).<sup>15</sup> In 2004, McCullough and coworkers also reported a similar preferential reaction using 2,5-dibromothiophene (Scheme 1.2, b).<sup>11</sup> These small molecule competition reactions then became widely used to identify suitable monomers and catalysts for CTP reactions.<sup>16</sup>

### Scheme 1.2. Small Molecule Competition Reactions. (Adapted with permission from *Macromolecules* **2013**, *46*, 8395-8405. Copyright 2013 American Chemical Society.)



The reaction requires 1 equivalent of the dihalogenated small molecule with 0.5 equivalent of the coupling partner in the presence of a catalyst and if a preferential double-substitution is observed, the associative  $\pi$ -complex is inferred (Scheme 1.2, c, path i). Otherwise, if the mono-substituted compound is formed as the major product, it is likely the catalyst dissociates after the first coupling event (Scheme 1.2, (c), path ii).

### 1.3 Catalysts Employed

Over the years, a variety of Pd or Ni based catalysts have been identified and successfully applied in the CTP process. Close examination of all the catalysts used in CTP demonstrate that they can strongly influence the polymerization.<sup>8</sup> According to different initiation rates, the catalyst used in CTP can be divided into two categories that are  $L_nMX_2$  and  $L_nM(Ar)X$  (L: ancillary ligands, X: leaving groups such as halogen atoms) (Figure 1.4).<sup>13</sup>

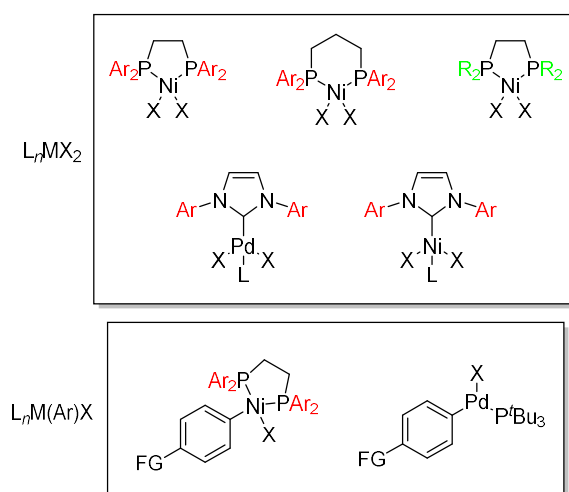


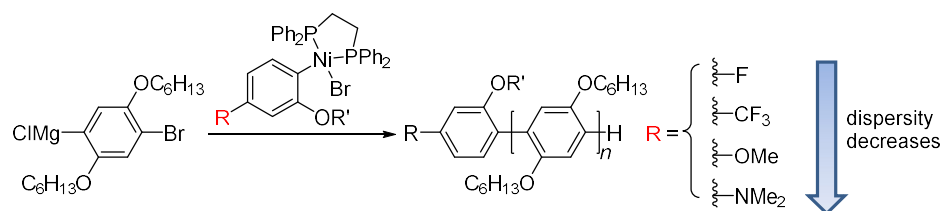
**Figure 1.4.** Selected Nickel and Palladium Precatalysts (X = Leaving Groups, Ar = Aryl Groups, FG = Functional Groups). (Adapted with permission from *Polym. Chem.* **2015**, *6*, 7781-7795. Copyright 2015 Royal Society of Chemistry.)

Precatalysts such as  $L_nMX_2$  can be easily synthesized, however have limited solubility in the polymerization solvent (THF). Catalysts like  $L_nM(Ar)X$  are soluble alternatives to  $L_nMX_2$  and initiate faster (one transmetalation step). Additional benefits of  $L_nM(Ar)X$  include distinct end

group formation from unidirectional propagation and modular initiation rates by modifying the Ar structure (Scheme 1.4).<sup>17</sup>

### Scheme 1.3. Electronic Influences of Substituents on Polymerization Initiation Rates.

(Adapted with permission from *Polym. Chem.* **2015**, *6*, 7781-7795. Copyright 2015 Royal Society of Chemistry.)



A variety of ancillary ligands have been used to promote chain-growth polymerizations such as monodentate phosphines ( $P^tBu_3$ ),<sup>18</sup> bidentate phosphines (dppp or dppe),<sup>19</sup> carbenes,<sup>20</sup> and diimines.<sup>21</sup> The steric and electronic properties of these ancillary ligands can be fine-tuned by modifying the substituent (Figure 1.5).<sup>14a,20</sup> Electron-rich ligands commonly outperform electron-poor ligands in promoting chain-growth polymerizations due to stronger  $\pi$ -binding between the metal and the polymer chain.<sup>16a,22</sup>

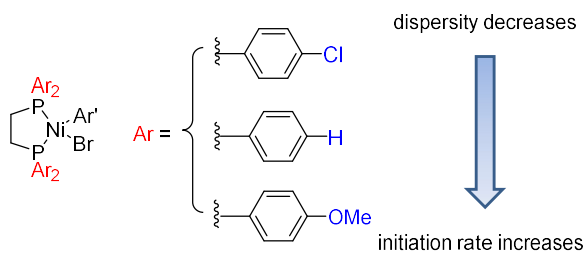


**Figure 1.5.** Electronic Influences of Ligands in Promoting Chain-Growth. (Adapted with permission from *Macromolecules* **2013**, *46*, 8395-8405. Copyright 2013 American Chemical Society.)

## 1.4 Monomer Scope

### 1.4.1 Electron-Rich Monomers

Since the first discovery of a CTP process for synthesizing polythiophene, chain-growth polymerization reactions have been successfully applied to many other conjugated monomers.

With extending to non-thiophene monomers in 2006<sup>23</sup> and utilizing palladium as an alternative catalyst to nickel in 2007,<sup>24</sup> the number of conjugated building blocks suitable for CTP rapidly increased over the last decade.

Among them, electron-rich monomers are more developed than electron-deficient monomers. Polythiophenes,<sup>11-12,25</sup> polyselenophenes,<sup>26</sup> polytellurophenes,<sup>27</sup> polypyrroles,<sup>28</sup> polyphenylenes,<sup>23</sup> polyfluorenes,<sup>24</sup> polycyclopentadithiophenes<sup>29</sup> and polydithienosiloles<sup>30</sup> have been obtained in a chain-growth fashion (Figure 1.6).

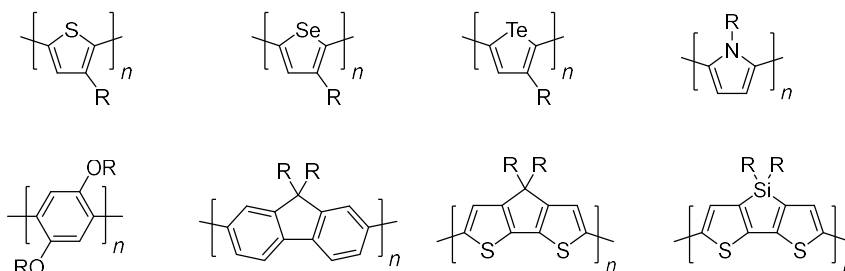


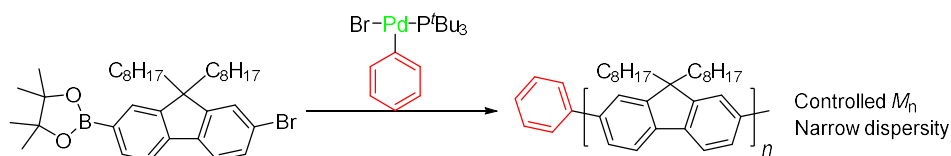
**Figure 1.6.** Selected Electron-Rich Polymers Synthesized using CTP.

Most of the CTP reactions utilize organometallic A-B type conjugated monomers which are generated by metal/halogen exchange between dihalogenated monomer precursors and aliphatic Grignard (*t*-BuMgCl or *i*-PrMgCl) or lithium reagents (*n*-BuLi). Upon addition of catalysts to *in situ* generated monomer solutions, chain-growth polymerization reactions rapidly take place at 0 °C or room temperature. To observe the ideal living chain-growth polymerization, incomplete consumption of Grignard or lithium reagents has to be avoided since residual metalating reagents can terminate the growing polymer chain prematurely. Moreover, starting dihalogenated monomer precursors should be slightly in excess compared to metalating reagents suppressing the formation of dimetalated species which might cause chain-termination or transfer. However, the highly reactive nature of Kumada or Negishi monomers ultimately limits the choice of functional groups attached to the polymer backbone.

By contrast, the introduction of A-B type Suzuki monomers in Pd-catalyzed chain-growth polymerizations significantly improves the scope of functional materials available by CTP

(Scheme 1.5).<sup>24</sup> Particularly, Suzuki monomers can be obtained in high purity with extensive column chromatography. The mild reactivity of boronic esters or acids allows for the preparation of polymers with functional groups which may not be accessed by Kumada or Negishi CTP. Well-developed Ir-catalyzed direct borylations in organic chemistry<sup>31</sup> also provide alternative methods in preparing Suzuki monomers circumventing the use of reactive metalating reagents. Though promising, Suzuki CTP often produces polymers with higher dispersities and lower molecular weights compared to those prepared by Kumada couplings, possibly due to the added water in the reaction mixture which is necessary to promote chain-growth polymerizations<sup>32</sup> but can lower the solubility of prepared polymers.

**Scheme 1.4. Representative Suzuki CTP to Synthesize Polyfluorenes.**



To date, the majority of donor monomers investigated in CTP have been thiophene related compounds, with a variety of side chain substituents appended to the polymer backbone such as carbon, oxygen, or sulfur-based solubilizing groups. Besides thiophene related monomers, other 5-membered heterocycles such as pyrroles,<sup>28</sup> selenophenes<sup>26</sup> and tellurophenes<sup>27</sup> have also been successfully applied in CTP. Thiophene fused aromatic monomers have been proven to be effective in polymerizing under a chain-growth fashion, but suffer for some complications when considering the livingness of the polymerization.<sup>29-30</sup> These limitations may arise from the extended length of fused monomers subsequently causing catalyst dissociation during the reaction. Kiriya and coworker have previously demonstrated that Ni catalysts can initiate efficient chain-growth polymerizations via intramolecular transfer over a ~1.1 nm long conjugated monomer.<sup>33</sup> It might also be the reason why fluorene polymerizations are often less controlled than “shorter” monomers like thiophenes. Significant improvements in controlled synthesis of polyfluorenes have not appeared until 2012, where Wang and coworkers used Ni(acac)<sub>2</sub>/dppp as the catalyst in

Kumada CTP leading to polyfluorenes with high molecular weights and extremely low dispersities.<sup>19a</sup>

### 1.4.2 Electron-Deficient Monomers

Despite the large number of donor monomers that can undergo CTP, controlled polymerizations of electron-deficient monomers remain a challenge. Theoretically, electron-deficient aromatic molecules should bind to metal catalysts (Ni or Pd) more strongly,<sup>34</sup> facilitating better chain-growth polymerizations. However, mechanistically both transmetalation and reductive elimination will be slow due to the electron-deficiency of the monomer. Most of electron-deficient monomer precursors are incompatible with metalating reagents to produce actual monomers *in situ*.

To date, efforts have been made to develop effective catalytic systems for improved control in the polymerization of electron-deficient monomers (Figure 1.7). In 2008, Rasmussen and coworkers have first polymerized thienopyrazine monomers using CTP,<sup>35</sup> followed by a 2014 report by Koeckelberghs and coworkers attempting to synthesize similar structures in a Kumada CTP process.<sup>36</sup> The rather uncontrolled nature of both indicates possible catalyst dissociation during the polymerization.

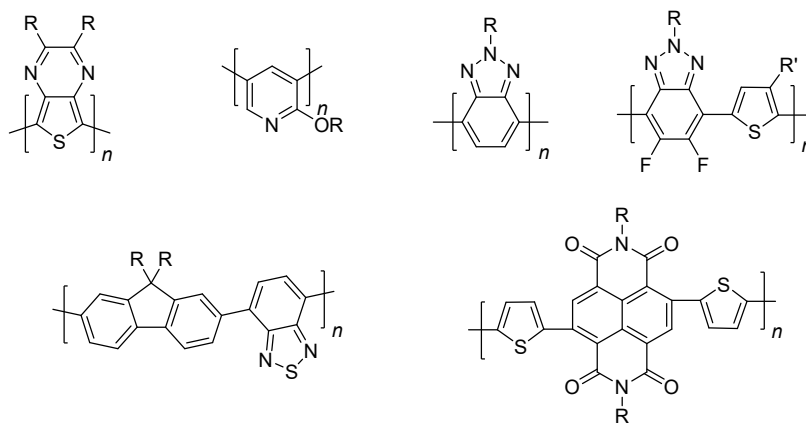
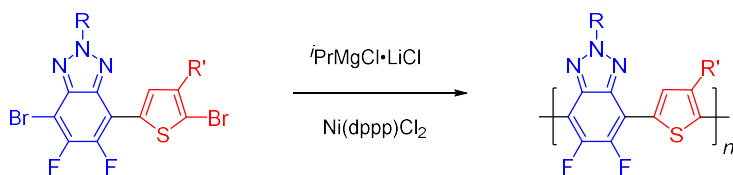


**Figure 1.7.** Selected Electron-Deficient Polymers Synthesized by CTP.

The first electron-deficient monomer that underwent controlled CTP was pyridine. In 2012 Yokozawa and coworkers reported the synthesis of poly(pyridine-3,5-diyl)s by Kumada CTP using Ni(dppp)Cl<sub>2</sub> as the catalyst.<sup>37</sup> Interestingly, the controlled synthesis of poly(pyridine-2,5-diyl)s is problematic despite different cross-coupling methods employed, stemming from the competitive disproportionation by the nitrogen atom.<sup>38</sup>

Another nitrogen-containing monomer benzotriazole has also been polymerized by CTP using computer-assisted rational design of catalysts.<sup>39</sup> By calculating the binding energy between different Ni-diimine catalysts and the monomer, Seferos and coworkers have been able to identify the best performing catalyst that initiates the controlled synthesis of polybenzotriazoles. Subsequent research by the same group has been focused on synthesizing donor-acceptor block copolymers and statistical copolymers.<sup>40</sup> Recently, Bielawski and coworkers first reported the controlled polymerization of an alternating donor-acceptor copolymer consisting of benzotriazole and hexylthiophene using Kumada CTP (Scheme 1.6).<sup>41</sup> Polymer samples with molecular weights up to 25 kg/mol and dispersities lower than 1.4 can be obtained, further demonstrating the feasibility of electron-deficient benzotriazole monomers in CTP conditions.

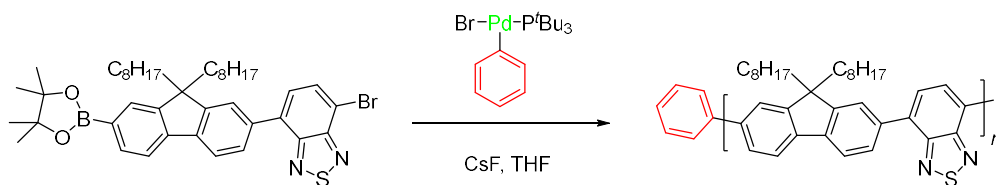
**Scheme 1.5. Alternating Donor-Acceptor Copolymers by Kumada CTP.**



Extensive research has also been conducted by Kiriy and coworkers. In 2011, they demonstrated a chain-growth synthesis of an alternating copolymer containing fluorene and benzothiadiazole by employing Pd-catalyzed Suzuki CTP (Scheme 1.7).<sup>42</sup> Although the prepared polymer has a low molecular weight, the strategy they used in designing the proper monomer by placing the halogen atom and boronic ester at different parts of the molecule provides certain guidance for others to construct more sophisticated building blocks. The same group is also known for their effort towards controlled synthesis of naphthalenediimide-based copolymers with

thiophenes.<sup>43</sup> Different from conventional Kumada and Negishi cross-couplings, the polymerization involves an unusual anion-radical based monomer produced upon adding activated Zn to the dihalogenated precursor. Polymers with controlled molecular weights up to 100 kg/mol can be obtained using Ni(dppe)Br<sub>2</sub> or Ph-Ni(dppe)Br as catalysts. It is worth noting since rylenediimides-related conjugated motifs represent a very important class of high performing electron-transporting materials, although complete investigation of the reaction mechanism is needed.

**Scheme 1.6. Alternating Donor-Acceptor Copolymers by Suzuki CTP.**



A tremendous amount of progress has been made in the last decade on expanding the monomer scope of CTP. Despite all the progress, conjugated monomers that can undergo CTP are still limited, especially those which are electron-deficient. Better understanding of the reaction mechanism is required to elucidate the reason why certain monomers are not amendable to CTP.

**1.5 Architectures**

Due to the living, chain-growth nature of CTP, a variety of polymeric architectures can be prepared using this method including all conjugated polymers and conjugated/nonconjugated polymers.

**1.5.1 All Conjugated Polymers**

Among many architectures and monomers investigated, thiophenes with other group 16 heterocycles such as selenophenes and tellurophenes are able to form the most diverse library of complex structures including block, gradient, and random copolymers when employing Kumada CTP (Figure 1.8).

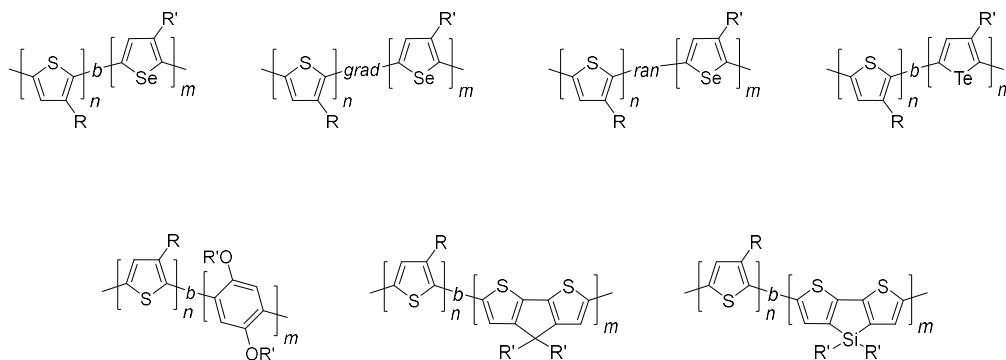


**Figure 1.8.** Selected All Conjugated Polymers.

Seferos and McNeil's group both prepared the random and block copolymer between thiophenes and selenophenes.<sup>44</sup> Gradient copolymers have also been reported by McNeil and coworkers.<sup>44c</sup> The successful preparation of these materials relies on the similar reactivity between different comonomers. Therefore, block copolymers are prepared by sequential monomer addition, where the second monomer is added to the reaction mixture after complete consumption of the first monomer. Similarly, gradient copolymers are synthesized via slow addition of the second monomer by syringe pump. These sequence-defined all conjugated polymers are of interest because they can phase separate and form unique thin-film morphology assisting charge separation in solar cells.

In 2016, Seferos reported the first controlled synthesis of polytellurophenes and subsequently synthesized a block copolymer of P3HT and poly(3-ethylheptyltellurophene)s.<sup>27</sup> Though complete characterizations of this polymer have not been conducted, they found the block copolymer can be only synthesized by choosing P3HT as the first block, a phenomenon that has been observed previously.<sup>45</sup>

Block copolymers between poly(2,5-bis(hexyloxy)-1,4-phenylene) (PPP) and P3HT were synthesized by Kumada CTP and characterized extensively.<sup>45-46</sup> By careful selection of solubilizing groups appended to the polymer backbone, thin film morphology can be tuned from phase separation to uniform segments.<sup>47</sup> Unique DNA-mimicking nanocaterpillar structures have also been overserved very recently.<sup>48</sup>

Complex block copolymers can also be produced using Kumada CTP. Koeckelberghs previously reported the controlled synthesis of polycyclopentadithiophenes and synthesized the block copolymer with P3HT.<sup>29</sup> Similar to the aforementioned synthesis of tellurophene-containing block copolymers, monomer addition sequence was found to be specific where more donor-type polycyclopentadithiophenes have to be the second block.

Block copolymers of polydithienosiloles and P3HT have been independently prepared by Dubois and Kiriy's group.<sup>30,49</sup> Comparing different cross-coupling reactions they adopted, Kiriy's method with Ni(dppe)Cl<sub>2</sub> and a Negishi-type dithienosilole monomer afforded block copolymers with better control.

### 1.5.2 Conjugated/Nonconjugated Polymers.

The ability to combine the conjugated segment with the nonconjugated aliphatic segment into one uniform polymer chain significantly increases the scope of functional materials consisting conjugated polymers (Figure 1.9). The drastic difference between two distinct blocks allows these block copolymers to self-assemble into ordered nanostructures. Solution processibility is improved because of the incorporation of aliphatic polymers. Nevertheless, a decreased conductivity was often observable among these block copolymers.

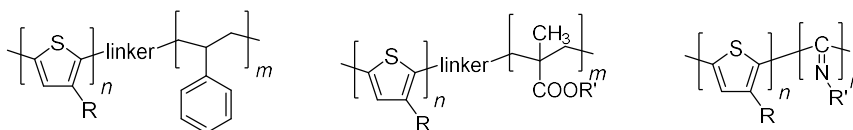


**Figure 1.9.** Selected Conjugated/Nonconjugated Polymers.

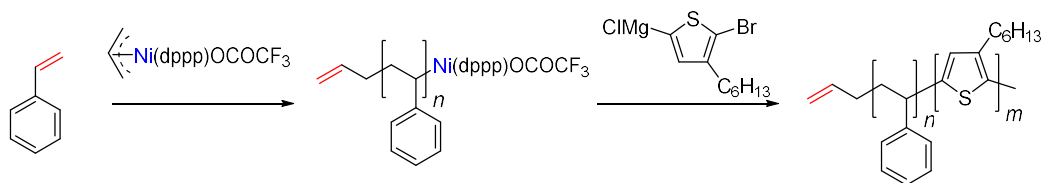
Pioneering research has been done by McCullough and coworkers, where they prepared several block copolymers of P3HT with polystyrenes or polyacrylates.<sup>50</sup> The nonconjugated block is typically synthesized from a polymeric macrorinitiator which is prepared by post-functionalization of the first conjugated block. Multiple steps including polymerizations and purifications are needed, inevitably limiting the application of this protocol.

In 2012, Bielawski and coworkers developed a one-pot synthesis route for the block copolymer of polythiophenes and polyisocyanides, merging two distinct mechanisms by using one single catalyst.<sup>51</sup> This method bypassed synthesizing macroinitiators in advance and reduced steps needed to produce the final block copolymer. However, monomers that are amendable to this protocol are limited.

In 2014, a one-pot copolymerization between thiophene monomers and vinyl-based monomers has been realized by Wu and coworkers.<sup>52</sup> Vinyl-based monomers such as styrene, butyl acrylate, and alkoxyallene were polymerized first using a  $\pi$ -allylnickel complex and then the active chain end of the first block was able to initiate the second thiophene block (Scheme 1.8). Moreover, a third block of polyalkoxyallenes can be further generated by successive monomer addition.

### Scheme 1.7. One-Pot Synthesis of the Block Copolymer Consisting Polystyrenes and P3HT.

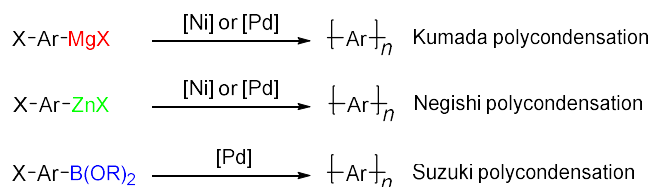
(Adapted with permission from *Chem. Rev.* **2016**, *116*, 1950-1968. Copyright 2016 American Chemical Society.)



## 1.6 Conclusions and Thesis Scope

Over the years, a variety of cross-coupling reactions such as Suzuki (organoboron), Kumada (organomagnesium) and Negishi (organozinc) have been successfully applied in the CTP process involving different metal catalysts (Scheme 1.8).

### Scheme 1.8. Representations of CTP using Different Cross-Coupling Reactions.



After a brief review of CTP protocols above, it is surprising that despite all the progress over the decade, there is no systematic evaluation of how catalysts behave in different cross-coupling reactions and it is important to synthesize the desired materials as to understand why some can only be prepared by certain catalysts using certain conditions. Several other pressing problems include (1) the still limited choice of catalysts that initiate CTP and the restricted scope of cross-coupling reactions, and (2) the lack of functional groups in conjugated polymers due to the high reactivity of Kumada or Negishi monomers.

The thesis work in the following chapters demonstrates some of our endeavor towards solving these problems and producing exciting materials using CTP.

In Chapter 2, we have successfully expanded the monomer scope to another group 16 heterocycle furan because furan is a “green” monomer and furan containing macromolecules often possess high planarity and rigidity. We have prepared regioregular head-to-tail and head-to-head poly(3-hexylfuran) using catalyst-transfer polycondensation. The resultant polyfurans have lower molecular weights but also low dispersities ( $D = 1.20\sim 1.25$ ). Extensive aggregation of the furan homopolymer led to investigation of an alternating furan-thiophene copolymer confirming that furyl-based monomers can polymerize in a chain-growth manner. The rather low stability of these furan related materials towards light and oxygen led us to the development of a mild and more functional group tolerant CTP protocol using different cross-coupling reactions other than Kumada.

In Chapter 3, we used a commercially available Pd-NHC precatalyst to initiate Stille CTP for P3HT synthesis. The molecular weight of the resultant poly(3-hexylthiophene) could be modulated by varying the catalyst concentration. Mass spectrometry data confirmed control over the polymer end-groups and a linear relationship between  $M_n$  and monomer conversion was observed. However, the limited monomer scope and complicated purification procedures using Stille CTP along with the toxicity concern regarding tin byproducts made us choose alternative protocols.

In Chapter 4, we have demonstrated a chain-growth Suzuki polycondensation of an ester-functionalized thiophene using commercially available nickel precatalysts to install functional groups into conjugated polymers. This is the first description of nickel-catalyzed Suzuki cross-coupling for catalyst-transfer polycondensation and to further illustrate the versatility of this method, block and alternating copolymers with 3-hexylthiophene were synthesized. An ester-functionalized furan monomer has also been polymerized using similar protocol. Though polymer samples were obtained with only moderate molecular weights, polyfurans consisting ester groups exhibited good end group fidelity and enhanced photostability.

In Chapter 5, though the results are preliminary, we sought to investigate a direct lithium-halogen cross-coupling protocol to synthesize conjugated polymers with ease and efficiency. Both electron-rich and electron-deficient polymers can be prepared using Pd or Ni catalysts. This method allows facile preparation of conjugated polymers with high yields. Molecular weight of the resultant polymer can be controlled by varying the catalyst loading. Interestingly, we have found that the same catalyst might behave differently regarding cross-coupling reactions used. A systematic evaluation of the catalyst performance in different cross-coupling strategies are necessary. And we believe that this should provide mechanistic insights of CTP and provide guidance for suitable combinations of catalysts and cross-coupling reactions to achieve the controlled synthesis of conjugated polymers.

## 1.7 References

- (1) *Controlled and Living Polymerizations*; Müller A. H. E. and Matyjaszewski K., Eds.; Wiley-VCH Verlag GmbH & Co. KGaA: Weinheim, Germany, **2009**.
- (2) (a) *Block Copolymers in Solution: Fundamentals and Applications*; Hamley, I., Eds.; John Wiley & Sons, Ltd: Chichester, UK, **2005**. (b) *Developments in Block Copolymer Science and Technology*; Hamley, I., Eds.; John Wiley & Sons, Ltd: Chichester, UK, **2004**.
- (3) Hadjichristidis, N.; Pitsikalis, M.; Pispas, S.; Iatrou, H. *Chem. Rev.* **2001**, *101*, 3747-3792.
- (4) Matyjaszewski, K.; Spanswick, J. *Mater. Today* **2005**, *8*, 26-33.
- (5) Bielawski, C. W.; Grubbs, R. H. *Prog. Polym. Sci.* **2007**, *32*, 1-29.
- (6) (a) Heeger, A. J. *Rev. Mod. Phys.* **2001**, *73*, 681-700. (b) MacDiarmid, A. G. *Rev. Mod. Phys.* **2001**, *73*, 701-712. (c) Shirakawa, H. *Rev. Mod. Phys.* **2001**, *73*, 713-718. (d) Chiang, C. K.; Druy, M. A.; Gau, S. C.; Heeger, A. J.; Louis, E. J.; MacDiarmid, A. G.; Park, Y. W.; Shirakawa, H. *J. Am. Chem. Soc.* **1978**, *100*, 1013-1015. (e) Chiang, C. K.; Fincher, C. R.; Park, Y. W.; Heeger, A. J.; Shirakawa, H.; Louis, E. J.; Gau, S. C.; MacDiarmid, A. G. *Phys. Rev. Lett.* **1977**, *39*, 1098-1101. (f) Shirakawa, H.; Louis, E. J.; MacDiarmid, A. G.; Chiang, C. K.; Heeger, A. J. *J. Chem. Soc., Chem. Commun.* **1977**, 578-580.
- (7) (a) Meager, I.; Ashraf, R. S.; Nielsen, C. B.; Donaghey, J. E.; Huang, Z.; Bronstein, H.; Durrant, J. R.; McCulloch, I. *Journal of Materials Chemistry C* **2014**, *2*, 8593-8598. (b) Lu, L.; Zheng, T.; Xu, T.; Zhao, D.; Yu, L. *Chemistry of Materials* **2015**, *27*, 537-543.
- (8) Bryan, Z. J.; McNeil, A. J. *Macromolecules* **2013**, *46*, 8395-8405.
- (9) *Principles of Polymerization*, 4th ed.; Odian, G., Eds.; John Wiley & Sons, Inc.: Hoboken, NJ, USA, **2004**.
- (10) Yokozawa, T.; Ohta, Y. *Chem. Rev.* **2016**, *116*, 1950-1968.
- (11) Sheina, E. E.; Liu, J.; Iovu, M. C.; Laird, D. W.; McCullough, R. D. *Macromolecules* **2004**, *37*, 3526-3528.
- (12) Yokoyama, A.; Miyakoshi, R.; Yokozawa, T. *Macromolecules* **2004**, *37*, 1169-1171.

- (13) Grisorio, R.; Suranna, G. P. *Polym. Chem.* **2015**, *6*, 7781-7795.
- (14) (a) Sylvester, K. T.; Wu, K.; Doyle, A. G. *J. Am. Chem. Soc.* **2012**, *134*, 16967-16970. (b) Ge, S.; Hartwig, J. F. *J. Am. Chem. Soc.* **2011**, *133*, 16330-16333. (c) Johnson, S. A.; Huff, C. W.; Mustafa, F.; Saliba, M. *J. Am. Chem. Soc.* **2008**, *130*, 17278-17280.
- (15) Kohei, T.; Koji, S.; Yoshihisa, K.; Michio, Z.; Akira, F.; Shun-ichi, K.; Isao, N.; Akio, M.; Makoto, K. *Bull. Chem. Soc. Jpn.* **1976**, *49*, 1958-1969.
- (16) (a) Bryan, Z. J.; McNeil, A. J. *Chem. Sci.* **2013**, *4*, 1620-1624. (b) Dong, C.-G.; Hu, Q.-S. *J. Am. Chem. Soc.* **2005**, *127*, 10006-10007.
- (17) Lee, S. R.; Bloom, J. W. G.; Wheeler, S. E.; McNeil, A. J. *Dalton Trans.* **2013**, *42*, 4218-4222.
- (18) (a) Zhang, H.-H.; Xing, C.-H.; Hu, Q.-S. *J. Am. Chem. Soc.* **2012**, *134*, 13156-13159. (b) Huddleston, N. E.; Sontag, S. K.; Bilbrey, J. A.; Sheppard, G. R.; Locklin, J. *Macromol. Rapid Commun.* **2012**, *33*, 2115-2120.
- (19) (a) Sui, A.; Shi, X.; Wu, S.; Tian, H.; Geng, Y.; Wang, F. *Macromolecules* **2012**, *45*, 5436-5443. (b) Kohn, P.; Huettner, S.; Komber, H.; Senkovskyy, V.; Tkachov, R.; Kiriy, A.; Friend, R. H.; Steiner, U.; Huck, W. T. S.; Sommer, J.-U.; Sommer, M. *J. Am. Chem. Soc.* **2012**, *134*, 4790-4805.
- (20) Bryan, Z. J.; Smith, M. L.; McNeil, A. J. *Macromol. Rapid Commun.* **2012**, *33*, 842-847.
- (21) Magurudeniya, H. D.; Sista, P.; Westbrook, J. K.; Ourso, T. E.; Nguyen, K.; Maher, M. C.; Alemseghed, M. G.; Biewer, M. C.; Stefan, M. C. *Macromol. Rapid Commun.* **2011**, *32*, 1748-1752.
- (22) Lee, S. R.; Bryan, Z. J.; Wagner, A. M.; McNeil, A. J. *Chem. Sci.* **2012**, *3*, 1562-1566.
- (23) Miyakoshi, R.; Shimono, K.; Yokoyama, A.; Yokozawa, T. *J. Am. Chem. Soc.* **2006**, *128*, 16012-16013.
- (24) Yokoyama, A.; Suzuki, H.; Kubota, Y.; Ohuchi, K.; Higashimura, H.; Yokozawa, T. *J. Am. Chem. Soc.* **2007**, *129*, 7236-7237.

- (25) Yokozawa, T.; Yokoyama, A. *Chem. Rev.* **2009**, *109*, 5595-5619.
- (26) Hollinger, J.; Jahnke, A. A.; Coombs, N.; Seferos, D. S. *J. Am. Chem. Soc.* **2010**, *132*, 8546-8547.
- (27) Ye, S.; Steube, M.; Carrera, E. I.; Seferos, D. S. *Macromolecules* **2016**, *49*, 1704-1711.
- (28) Yokoyama, A.; Kato, A.; Miyakoshi, R.; Yokozawa, T. *Macromolecules* **2008**, *41*, 7271-7273.
- (29) Willot, P.; Govaerts, S.; Koeckelberghs, G. *Macromolecules* **2013**, *46*, 8888-8895.
- (30) Boon, F.; Hergue, N.; Deshayes, G.; Moerman, D.; Desbief, S.; De Winter, J.; Gerbaux, P.; Geerts, Y. H.; Lazzaroni, R.; Dubois, P. *Polym. Chem.* **2013**, *4*, 4303-4307.
- (31) Mkhallid, I. A. I.; Barnard, J. H.; Marder, T. B.; Murphy, J. M.; Hartwig, J. F. *Chem. Rev.* **2010**, *110*, 890-931.
- (32) Kosaka, K.; Ohta, Y.; Yokozawa, T. *Macromol. Rapid Commun.* **2015**, *36*, 373-377.
- (33) Beryozkina, T.; Senkovskyy, V.; Kaul, E.; Kiriya, A. *Macromolecules* **2008**, *41*, 7817-7823.
- (34) (a) Ateşin, T. A.; Li, T.; Lachaize, S.; García, J. J.; Jones, W. D. *Organometallics* **2008**, *27*, 3811-3817. (b) Tolman, C. A. *J. Am. Chem. Soc.* **1974**, *96*, 2780-2789.
- (35) Wen, L.; Duck, B. C.; Dastoor, P. C.; Rasmussen, S. C. *Macromolecules* **2008**, *41*, 4576-4578.
- (36) Willot, P.; Moerman, D.; Leclère, P.; Lazzaroni, R.; Baeten, Y.; Van der Auweraer, M.; Koeckelberghs, G. *Macromolecules* **2014**, *47*, 6671-6678.
- (37) Nanashima, Y.; Yokoyama, A.; Yokozawa, T. *Macromolecules* **2012**, *45*, 2609-2613.
- (38) Nanashima, Y.; Shibata, R.; Miyakoshi, R.; Yokoyama, A.; Yokozawa, T. *J. Polym. Sci., Part A: Polym. Chem.* **2012**, *50*, 3628-3640.
- (39) Bridges, C. R.; McCormick, T. M.; Gibson, G. L.; Hollinger, J.; Seferos, D. S. *J. Am. Chem. Soc.* **2013**, *135*, 13212-13219.
- (40) (a) Pollit, A. A.; Bridges, C. R.; Seferos, D. S. *Macromol. Rapid Commun.* **2015**, *36*, 65-70. (b) Bridges, C. R.; Yan, H.; Pollit, A. A.; Seferos, D. S. *ACS Macro Lett.* **2014**, *3*, 671-674.

- (41) Todd, A. D.; Bielawski, C. W. *ACS Macro Lett.* **2015**, *4*, 1254-1258.
- (42) Elmalem, E.; Kiriy, A.; Huck, W. T. S. *Macromolecules* **2011**, *44*, 9057-9061.
- (43) Senkovskyy, V.; Tkachov, R.; Komber, H.; Sommer, M.; Heuken, M.; Voit, B.; Huck, W. T. S.; Kataev, V.; Petr, A.; Kiriy, A. *J. Am. Chem. Soc.* **2011**, *133*, 19966-19970.
- (44) (a) Hollinger, J.; Sun, J.; Gao, D.; Karl, D.; Seferos, D. S. *Macromol. Rapid Commun.* **2013**, *34*, 437-441. (b) Hollinger, J.; DiCarmine, P. M.; Karl, D.; Seferos, D. S. *Macromolecules* **2012**, *45*, 3772-3778. (c) Palermo, E. F.; McNeil, A. J. *Macromolecules* **2012**, *45*, 5948-5955.
- (45) Ryo, M.; Akihiro, Y.; Tsutomu, Y. *Chem. Lett.* **2008**, *37*, 1022-1023.
- (46) (a) Yu, X.; Yang, H.; Wu, S.; Geng, Y.; Han, Y. *Macromolecules* **2012**, *45*, 266-274. (b) Wu, S.; Bu, L.; Huang, L.; Yu, X.; Han, Y.; Geng, Y.; Wang, F. *Polymer* **2009**, *50*, 6245-6251.
- (47) Lee, Y.-H.; Chen, W.-C.; Yang, Y.-L.; Chiang, C.-J.; Yokozawa, T.; Dai, C.-A. *Nanoscale* **2014**, *6*, 5208-5216.
- (48) Lee, I.-H.; Amaladass, P.; Choi, I.; Bergmann, V. W.; Weber, S. A. L.; Choi, T.-L. *Polym. Chem.* **2016**, *7*, 1422-1428.
- (49) Erdmann, T.; Back, J.; Tkachov, R.; Ruff, A.; Voit, B.; Ludwigs, S.; Kiriy, A. *Polym. Chem.* **2014**, *5*, 5383-5390.
- (50) (a) Iovu, M. C.; Zhang, R.; Cooper, J. R.; Smilgies, D. M.; Javier, A. E.; Sheina, E. E.; Kowalewski, T.; McCullough, R. D. *Macromol. Rapid Commun.* **2007**, *28*, 1816-1824. (b) Iovu, M. C.; Jeffries-El, M.; Zhang, R.; Kowalewski, T.; McCullough, R. D. *J. Macromol. Sci., Part A: Pure Appl. Chem.* **2006**, *43*, 1991-2000. (c) Iovu, M. C.; Jeffries-El, M.; Sheina, E. E.; Cooper, J. R.; McCullough, R. D. *Polymer* **2005**, *46*, 8582-8586.
- (51) Wu, Z.-Q.; Radcliffe, J. D.; Ono, R. J.; Chen, Z.; Li, Z.; Bielawski, C. W. *Polym. Chem.* **2012**, *3*, 874-881.
- (52) Gao, L.-M.; Hu, Y.-Y.; Yu, Z.-P.; Liu, N.; Yin, J.; Zhu, Y.-Y.; Ding, Y.; Wu, Z.-Q. *Macromolecules* **2014**, *47*, 5010-5018.

## CHAPTER 2

### Synthesis of Polyfuran and Thiophene-Furan Alternating Copolymers Using Catalyst-Transfer Polycondensation

#### 2.1 Introduction

In the extensive exploration of organic semiconductors for optoelectronics, polythiophenes (PTs) are some of the most widely studied materials.<sup>1</sup> Typically, a highly planar  $\pi$ -conjugated backbone is necessary to obtain good  $\pi$ - $\pi$  stacking in the solid state, leading to materials with enhanced charge carrier mobility.<sup>2</sup> For PTs, the energy required to twist the backbone is quite low,<sup>3</sup> and consequently, solubilizing substituents must be incorporated in a controlled manner to obtain solution-processable materials without sacrificing planarity. The preparation of regioregular head-to-tail poly(3-hexylthiophene) (*rr*-P3HT) was an important synthetic achievement to this end,<sup>4</sup> producing a material with superior electronic properties compared to its regioirregular analogues.<sup>5</sup>

Additionally, the polycondensation process to synthesize P3HT was determined to proceed by a chain-growth mechanism,<sup>6</sup> affording materials with controllable molecular weights and low dispersities. This controlled process CTP provides access to more complex semiconducting architectures as a means to further tune solid-state organization.<sup>7</sup> With the exploration of chain-growth polymerization for PTs and polyselenophenes,<sup>8</sup> it is surprising that controlled methods for the lighter group 16 heterocycle (furan) have not yet been reported.<sup>9</sup>

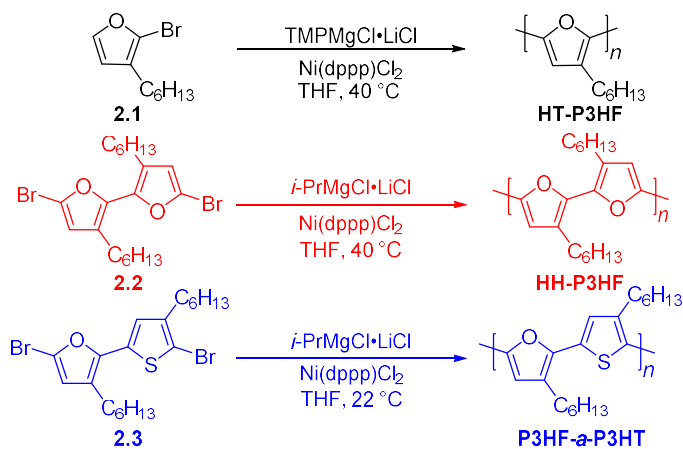
The environmental impact regarding manufacturing and disposal of organic electronics is a concern.<sup>10</sup> Furan is a biodegradable monomer that can be obtained from biomass, making it a green conjugated building block.<sup>11</sup> The challenging synthesis of furan-based monomers as well as the suspicion of polyfuran instability<sup>12</sup> have likely contributed to the limited examination of these polymers. Recent reports on oligofurans have illustrated that these materials are relatively stable;<sup>13</sup> and they exhibit increased solubility, higher fluorescence and a lower propensity to twist

as compared to oligothiophenes.<sup>14</sup> Oligofurans are highly planar even with substituents in a head-to-head orientation (HH-3,3' substitution on adjacent rings).<sup>14b</sup> The steric strain between adjacent furan rings is lower due to the smaller oxygen atom as compared to sulfur. Moreover, the lower aromaticity of furan enhances quinoidal character in the polymer, resulting in shorter inter-ring bonds.<sup>15</sup>

## 2.2 Results and Discussion

In order to thoroughly investigate poly(3-hexylfuran) (P3HF), we prepared two different regioregular materials, one with the typical head-to-tail (HT) substitution similar to *rr*-P3HT, and the other with HH enchainment of the hexyl tails (Scheme 2.1). These polyfurans exhibit remarkably similar solid-state conformations regardless of the side-chain pattern, confirming the limited effect of the substituent orientation on polymer organization. While neither polymerization proceeded to high molecular weights, the low dispersities were an indicator of a possible chain-growth process. Extensive aggregation during polymerization led us to explore an alternating furan-thiophene copolymer to confirm that furan is amenable to chain-growth polymerization protocols.

**Scheme 2.1. Synthesis of HT-P3HF, HH-P3HF and P3HF-*a*-P3HT**



Furan-containing molecules are often sensitive to light and acid,<sup>13,16</sup> and aqueous acidic work-ups are not suitable for any of the monomers synthesized (Compounds **2.1-2.3**) in this

work. The brominated furans are especially sensitive to acidic conditions. Column chromatography using standard silica gel is problematic though basic alumina can be used as a substitute.

Both **HT-P3HF** and **HH-P3HF** were synthesized using nickel-catalyzed Kumada coupling. The active monomer for **HT-P3HF** was generated by treatment of 2-bromo-3-hexylfuran **2.1** (Scheme 2.3) with 2,2,6,6-tetramethylpiperidinylmagnesium chloride lithium chloride complex (TMPMgCl·LiCl), similar to previously reported protocols for PT.<sup>17</sup> We conducted a quenching study of the monomer to confirm metallation at the 5-position and the major product was the expected 2-bromo-3-hexyl-5-iodofuran. The HH furan dimer (**2.2**) was converted into the active monomer species by combination with isopropylmagnesium chloride lithium chloride complex (*i*-PrMgCl·LiCl). Both polymerization reactions were initiated by adding Ni(dppp)Cl<sub>2</sub> into the active monomer solution at 40 °C, and after 20 min, the reactions were quenched using 6 M methanolic HCl solution. Gel permeation chromatography (GPC) relative to polystyrene (THF) indicated modest molecular weights with relatively narrow dispersities ( $D = 1.20\sim 1.25$ , Table 2.1). However, when lower catalyst loadings were used, higher molecular weights could not be obtained.

**Table 2.1. Comparison of furan-containing polymers**

Entry	Sample	% cat	$M_n(\text{GPC})^a$ [g/mol]	$D$	Yield
1	HT-P3HF	20	3600	1.20	55%
2	HT-P3HF	10	4100	1.25	73%
3	HH-P3HF	10	2900	1.22	42%
4	P3HF- <i>a</i> -P3HT	5	7700	1.58	46%
5	P3HF- <i>a</i> -P3HT	2.5	10000	1.50	57%
6	P3HF- <i>a</i> -P3HT	1.25	11900	1.41	35%

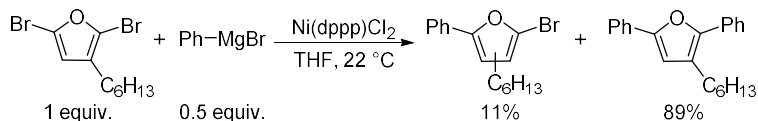
<sup>a</sup>GPC was recorded at 40 °C in THF versus polystyrene standards.

During the polymerization of both the HT and HH polyfuran, significant aggregation was observed. We suspect that the polymer aggregates as the reaction progresses and consequently, the growing macromolecule precipitates from solution with premature termination of chain-

growth. The dispersities observed for the isolated polymer samples were encouraging that furan would still be suitable for CTP (Table 2.1, Entries 1-3).

A metal polymer  $\pi$ -complex has been proposed as an intermediate in the catalytic cycle for these chain-growth processes, resulting in selective intramolecular oxidative addition at the polymer chain-end during polymerization.<sup>18</sup> Small molecule experiments with a dihalogenated compound and a Grignard reagent can provide indirect evidence of the  $\pi$ -complex if exclusive double substitution is observed.<sup>6a</sup> When 1 equivalent of 2,5-dibromo-3-hexylfuran was combined with 0.5 equivalents of phenylmagnesium bromide in the presence of Ni(dppp)Cl<sub>2</sub>, 2,5-diphenyl-3-hexylfuran was obtained preferentially (Scheme 2.2). This provides further evidence for nickel association to the furan ring and that aggregation is the barrier to obtaining higher molecular weight P3HF.

**Scheme 2.2. Preferential double substitution with furan, the percent yields are relative to Ph-MgBr.**



To probe whether furan is amenable to CTP, an alternating copolymer containing furan and thiophene was envisioned. This structure would lower the furan content along the polymer chain and provide a certain amount of torsion within the backbone to improve solubility. The thiophene-furan dimer (**2.3**) was synthesized (Scheme 2.4), activated using *i*-PrMgCl·LiCl and polymerized in THF.<sup>19</sup> In the activation step, two possible sites (thiophene or furan) can be metalated by the Grignard reagent to produce the desired AB monomer. In 2,5-dibromo-3-hexylthiophene, metalation at the less hindered 5-position is favored (monomer ratio ~ 4:1).<sup>20</sup> Interestingly, we observed a ~4:1 mixture of metalated monomers when activating **2.3**, but quenching studies indicated preferential activation of the bromine on the thiophene ring.

This result was surprising considering the halogen on the thiophene ring is more sterically hindered. To examine this further, a competition experiment was conducted by adding *i*-PrMgCl·LiCl to an equimolar mixture of 2-bromofuran and 2-bromo-3-hexylthiophene. A preference for insertion into thiophene was observed, providing further support for the higher reactivity of this heterocycle towards Mg exchange. A similar reactivity preference has been noted previously.<sup>21</sup>

The unexpected monomer activation does not inhibit polymerization, since a range of molecular weights could be achieved by manipulating the catalyst loading (Table 2.1, Entries 4,5,6). The “reversed” thiophene isomer is not normally consumed in a Grignard metathesis polymerization however,<sup>20,22</sup> in the presence of LiCl, the “reversed” monomer can be polymerized.<sup>23</sup> The LiCl may play a similar role in the polymerization of monomer **2.3**.

A  $M_n$  versus conversion plot was obtained (Figure 2.1) for polymerization of **2.3** using 1.25 mol % of Ni(dppp)Cl<sub>2</sub>. The two isomers were formed in a nearly 4:1 ratio upon activation with a small amount (~2%) of bismetallated monomer. Over the first 2 min, consumption of both isomers is observed after which time, the concentration of the minor isomer does not change dramatically while the major isomer is still consumed (Figure 2.4 and Table 2.2). The moderately linear relationship between  $M_n$  and total monomer conversion was indicative of a chain-growth process and the dispersities remained relatively constant (1.4-1.5).

The higher dispersity is consistent with the previous report for the polymerization of a “reversed” thiophene monomer.<sup>23</sup> Geng and co-workers observed the LiCl was necessary to produce HH enchainment of two thiophene monomers initially.<sup>23</sup> They also noted HH coupling was much slower than HT or tail-to-tail (TT) and the HH event was responsible for slow initiation and low molecular weight tailing. We also observe tailing in the chromatograms for **P3HF-*a*-P3HT**, suggesting slow initiation or some other complication. Initiation for **2.3** could also involve both the major and minor species and further studies are necessary to probe this behavior in more detail. The controlled molecular weights and  $M_n$  versus conversion plot for the furan-thiophene

dimer indicated CTP is applicable to furan-based monomers though typical insertion of Grignard reagents must be explored carefully.

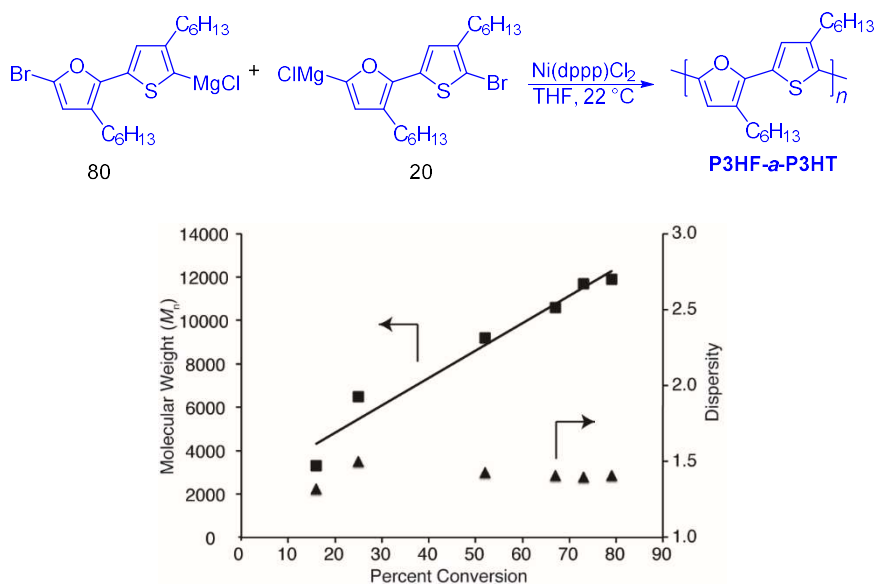


**Figure 2.1.** Plot of  $M_n$  versus conversion for polymerization of P3HF-*a*-P3HT using 1.25 mol %  $\text{Ni(dppp)Cl}_2$ .

The  $^1\text{H}$  NMR spectra obtained for all three polymers are shown in Figure 2.2. Close examination of the aromatic region (A, C, F and E) and the methylene signals of the hexyl chains (B, D, H and G) reveal primarily regioregular enchainment. In **HT-P3HF**, some signals appear slightly downfield of the major aromatic resonance at 6.47 ppm. 2D NMR analysis confirmed that these signals are part of the polymer backbone and reveal two other families of triads, we speculate that these are regiodefects in the polymer chain, similar to those reported for P3HT,<sup>24</sup> but further studies with model compounds are necessary to confirm this. We also observe primarily H/H terminated end-groups in this polymer. The major end group appears as two small aromatic signals at 7.22 and 6.39 ppm, which corresponds to an HT end-group. Interestingly, there is a similar end group observed in the long range COSY that indicates another HT end group affected by a nearby irregularity (likely a TT). Finally, a minor end group signal (7.18 ppm) likely corresponds to a TT end-group though again, model compounds are necessary to confirm

this. Overall, the major end group observed is HT and suggests bidirectional chain-walking as observed previously for P3HT.<sup>22b,25</sup>

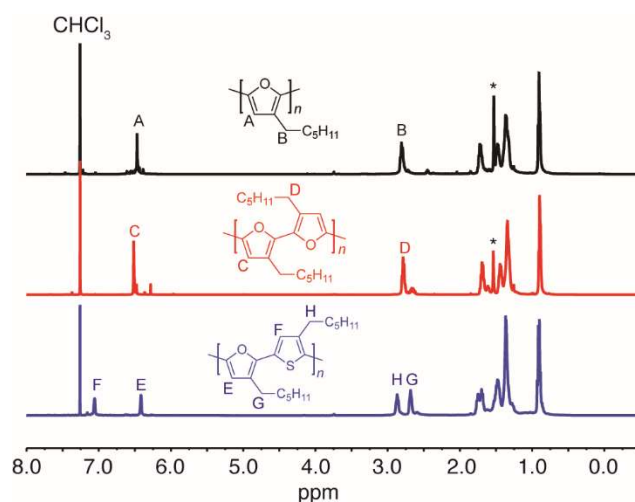


**Figure 2.2.**  $^1\text{H}$  NMR spectra of HT-P3HF, HH-P3HF and P3HF-*a*-P3HT collected at 22 °C in  $\text{CDCl}_3$ , the \* indicates  $\text{H}_2\text{O}$ .

In **HH-P3HF**, the polymer is highly regioregular, which is not surprising considering the regiochemistry of dimer **2.2**. Two end groups are observed and are labeled in the supporting information (6.29 ppm for the Br terminated end group and 7.37 ppm, 6.37 ppm for the H terminated end group). In contrast to **HT-P3HF**, the major end group corresponds to a bromine and suggests some Br/Br chains. Both the **HT** and **HH-P3HF** end groups suggest competitive termination reactions in these polymerizations and are consistent with the inability to alter molecular weight by changing catalyst loading.

Long range  $^1\text{H}$ - $^{13}\text{C}$  coupling in the HMBC spectrum of **P3HF-*a*-P3HT** revealed the expected correlations for the ring resonances and confirmed the highly alternating nature of the polymer chain. The  $^1\text{H}$  NMR spectrum of the alternating polymer was slightly broader than that of the homopolymers and it was difficult to conduct end-group analysis or determine regioregularity. We have also noted the color of all three polymers faded over a period of several hours in solution, which is caused by exposure to  $\text{O}_2$  and light.

Optical properties of all three polymers were probed both in solution and in the solid-state (Figure 2.3 and Table 2.3). In THF, **HT-P3HF** and **HH-P3HF** have very similar maximum absorption peaks at 465 and 458 nm respectively, which are red-shifted from *rr*-P3HT (450 nm).<sup>26</sup> Both HT and HH polyfuran exhibit shoulders near 480-490 nm. These result from interchain excitons and vibronic couplings, indicating aggregation in solution.<sup>5</sup> The well-defined absorption peaks of **HT-P3HF** and **HH-P3HF** suggest both polymers adopt a planar and rod-like structure in solution. In contrast, a featureless absorption profile was recorded for *rr*-P3HT (Figure 2.3). The alternating **P3HF-*a*-P3HT** produced a maximum absorption (476 nm) that is red shifted from both P3HF and *rr*-P3HT in solution. This may be attributed to a more planar backbone structure from lower strain between adjacent rings. Replacing different heterocycles with furan could potentially be used to enhance planarity in conjugated polymers as has been observed previously in donor-acceptor copolymers.<sup>27</sup>

The maximum absorptions of P3HF closely match that of the previously reported HT-poly(3-octylfuran) ( $\lambda_{\text{max}} = 466$  nm) in solution, suggesting a similar effective conjugation length.<sup>9c</sup> The previous report describing poly(3-octylfuran) indicated that regiorandom orientations of the repeat unit produced a blue shift in the UV-Vis spectrum ( $\lambda_{\text{max}} = 372$  nm) as compared to the HT derivative.<sup>9c</sup> Considering the absorption spectra for **HH-P3HF** and **HT-P3HF** are so similar, the HH orientation of the hexyl chains in a regioregular polymer exhibits little effect on the polymer conformation. This is consistent with recent reports on HH-enriched furan oligomers.<sup>14a,14b</sup> Remarkably, the solid-state absorption spectra for **HT-P3HF** and **HH-P3HF** are nearly indistinguishable with similar  $\lambda_{\text{max}}$  values and red-shifted shoulders. The optical bandgap (2.19 eV) calculated from the onset absorption wavelength for both P3HF polymers were the same. The regiocontrolled HH defect seems to have a negligible effect on backbone planarity in polyfuran, which correlates well with recent DFT calculations.<sup>14a</sup> In contrast, regioregular HH-P3HT has been synthesized and is significantly blue shifted from its HT analog.

In the solid state, regioregular HH-P3HT has a  $\lambda_{\max} = 428 \text{ nm}$  ( $E_g$  edge = 2.9 eV) which is blue shifted by 133 nm from the  $\lambda_{\max}$  of HT-P3HT (561 nm,  $E_g$  edge = 1.9 eV).<sup>28</sup> Clearly, the smaller oxygen atom plays a role in minimizing steric interactions between adjacent aromatic rings with substituents. The absorption maximum of the **P3HF-*a*-P3HT** thin film (531 nm) was situated between its two homopolymers, showing good agreement of a balanced bandgap (2.00 eV).

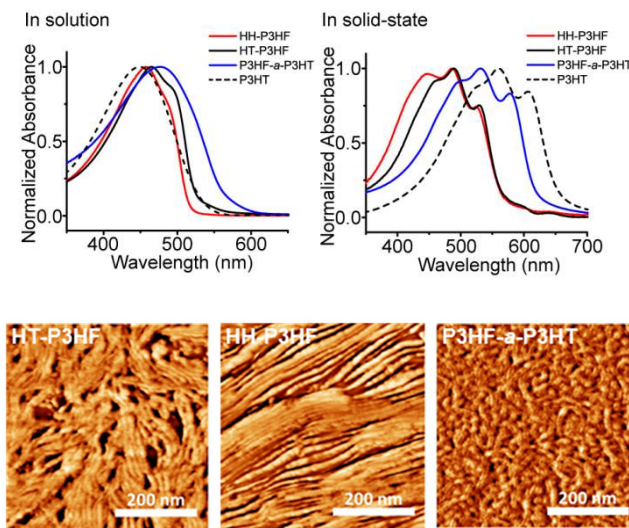


**Figure 2.3.** Top Left - UV-Vis absorption spectra in THF for HT-P3HF, HH-P3HF and P3HF-*a*-P3HT compared with *rr*-P3HT. Top Right - Solid-state UV-Vis of the 3 polymer samples compared with *rr*-P3HT. Bottom - Tapping-mode AFM phase images showing nanofibrillar structures of HT-P3HF, HH-P3HF and P3HF-*a*-P3HT.

Tapping mode AFM images of the three polymer samples were obtained to further confirm the well-defined solid-state organization (Figure 2.3). The observed nanofibrillar structures indicate the formation of  $\pi$ - $\pi$  stacked polymer chains, which is well known for *rr*-P3HT with narrow dispersity.<sup>29</sup> Both **HT** and **HH-P3HF** tended to form elongated fibrils. The fibril widths determined from AFM images were equal to  $\sim 10 \text{ nm}$  for the homopolymers, and were comparable with the average fully extended lengths of polymer chains based on their degree of polymerization (DP). Similar observations have been noted for moderate length (DP $\sim$ 60) narrow

dispersity *rr*-P3HT, and has been attributed to the perpendicular orientation of  $\pi$ - $\pi$  stacked polymer chains with respect to the nanofibril axis.<sup>29</sup>

Notably, the nanofibrils formed from the alternating polymer were much less distinct and uniform, which can be attributed to significantly higher dispersity of the **P3HF-*a*-P3HT** sample. The alternating polymer also exhibited marked sensitivity to light exposure during AFM characterization, with the surface morphology visibly deteriorating upon rescanning. The appearance of those regions under optical microscope also changed, in a manner consistent with photobleaching.

Electrochemical properties of all three polymers were probed using cyclic voltammetry (CV) on a platinum disk working electrode in dry acetonitrile. Both **HT** and **HH-P3HF** showed quasireversible oxidation peaks with onset potentials at -0.013 and -0.039 V, respectively (referenced to the ferrocene/ferrocenium couple). The corresponding HOMO energy level was determined to be -5.09 eV for **HT-P3HF** and -5.06 eV for **HH-P3HF**. The LUMO levels were calculated from the optical bandgap, since a reduction peak for polyfuran could not be obtained in acetonitrile (-2.90 eV for **HT-P3HF** and -2.87 eV for **HH-P3HF**). Both onset oxidation (0.09 V) and reduction (-1.93 V) potentials were obtained for **P3HF-*a*-P3HT**, indicating an electrochemical HOMO-LUMO gap of 2.02 eV.

When characterizing all three polymers, we have noticed their sensitivity towards ambient light and oxygen. To compare polymer samples before and after exposure to both light and oxygen, we have conducted NMR, GPC and UV-Vis experiments using **P3HF-*a*-P3HT**. After each measurement, the polymer sample was placed under sunlight for 24 hours before retesting. NMR spectra before and after exposure are shown in Figure 2.4. The appearance of new peaks in NMR indicated structural changes due to possible ring opening reactions. Particularly, signals near 4.16 ppm might arise from allyl CH<sub>2</sub> peaks which are adjacent to a thiophene ring after ring opening.<sup>9c</sup> The decreasing molecular weight evidenced by GPC spectra is possibly due to the loss of rigid configuration through the polymer backbone (Figure 2.5).<sup>30</sup> The blue shifted

UV-Vis spectrum (Figure 2.6) after exposure to light indicated a decrease in effective conjugation length because of the same structural changes. However, other experiments are needed to further illustrate this.

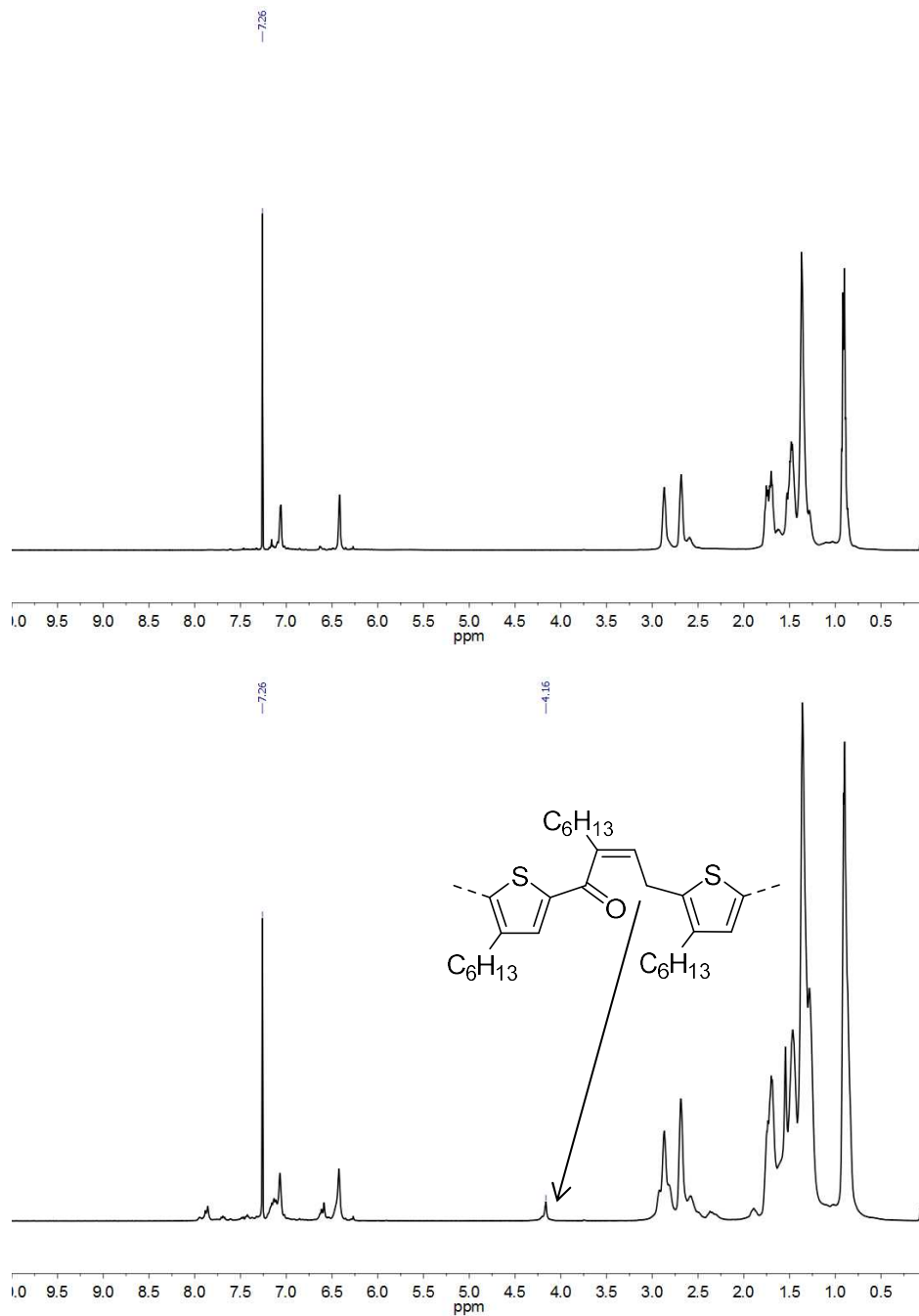


**Figure 2.4.** P3HF-*a*-P3HT NMR spectra before and after exposure to light and oxygen (top – before exposure. Bottom – after exposure.)

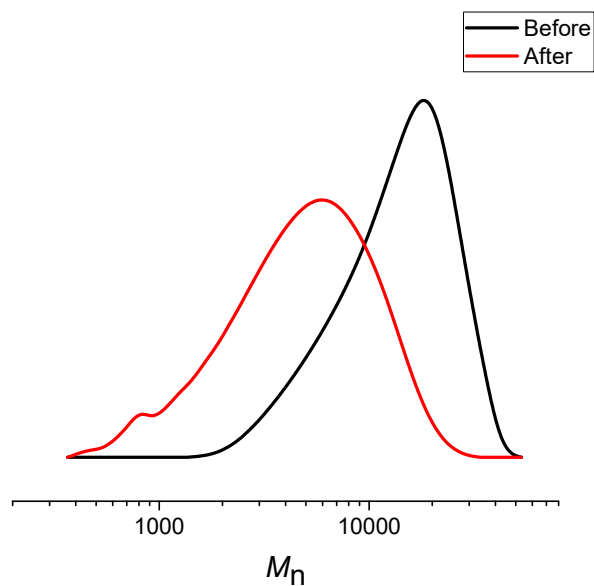


**Figure 2.5.** P3HF-*a*-P3HT GPC spectra before and after exposure to light and oxygen.

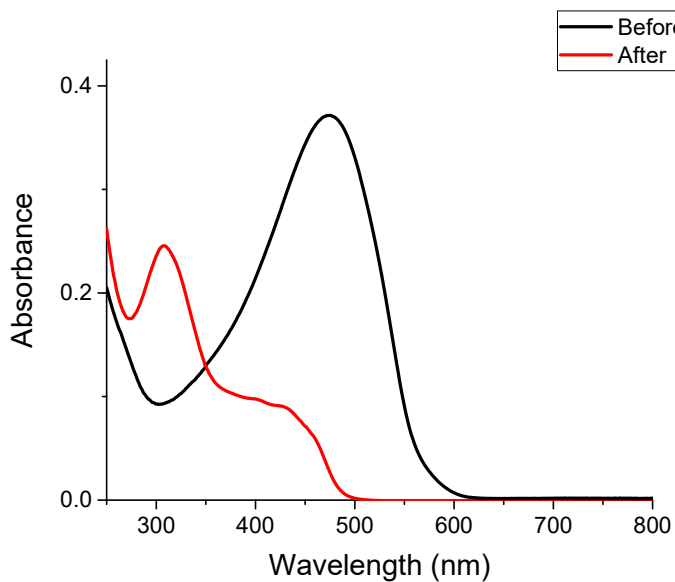


**Figure 2.6.** P3HF-*a*-P3HT UV-Vis spectra before and after exposure to light and oxygen.

### 2.3 Conclusions

In conclusion, we have designed and synthesized two regioregular poly(3-hexylfuran)s with head-to-tail and head-to-head side-chain substitution. These materials were prepared using catalyst-transfer polycondensation but aggregation during polymerization limited the molecular

weight of the samples. An alternating furan-thiophene polymer was also prepared to confirm that furan is amenable to chain-growth polymerization. Both polyfuran homopolymers adopt nearly identical backbone conformations in solution and in the solid-state, regardless of the solubilizing group regiochemistry. The data confirms that there is little steric strain from HH enchainment of alkyl groups in regioregular polyfuran. The ability to incorporate a biorenewable monomer into precise conjugated materials along with its impressive effects on polymer backbone conformation, should afford an array of unique new polymers for future investigation. However, the rather low stability of these furan related materials towards light and oxygen led us to the investigation of milder and more functional group tolerant CTP protocols using different cross-coupling reactions other than Kumada, which will be discussed in the following chapters.

## 2.4 Experimental

**Materials and Methods.** All reactions and manipulations of air or water sensitive compounds were carried out under dry nitrogen using an mBraun glovebox or standard Schlenk techniques unless otherwise stated. Tetrahydrofuran was purchased from commercial sources, degassed with argon, and dried prior to use. Anhydrous dioxane was purchased and degassed with nitrogen prior to use. N-bromosuccinimide (NBS) was recrystallized from hot water prior to use. Ni(dppp)Cl<sub>2</sub> was obtained from Accela and 3-bromofuran from ChemImpex. All other solvents and chemicals were used as received from commercial sources.

TMPMgCl·LiCl and *i*-PrMgCl·LiCl were titrated against benzoic acid using fluorene as the indicator. 2-(4-hexylthiophen-2-yl)-4,4,5,5-tetramethyl-1,3,2-dioxaborolane<sup>31</sup> and 5,5'-dibromo-3,3'-dihexyl-2,2'-bifuran (**2.2**)<sup>14b</sup> were prepared according to literature procedures. 2,5-dibromo-3-hexylfuran was prepared similarly to 2,5-dibromo-3-octylfuran.<sup>9c</sup> Poly(3-hexylthiophene) ( $M_n = 23,800$ ,  $D = 1.3$  determined versus polystyrene standards in CHCl<sub>3</sub>) used in the UV-Vis study was prepared according to a literature procedure.<sup>32</sup>

Polymer samples were precipitated with methanol and washed with both methanol and acetone before GPC analysis (Table 2.1). Polymer samples used for NMR analysis, UV-Vis spectroscopy,

atomic force microscopy and cyclic voltammetry were further purified by Soxhlet extraction using methanol, acetone, hexanes and chloroform. The chloroform extracts were used in the analysis.

**NMR Analysis.** All NMR experiments were collected at 300 K on a two-channel Bruker Avance<sup>TM</sup> III NMR instrument equipped with a Broad Band Inverse (BBI) probe, operating at 500 MHz for <sup>1</sup>H (126 MHz for <sup>13</sup>C). <sup>1</sup>H NMR spectra are referenced to residual protio solvent (7.26 for CHCl<sub>3</sub>) and <sup>13</sup>C NMR spectra are referenced to the solvent signal ( $\delta$  77.23 for CDCl<sub>3</sub>). Long-range COSY (cosylrqlf), edited-HSQC (hsqceedetgpsisp2.2) and echo/antiecho-HMBC with triple low-pass filter to remove one-bond correlations (hmbcetgpl3nd) are standard experiments from the Bruker pulseprogram library in TopSpin 3.1. The F2 proton-coupled HSQC was performed using the recently published Perfect-HSQC pulse program,<sup>33</sup> kindly provided by Dr. Teodor Parella (<http://sermn.uab.cat/2014/10/perfect-hsqc-experiments-pure-in-phase-spectra/>). The HMBC experiments were optimized for 4 and 8 Hz long-range proton-coupling (<sup>n</sup>J<sub>CH</sub>).

**Mass Spectrometry.** High-resolution mass spectrometry experiments (electrospray and electron impact) were performed in the School of Chemical Sciences Mass Spectrometry Laboratory at the University of Illinois, Urbana-Champaign.

**Gel-Permeation Chromatography.** GPC measurements were performed on a Waters Instrument equipped with a 717 plus autosampler, a Waters 2414 refractive index (RI) detector and two SDV columns (Porosity 1000 and 100000 Å; Polymer Standard Services) with THF as the eluent (flow rate 1 mL/min, 40 °C). A 10-point calibration based on polystyrene standards (Polystyrene, ReadyCal Kit, Polymer Standard Services) was applied for determination of molecular weights. All polymer aliquots subjected to GPC were prepared by quenching ~0.2 mL of the polymer solution with ~1.0 mL of 6 M methanolic HCl. The precipitate was filtered and washed with cold methanol. The resultant polymer was dissolved in ~1 mL of THF, filtered through a 0.22  $\mu$ m PTFE syringe filter, and analyzed.

**GC-MS Analysis.** GC-MS analysis was performed on a Hewlett-Packard Agilent 6890-5973 GC-MS workstation. The GC column was a Hewlett-Packard fused silica capillary column cross-linked with 5% phenylmethylsiloxane. Helium was used as the carrier gas. The following conditions were used for all GC-MS analyses: injector temperature, 250 °C; initial temperature, 70 °C; temperature ramp, 10 °C/min; final temperature, 280 °C. All polymer aliquots subjected to GC-MS were prepared by quenching ~0.2 mL of the polymer solution with ~1.0 mL of acidic methanol (HCl:methanol, 1:200 v/v). This was diluted with 1 mL of diethyl ether in a 20 mL scintillation vial. 0.2 mL of this resultant solution was filtered through a 0.22 µm PTFE syringe filter into a 2 mL vial and diethyl ether was added to fill the vial. Due to hydrolysis of the monomer in acidic methanol, conversion was calculated by integration of the nonadecane internal standard to protonated monomer.

**UV-Vis Spectroscopy.** UV-Vis spectra of all three polymers were recorded on a Varian Cary 5000 spectrophotometer. Solution measurements were conducted in THF at 0.005 mg/mL concentration. In the dark, under a dry nitrogen environment in a VAC glovebox, thin film samples were prepared from a spin-coating process. 22 × 22 mm glass cover slips were cleaned by spraying with fresh acetone, isopropanol and dried under a jet of filtered, dry N<sub>2</sub>. 5 mg/mL solutions of **HT-P3HF**, **HH-P3HF**, **P3HF-*a*-P3HT** and P3HT in dry toluene were heated to 80 °C in amber glass vials for 10 min, filtered through a 0.22 µm PTFE syringe filter using a glass syringe, and re-heated for 5 min prior to spin-casting from hot solutions. The spin-coating conditions consisted of three cycles, a 400 RPM spreading cycle for 5 s, a 1000 RPM main cycle for 30 s and a 2000 RPM wicking cycle for 15 s. The films were annealed at 150 °C for 1 h under N<sub>2</sub>.

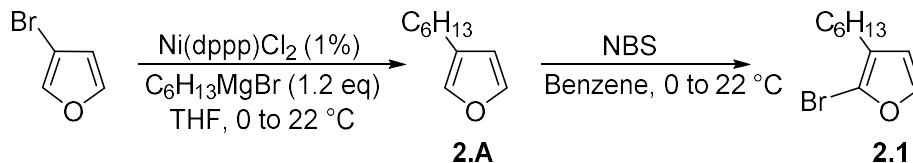
**Cyclic Voltammetry.** Electrochemical potentials were determined using a CH Instruments Model 600C Series Electrochemical Analyzer/Workstation and a three electrode system consisting of a 1 mm<sup>2</sup> platinum disk working electrode, a coiled platinum counter electrode, and a silver wire pseudo-reference electrode. Acetonitrile was degassed using Ar prior to use. A

solution of the polymer (0.5 mg/mL in toluene) was drop cast onto the working electrode. The electrode was immersed in acetonitrile with 0.1 M tetrabutylammonium hexafluorophosphate (Fluka, electrochemical grade) as the supporting electrolyte. Scans were collected under a constant argon purge at a scan rate of 100 mV/s. Ferrocene was used as an internal standard and measurements were referenced to  $\text{Fc}/\text{Fc}^+$ . Considering the oxidation potential of ferrocene is +0.40 V versus SCE in acetonitrile and the SCE electrode is -4.7 eV from vacuum,<sup>34</sup> the HOMO and LUMO energy levels were estimated according to:

$$E_{\text{HOMO}} = - (E_{[\text{onset, ox vs. Fc/Fc}^+]} + 5.1) \text{ (eV)} \quad E_{\text{LUMO}} = - (E_{[\text{onset, red vs. Fc/Fc}^+]} + 5.1) \text{ (eV)}.$$

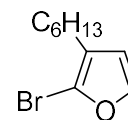
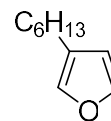
**Atomic Force Microscopy.** The **HT-P3HF** and **HH-P3HF** samples were prepared under a dry nitrogen environment in a glovebox, whereas the **P3HF-*a*-P3HT** sample was prepared under ambient conditions. All samples were prepared from 0.5 mg/mL solutions in dry toluene, on  $2 \times 2$  cm silicon wafers with native oxide. In the dark, the solutions were heated to 80 °C in amber glass vials for 30 min, filtered through a 0.22  $\mu\text{m}$  PTFE syringe filter using a glass syringe, and re-heated for 5 min prior to drop-casting hot solutions onto the wafers. The wafers were cleaned by spraying with fresh acetone and isopropanol and dried under a jet of filtered, dry nitrogen, followed by UV/Ozone treatment at 120 °C for 45 min, followed by an incubation period of 45 min until cooled to 42 °C (Novascan PSD-UVT). The wafers were then placed under vacuum (10 mTorr) for 90 min. The as-treated wafers were placed in a petri dish, completely covered with a minimum amount of solution, and allowed to dry slowly. The as-obtained films were imaged with a Bruker Dimension V hybrid AFM in tapping mode.

**Scheme 2.3.** Synthesis of Monomer **2.1**



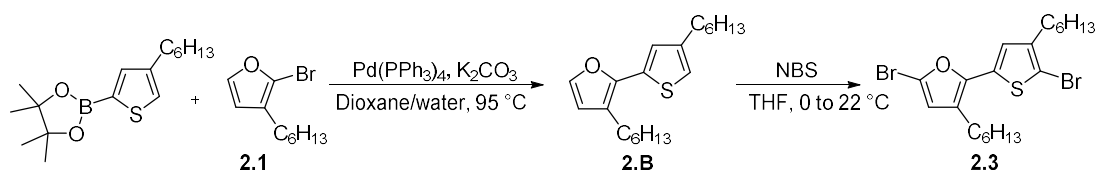
3-hexylfuran (**2.A**). An oven-dried 500 mL Schlenk flask was charged with 3-hexylfuran (15.0 g, 0.102 mol), Ni(dppp)Cl<sub>2</sub> (0.555 g, 1.02 mmol) and 200 mL of dry THF. The flask was cooled to 0 °C using an ice-water bath. Hexylmagnesium bromide solution (2.0 M, 61.2 mL, 0.122 mol) was added dropwise to the solution by syringe. After stirring at 0 °C for 0.5 h, the mixture was warmed to room temperature overnight. The reaction was carefully quenched with saturated NaHCO<sub>3</sub> solution at 0 °C and stirred for another 0.5 h before filtration through Celite. The solution was diluted with 150 mL of diethyl ether and transferred to a 500 mL separatory funnel. The organic layer was separated, washed with additional saturated NaHCO<sub>3</sub> solution, dried over Na<sub>2</sub>SO<sub>4</sub> and concentrated using rotary evaporation. The resultant yellow oily product was dissolved in 100 mL of hexanes and filtered through a basic alumina plug to remove residual catalyst and other impurities. The final product was purified by distillation at 55 °C under static vacuum and obtained as a clear liquid (6.24 g, 40%). Dodecane is typically observed as a byproduct in these reactions and co-distills with the desired product. It is present in the <sup>1</sup>H and <sup>13</sup>C NMR spectra and there is some overlap with the alkyl signals of the 3-hexylfuran. <sup>1</sup>H NMR (500 MHz, CDCl<sub>3</sub>) δ 7.34 (t, *J* = 1.7 Hz, 1H), 7.21 – 7.19 (m, 1H), 6.28 – 6.25 (m, 1H), 2.41 (t, *J* = 7.6 Hz, 2H), 1.59 – 1.50 (m, 2H), 1.38 – 1.28 (m, 6H), 0.91 – 0.86 (m, 3H). <sup>13</sup>C NMR (126 MHz, CDCl<sub>3</sub>) δ 142.8, 138.9, 125.6, 111.3, 31.9, 30.2, 29.2, 25.0, 22.8, 14.3. HR-EIMS (*m/z*): [M]<sup>+</sup> calculated for C<sub>10</sub>H<sub>16</sub>O: 152.1201; found 152.1202.

2-bromo-3-hexylfuran (**2.1**). In a 250 mL round-bottom flask, 3-hexylfuran (**2.A**) (6.24 g, 0.041 mol) was dissolved in 100 mL of benzene. The flask was cooled to 0 °C using an ice-water bath. NBS (7.44 g, 0.042 mol) was added into the solution in one portion and the reaction mixture was protected from ambient light. The mixture was slowly warmed to room temperature and stirred overnight. The reaction was quenched with saturated NaHCO<sub>3</sub> solution and transferred to a 500 mL of separatory funnel. The organic layer was separated and the aqueous layer was extracted two more times using diethyl ether (2 × 50 mL). The organic extracts



were combined and washed with saturated NaHCO<sub>3</sub> solution, dried over Na<sub>2</sub>SO<sub>4</sub> and concentrated using rotary evaporation. The resultant crude product was dissolved in 100 mL of hexanes and filtered through a basic alumina plug to remove succinimide. The crude product was purified by distillation at 43 °C (100 mtorr) and the final product was obtained as a clear liquid (5.10 g, 54%). <sup>1</sup>H NMR (500 MHz, CDCl<sub>3</sub>) δ 7.37 (d, *J* = 2.1 Hz, 1H), 6.29 (d, *J* = 2.0 Hz, 1H), 2.33 (t, *J* = 7.6 Hz, 2H), 1.57 – 1.48 (m, 2H), 1.36 – 1.27 (m, 6H), 0.92 – 0.84 (m, 3H). <sup>13</sup>C NMR (126 MHz, CDCl<sub>3</sub>) δ 143.7, 124.2, 119.9, 113.2, 31.8, 29.6, 29.0, 25.3, 22.8, 14.3. HR-EIMS (*m/z*): [M]<sup>+</sup> calculated for C<sub>10</sub>H<sub>15</sub>BrO: 230.0306; found 230.0313.

**Scheme 2.4.** Synthesis of Monomer **2.3**



*3-hexyl-2-(4-hexylthiophen-2-yl)furan (2.B)*. In a N<sub>2</sub> filled glovebox, a 20 mL scintillation vial was charged with compound **2.1** (1.71 g, 7.40 mmol),

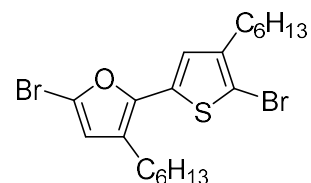
2-(4-hexylthiophen-2-yl)-4,4,5,5-tetramethyl-1,3,2-dioxaborolane (2.17 g,

7.40 mmol), Pd(PPh<sub>3</sub>)<sub>4</sub> (0.43 g, 0.37 mmol), K<sub>2</sub>CO<sub>3</sub> (3.07 g, 22 mmol) and 10 mL of dioxane. The vial was removed from the glovebox and 4 mL of water was added into the vial by syringe. The vial was immersed in an oil bath at 95 °C and the solution was stirred for 36 h before cooling to room temperature. The mixture was transferred to a separatory funnel, diluted with 100 mL of diethyl ether and washed with saturated NaHCO<sub>3</sub> solution. The organic layer was dried over Na<sub>2</sub>SO<sub>4</sub> and concentrated using rotary evaporation. The crude material was purified using column chromatography on silica gel using hexanes (*R<sub>f</sub>* ~0.7) to afford the final product as a clear liquid

(1.89 g, 80%). <sup>1</sup>H NMR (500 MHz, CDCl<sub>3</sub>) δ 7.30 (d, *J* = 1.8 Hz, 1H), 7.05 (d, *J* = 1.4 Hz, 1H), 6.83 (q, *J* = 1.1 Hz, 1H), 6.33 (d, *J* = 1.8 Hz, 1H), 2.65 – 2.57 (m, 4H), 1.68 – 1.57 (m, 4H), 1.45 – 1.24 (m, 12H), 0.93 – 0.85 (m, 6H). <sup>13</sup>C NMR (126 MHz, CDCl<sub>3</sub>) δ 145.0, 143.7, 140.8, 133.6, 124.3, 121.3, 118.7, 113.5, 31.9, 30.7, 30.6, 29.9, 29.4, 29.2, 25.9, 22.9, 14.32 and 14.30 (two

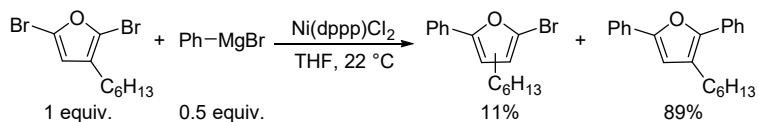
overlapping signals). Note: only 10 of the 12 possible signals from the hexyl chains are visible due to similarities between chemical environments. HRMS (ESI-TOF) ( $m/z$ ):  $[M + H]^+$  calculated for  $C_{20}H_{31}OS$ : 319.2096; found 319.2095.

*5-bromo-2-(5-bromo-4-hexylthiophen-2-yl)-3-hexylfuran (2.3)*. In a 250 mL round-bottom flask, compound **2.B** (1.70 g, 5.34 mmol) was dissolved in 100 mL of THF. The flask was cooled to 0 °C using an



ice-water bath, and NBS (1.94 g, 10.9 mmol) was slowly added to the solution under protection from ambient light. The reaction mixture was slowly warmed to room temperature and stirred overnight. The mixture was quenched with saturated  $NaHCO_3$  solution and transferred to a 500 mL of separatory funnel. The organic layer was separated and the aqueous layer was extracted two more times using diethyl ether ( $2 \times 50$  mL). The organic extracts were combined and washed with saturated  $NaHCO_3$  solution, dried over  $Na_2SO_4$  and concentrated using rotary evaporation. The crude material was purified using column chromatography on basic alumina using hexanes ( $R_f \sim 0.8$ ) to afford the final product as a clear yellow liquid (1.69 g, 66%).  $^1H$  NMR (500 MHz,  $CDCl_3$ )  $\delta$  6.89 (br s, 1H), 6.24 (br s, 1H), 2.59 – 2.48 (m, 4H), 1.64 – 1.50 (m, 4H), 1.41 – 1.23 (m, 12H), 0.93 – 0.82 (m, 6H).  $^{13}C$  NMR (126 MHz,  $CDCl_3$ )  $\delta$  146.3, 142.6, 132.0, 124.5, 124.2, 120.9, 115.1, 108.4, 31.8, 29.9, 29.73 and 29.72 (two overlapping signals), 29.3, 29.1, 25.8, 22.82 and 22.81 (2 overlapping signals), 14.31 and 14.29 (2 overlapping signals). Note: only 11 of the 12 possible signals from the hexyl chains are visible due to similarities between chemical environments. HRMS (ESI-TOF) ( $m/z$ ):  $[M + H]^+$  calculated for  $C_{20}H_{29}Br_2OS$ : 475.0306; found 475.0304.

### Model Compound Reaction

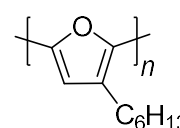


In a  $N_2$  filled glovebox, a 20 mL vial was charged with 2,5-dibromo-3-hexylfuran (1.0 equiv. 0.25 g, 0.81 mmol),  $Ni(dppp)Cl_2$  (2 mol %, 0.0087 g, 0.016 mmol), nonadecane as the internal

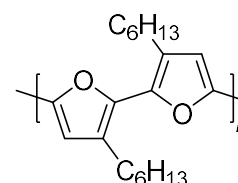
standard (0.206 g, 0.77 mmol) and 5 mL of THF. After 30 s of stirring inside the glovebox, an aliquot was withdrawn from the solution and subjected to GC-MS analysis to determine the initial ratios of starting material to the internal standard. Phenylmagnesium bromide (1.6 M, 0.25 mL, 0.4 mmol) was then added to the vial dropwise at room temperature. After stirring for 1 h, an aliquot was removed and GC-MS analysis was performed to determine the relative ratio of 2,5-diphenyl-3-hexylfuran and the bromophenylfuran isomers.

### General Polymerization Conditions

**HT-P3HF.** The polymerization reaction was conducted under a N<sub>2</sub> atmosphere. A 100 mL Schlenk flask was charged with compound **2.1** (0.28 g, 1.21 mmol) and 40 mL of THF. TMPMgCl·LiCl solution (0.76 M, 1.6 mL, 1.22 mmol) was slowly added to the reaction solution at room temperature. The flask was then immersed in an oil bath at 40 °C. After stirring at 40 °C for 1 h, a calculated amount of Ni(dppp)Cl<sub>2</sub> (20 or 10 mol %) was quickly added into the solution in one portion. The polymerization was stirred at 40 °C for 20 min and subsequently quenched with 6 M methanolic HCl. 200 mL of methanol was then added to the red polymer suspension along with dimethylglyoxime to scavenge the nickel catalyst. The resultant mixture was stirred at room temperature for 1 h under protection from ambient light. The final polymer was collected by centrifugation, dried in *vacuo* and stored in the glovebox as a red powder. Yield: Entry 1 (0.10 g, 55%), Entry 2 (0.13 g, 73%) from Table 2.1. Note: The integrations include the small aromatic signals observed downfield from the major signal at 6.47 ppm. <sup>1</sup>H NMR (500 MHz, CDCl<sub>3</sub>) δ 6.47 (s, 1H), 2.90 – 2.75 (m, 2H), 1.79 – 1.65 (m, 2H), 1.52 – 1.43 (m, 2H), 1.43 – 1.22 (m, 4H), 0.97 – 0.81 (m, 3H). <sup>13</sup>C NMR (126 MHz, CDCl<sub>3</sub>) δ 146.0, 140.9, 124.5, 109.0, 32.0, 30.3, 29.5, 25.6, 22.9, 14.4.

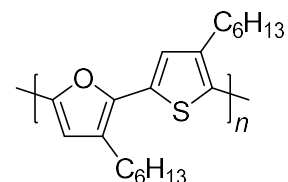


**HH-P3HF.** The polymerization reaction was conducted under a N<sub>2</sub> atmosphere. A 100 mL Schlenk flask was charged with compound **2.2**



(0.57 g, 1.24 mmol) and 40 mL of THF. *i*-PrMgCl·LiCl solution (1.3 M, 0.9 mL, 1.17 mmol) was slowly added to the reaction at room temperature. The flask was then immersed in an oil bath at 40 °C. After stirring at 40 °C for 1 h, an aliquot was withdrawn and subjected to GC-MS analysis to determine the monomer content (84% active monomer, 11% starting material, 5% bismetallated compound). Ni(dppp)Cl<sub>2</sub> (66.7 mg, 0.12 mmol) was then quickly added into the solution in one portion. The polymerization was stirred at 40 °C for 20 min and subsequently quenched with 6 M methanolic HCl. 200 mL of methanol was then added to the red polymer suspension along with dimethylglyoxime to scavenge the nickel catalyst. The resultant mixture was stirred at room temperature for 1 h under protection from ambient light. The final polymer was collected by centrifuge, dried in *vacuo* and stored in the glovebox as a red powder. Yield: Entry 3 (0.16 g, 42%) from Table 2.1. <sup>1</sup>H NMR (500 MHz, CDCl<sub>3</sub>) δ 6.52 (s, 2H), 2.85 – 2.70 (m, 4H), 1.75 – 1.65 (m, 4H), 1.50 – 1.40 (m, 4H), 1.40 – 1.21 (m, 8H), 0.95 – 0.80 (m, 6H). <sup>13</sup>C NMR (126 MHz, CDCl<sub>3</sub>) δ 145.0, 142.0, 124.9, 108.8, 32.0, 30.5, 29.5, 25.6, 23.0, 14.3.

**P3HF-*a*-P3HT.** The polymerization reaction was conducted under a N<sub>2</sub> atmosphere. A 50 mL Schlenk flask was charged with compound **2.3** (0.29 g, 0.61 mmol) and 20 mL of THF. The flask was cooled to 0



°C, and *i*-PrMgCl·LiCl solution (1.3 M, 0.46 mL, 0.60 mmol) was slowly added to the reaction mixture. After stirring at 0 °C for 15 min, the flask was immersed in an oil bath at 35 °C and stirred for 0.5 h. An aliquot was then withdrawn and subjected to GC-MS analysis to determine the content of active monomer (70% major, 17% minor, 11% starting material and 2% bismetallated compound). The mixture was cooled to room temperature and stirred for another 0.5 h. A calculated amount of Ni(dppp)Cl<sub>2</sub> (5, 2.5 and 1.25 mol %) was then quickly added into the solution in one portion. The polymerization was stirred at 22 °C for 30 to 40 min then quenched with 6 M methanolic HCl. 200 mL of methanol was then added to the red polymer suspension along with dimethylglyoxime to scavenge the nickel catalyst. The resultant mixture was stirred at room temperature for 1 h under protection from ambient light. The final polymer

was collected by suction filtration, washed with methanol and acetone, dried in *vacuo* and stored in the glovebox as a red powder. Yield: Entry 4 (0.09 g, 46%), Entry 5 (0.11 g, 57%) and Entry 6 (0.07 g, 35%) from Table 2.1.  $^1\text{H}$  NMR (500 MHz,  $\text{CDCl}_3$ )  $\delta$  7.06 (br s, 1H), 6.42 (br s, 1H), 2.97 – 2.78 (m, 2H), 2.73 – 2.63 (m, 2H), 1.81 – 1.65 (m, 4H), 1.58 – 1.43 (m, 4H), 1.42 – 1.20 (m, 8H), 0.96 – 0.80 (m, 6H).  $^{13}\text{C}$  NMR (126 MHz,  $\text{CDCl}_3$ )  $\delta$  147.7, 143.9, 140.0, 131.0, 125.8, 125.7, 124.3, 110.6, 32.1, 32.0, 30.5, 30.2, 29.8, 29.4, 26.2, 23.0, 22.9, 14.4. Note: only 10 of the 12 possible signals from the hexyl chains are visible due to similarities between chemical environments.

### Procedure for obtaining $M_n$ versus conversion plot

The polymerization reaction was conducted under a  $\text{N}_2$  atmosphere. A 50 mL Schlenk flask was charged with compound **2.3** (0.29 g, 0.61 mmol), nonadecane as internal standard and 20 mL of THF. The flask was cooled to 0 °C using an ice-water bath, and *i*-PrMgCl·LiCl solution (1.3 M, 0.46 mL, 0.60 mmol) was slowly added to the reaction mixture. After stirring at 0 °C for 15 min, the flask was immersed into an oil bath at 35 °C and stirred for 0.5 h. An aliquot was then withdrawn and subjected to GC-MS analysis to determine the initial ratio of monomer to the internal standard. The mixture was cooled to room temperature and stirred for another 0.5 h. Ni(dppp)Cl<sub>2</sub> (4.2 mg, 0.0077 mmol) was then quickly added into the solution in one portion. Aliquots (~0.4 mL) were withdrawn after 0.5, 2, 5, 10, 20 and 40 min to determine the monomer conversion (major + minor using GC-MS) and polymer molecular weight (GPC). All results are summarized in Table 2.2 below.

**Table 2.2.** Data used to construct  $M_n$  versus total monomer conversion plot.

Time (min)	Total Monomer Conv.	Molecular Weight ( $M_n$ )	Dispersity
0.5	16	3300	1.32
2	25	6500	1.50
5	52	9200	1.43
10	67	10600	1.41
20	73	11700	1.40
40	79	11900	1.41

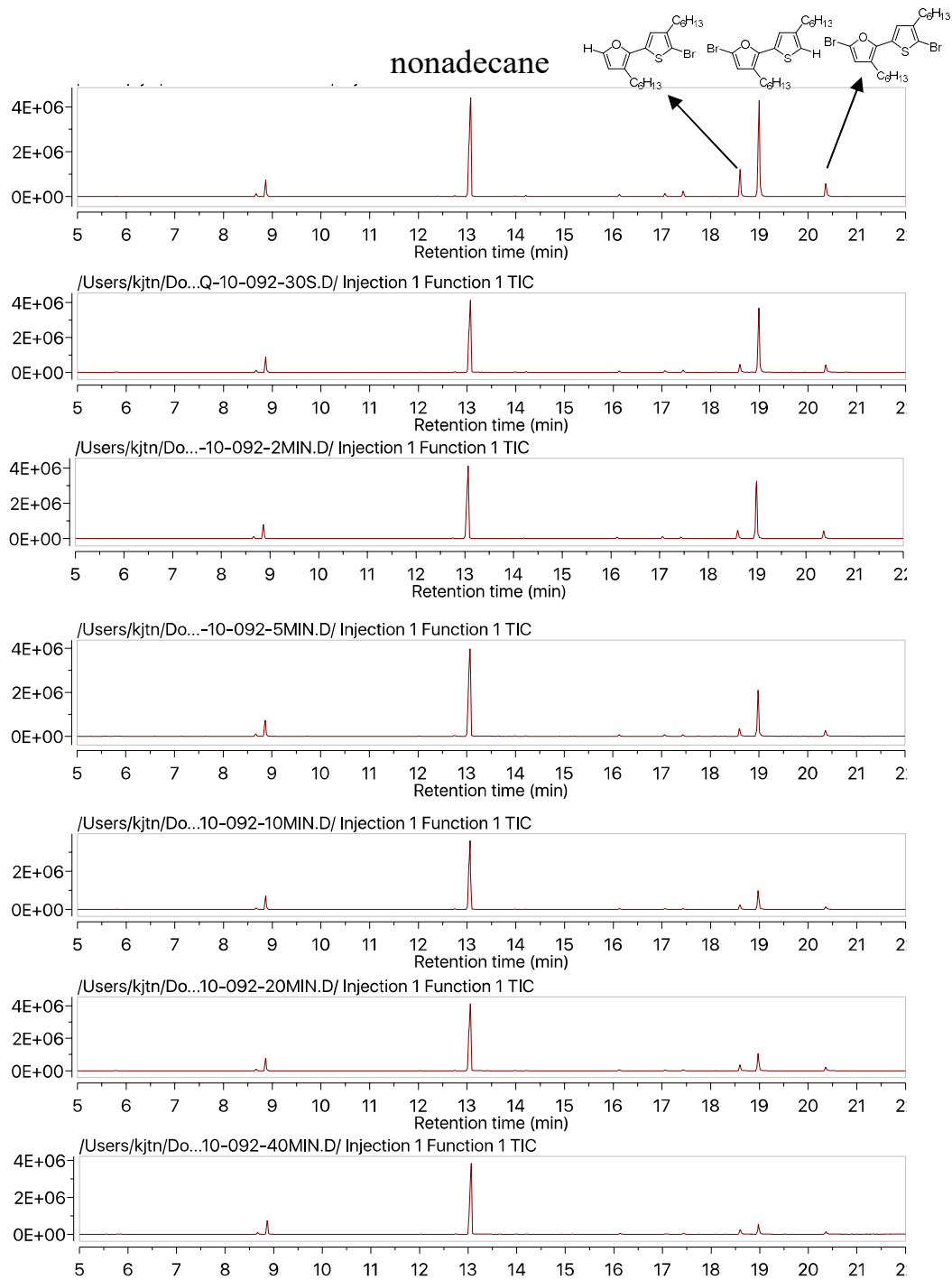


**Figure 2.7.** Stack Plot of GC-MS Traces from the  $M_n$  versus conversion plot. The signal at ~13 min corresponds to nonadecane which was used to determine conversion. The two isomers correspond to H-terminated monomer and are observed near 19 min. The dibromo starting material **2.3** is observed at ~21 min.

**Table 2.3.** Summary of optical and electrochemical properties of HT-P3HF, HH-P3HF and P3HF-*a*-P3HT.

	$\lambda_{\max}$ (nm) THF	$\lambda_{\max}$ (nm) film	$E_g^{\text{opt}}$ (eV) <sup>a</sup>	$E_{\text{ox}}$ (eV) <sup>b</sup>	$E_{\text{red}}$ (eV) <sup>b</sup>	HOMO AVG (eV) <sup>c</sup>	LUMO AVG (eV)	$E_g^{\text{CV}}$ (eV)
<b>HT-P3HF</b>	465	489	2.19	-0.013 +/- 0.037	-	-5.09	-2.90 <sup>d</sup>	–
<b>HH-P3HF</b>	458	486	2.19	-0.039 +/- 0.030	-	-5.06	-2.87 <sup>d</sup>	–
<b>P3HF-<i>a</i>-P3HT</b>	476	531	2.00	0.090 +/- 0.034	-1.93 +/- 0.030	-5.19	-3.17 <sup>c</sup>	2.02

<sup>a</sup>Determined by the onset of absorption edge (UV-Vis). <sup>b</sup>Determined by the average of initial onset and derivative onsets of oxidation and reduction potentials by cyclic voltammetry.

<sup>c</sup>Estimated by the average onset of oxidation and reduction potentials by cyclic voltammetry.

<sup>d</sup>Determined from the optical bandgap.

## 2.5 References

- (1) *Handbook of Thiophene-Based Materials*; Perepichka, I. F.; Perepichka, D. F., Eds.; John Wiley & Sons, Ltd: Chichester, UK, **2009**.
- (2) Salleo, A.; Kline, R. J.; DeLongchamp, D. M.; Chabinyc, M. L. *Adv. Mater.* **2010**, *22*, 3812-3838.
- (3) Zade, S. S.; Bendikov, M. *Chem.-Eur. J.* **2007**, *13*, 3688-3700.
- (4) McCullough, R. D.; Lowe, R. D. *J. Chem. Soc., Chem. Commun.* **1992**, 70-72.
- (5) Ewbank, P. C.; Stefan, M. C.; Sauvé, G.; McCullough, R. D. Synthesis, Characterization and Properties of Regioregular Polythiophene-Based Materials. In *Handbook of Thiophene-Based Materials*; Perepichka, I. F., Perepichka, D. F., Eds.; John Wiley & Sons, Ltd: Chichester, UK, 2009, pp 157-217.
- (6) (a) Sheina, E. E.; Liu, J.; Iovu, M. C.; Laird, D. W.; McCullough, R. D. *Macromolecules* **2004**, *37*, 3526-3528. (b) Yokoyama, A.; Miyakoshi, R.; Yokozawa, T. *Macromolecules* **2004**, *37*, 1169-1171. (c) Miyakoshi, R.; Yokoyama, A.; Yokozawa, T. *Macromol. Rapid Commun.* **2004**, *25*, 1663-1666.
- (7) (a) Bryan, Z. J.; McNeil, A. J. *Macromolecules* **2013**, *46*, 8395-8405. (b) Ohta, Y.; Yokozawa, T. *Adv. Polym. Sci.* **2013**, *262*, 191-238. (c) Yokozawa, T.; Nanashima, Y.; Kohno, H.; Suzuki, R.; Nojima, M.; Ohta, Y. *Pure Appl. Chem.* **2013**, *85*, 573-587. (d) Okamoto, K.; Luscombe, C. K. *Polym. Chem.* **2011**, *2*, 2424-2434. (e) Kiriya, A.; Senkovskyy, V.; Sommer, M. *Macromol. Rapid Commun.* **2011**, *32*, 1503-1517.
- (8) (a) Verswyvel, M.; Steverlynck, J.; Mohamed, S. H.; Trabelsi, M.; Champagne, B.; Koeckelberghs, G. *Macromolecules* **2014**, *47*, 4668-4675. (b) Yan, H.; Hollinger, J.; Bridges, C. R.; McKeown, G. R.; Al-Faouri, T.; Seferos, D. S. *Chem. Mater.* **2014**, *26*, 4605-4611. (c) Hollinger, J.; Seferos, D. S. *Macromolecules* **2014**, *47*, 5002-5009. (d) Palermo, E. F.; McNeil, A. J. *Macromolecules* **2012**, *45*, 5948-5955. (e) Heeney, M.; Zhang, W.; Crouch, D. J.; Chabinyc, M.

- L.; Gordeyev, S.; Hamilton, R.; Higgins, S. J.; McCulloch, I.; Skabara, P. J.; Sparrowe, D.; Tierney, S. *Chem. Commun.* **2007**, 5061-5063.
- (9) (a) Jeffries-EL, M.; Kobilka, B. M.; Hale, B. J. *Macromolecules* **2014**, *47*, 7253-7271. (b) Streifel, B. C. and Tovar, J. D. 2012.  $\pi$ -Conjugated Furan-Based Polymers. Encyclopedia Of Polymer Science and Technology. (c) Politis, J. K.; Nemes, J. C.; Curtis, M. D. *J. Am. Chem. Soc.* **2001**, *123*, 2537-2547.
- (10) (a) Po, R.; Bernardi, A.; Calabrese, A.; Carbonera, C.; Corso, G.; Pellegrino, A. *Energy Environ. Sci.* **2014**, *7*, 925-943. (b) Burke, D. J.; Lipomi, D. J. *Energy Environ. Sci.* **2013**, *6*, 2053-2066. (c) Lizin, S.; Van Passel, S.; De Schepper, E.; Maes, W.; Lutsen, L.; Manca, J.; Vanderzande, D. *Energy Environ. Sci.* **2013**, *6*, 3136-3149.
- (11) (a) *Monomers, Polymers and Composites from Renewable Resources*; Belgacem, M. N.; Gandini, A., Eds.; Elsevier: Amsterdam, **2008**. (b) Gandini, A. *Macromolecules* **2008**, *41*, 9491-9504.
- (12) Distefano, G.; Jones, D.; Guerra, M.; Favaretto, L.; Modelli, A.; Mengoli, G. *J. Phys. Chem.* **1991**, *95*, 9746-9753.
- (13) Gidron, O.; Diskin-Posner, Y.; Bendikov, M. *J. Am. Chem. Soc.* **2010**, *132*, 2148-2150.
- (14) (a) Sheberla, D.; Patra, S.; Wijsboom, Y. H.; Sharma, S.; Sheynin, Y.; Haj-Yahia, A.-E.; Barak, A. H.; Gidron, O.; Bendikov, M. *Chem. Sci.* **2015**, *6*, 360-371. (b) Jin, X.-H.; Sheberla, D.; Shimon, L. J. W.; Bendikov, M. *J. Am. Chem. Soc.* **2014**, *136*, 2592-2601. (c) Gidron, O.; Bendikov, M. *Angew. Chem. Int. Ed.* **2014**, *53*, 2546-2555.
- (15) (a) Sharma, S.; Zamoshchik, N.; Bendikov, M. *Isr. J. Chem* **2014**, *54*, 712-722. (b) Sharma, S.; Bendikov, M. *Chem.-Eur. J.* **2013**, *19*, 13127-13139.
- (16) Joule, J. A.; Mills, K. *Heterocyclic chemistry*; 5th ed.; Wiley: Hoboken, N.J., 2009.
- (17) (a) Tamba, S.; Mitsuda, S.; Tanaka, F.; Sugie, A.; Mori, A. *Organometallics* **2012**, *31*, 2263-2267. (b) Tamba, S.; Shono, K.; Sugie, A.; Mori, A. *J. Am. Chem. Soc.* **2011**, *133*, 9700-9703. (c)

- McCullough, R. D.; Lowe, R. D.; Jayaraman, M.; Anderson, D. L. *J. Org. Chem.* **1993**, *58*, 904-912.
- (18) Osaka, I.; McCullough, R. D. *Acc. Chem. Res.* **2008**, *41*, 1202-1214.
- (19) (a) Loewe, R. S.; Khersonsky, S. M.; McCullough, R. D. *Adv. Mater.* **1999**, *11*, 250-253. (b) Loewe, R. S.; Ewbank, P. C.; Liu, J.; Zhai, L.; McCullough, R. D. *Macromolecules* **2001**, *34*, 4324-4333.
- (20) Iovu, M. C.; Sheina, E. E.; Gil, R. R.; McCullough, R. D. *Macromolecules* **2005**, *38*, 8649-8656.
- (21) Shi, L.; Chu, Y.; Knochel, P.; Mayr, H. *Org. Lett.* **2009**, *11*, 3502-3505.
- (22) (a) Boyd, S. D.; Jen, A. K.-Y.; Luscombe, C. K. *Macromolecules* **2009**, *42*, 9387-9389. (b) Tkachov, R.; Senkovskyy, V.; Komber, H.; Sommer, J.-U.; Kiriy, A. *J. Am. Chem. Soc.* **2010**, *132*, 7803-7810.
- (23) Wu, S.; Huang, L.; Tian, H.; Geng, Y.; Wang, F. *Macromolecules* **2011**, *44*, 7558-7567.
- (24) Barbarella, G.; Bongini, A.; Zambianchi, M. *Macromolecules* **1994**, *27*, 3039-3045.
- (25) Kohn, P.; Huettner, S.; Komber, H.; Senkovskyy, V.; Tkachov, R.; Kiriy, A.; Friend, R. H.; Steiner, U.; Huck, W. T. S.; Sommer, J.-U.; Sommer, M. *J. Am. Chem. Soc.* **2012**, *134*, 4790-4805.
- (26) *rr*-P3HT was prepared according to: Qiu, Y.; Mohin, J.; Tsai, C.-H.; Tristram-Nagle, S.; Gil, R. R.; Kowalewski, T.; Noonan, K. J. T. *Macromol. Rapid Commun.* **2015**, *36*, 840-844.
- (27) Luzio, A.; Fazzi, D.; Nuebling, F.; Matsidik, R.; Straub, A.; Komber, H.; Giussani, E.; Watkins, S. E.; Barbatti, M.; Thiel, W.; Gann, E.; Thomsen, L.; McNeill, C. R.; Caironi, M.; Sommer, M. *Chem. Mater.* **2014**, *26*, 6233-6240.
- (28) Di Maria, F.; Gazzano, M.; Zanelli, A.; Gigli, G.; Loiudice, A.; Rizzo, A.; Biasiucci, M.; Salatelli, E.; D' Angelo, P.; Barbarella, G. *Macromolecules* **2012**, *45*, 8284-8291.

- (29) Zhang, R.; Li, B.; Iovu, M. C.; Jeffries-EL, M.; Sauv e, G.; Cooper, J.; Jia, S.; Tristram-Nagle, S.; Smilgies, D. M.; Lambeth, D. N.; McCullough, R. D.; Kowalewski, T. *J. Am. Chem. Soc.* **2006**, *128*, 3480-3481.
- (30) (a) Liu, J.; Loewe, R. S.; McCullough, R. D. *Macromolecules* **1999**, *32*, 5777-5785. (b) Wong, M.; Hollinger, J.; Kozycz, L. M.; McCormick, T. M.; Lu, Y.; Burns, D. C.; Seferos, D. S. *ACS Macro Lett.* **2012**, *1*, 1266-1269.
- (31) Li, J. C.; Lee, S. H.; Hahn, Y. B.; Kim, K. J.; Zong, K.; Lee, Y. S. *Synth. Met.* **2008**, *158*, 150-156.
- (32) Qiu, Y.; Mohin, J.; Tsai, C.-H.; Tristram-Nagle, S.; Gil, R. R.; Kowalewski, T.; Noonan, K. J. T. *Macromol. Rapid Commun.* **2015**, *36*, 840-844.
- (33) Casta nar, L.; Sistar e, E.; Virgili, A.; Williamson, R. T.; Parella, T. *Magn. Reson. Chem.* **2015**, *53*, 115-119.
- (34) *Electrochemical Methods: Fundamentals and Applications*; Bard, A. J.; Faulkner, L. R., eds.; John Wiley & Sons, Inc.: New York, USA, **2001**.

## CHAPTER 3

### Stille Catalyst-Transfer Polycondensation using Pd-PEPPSI-IPr for High Molecular Weight Regioregular Poly(3-hexylthiophene)

#### 3.1 Introduction

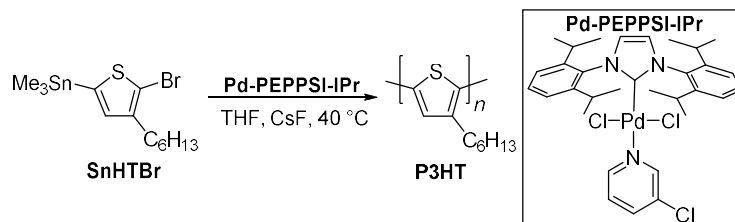
Condensation polymerization, which is commonly employed to prepare  $\pi$ -conjugated materials for organic electronics, proceeds by a step-growth mechanism making it difficult to tailor molecular weight and dispersity. The development of catalyst-transfer polycondensation (CTP) in 2004<sup>1</sup> has enabled the synthesis of precision  $\pi$ -conjugated materials through a chain-growth polymerization process.<sup>2</sup> Selection of a suitable monomer and catalyst will result in controlled molecular weights and low dispersity, typically using Kumada and Suzuki-Miyaura cross-coupling protocols.<sup>2</sup> However, the number of conjugated building blocks which undergo CTP is still limited, which can be improved through enhanced mechanistic understanding of the reaction, catalyst development and alternative transmetallating agents.<sup>2a</sup>

Stille coupling is one of the most versatile methods for preparing highly functional semiconducting polymers via step-growth polycondensation of A-A B-B monomers.<sup>3</sup> Surprisingly, exploration of chain-growth polymerization with tin-based transmetallating agents remains limited.<sup>4</sup> Stille coupling should provide access to chain-growth polymerization of conjugated monomers that may be sensitive to nucleophilic Grignard reagents (n-type monomers).<sup>5</sup> Herein, a commercially available palladium N-heterocyclic carbene (NHC) complex (**Pd-PEPPSI-IPr**) was used to induce Stille CTP of the A-B monomer **SnHTBr** (Scheme 3.1). The resultant poly(3-hexylthiophene) (**P3HT**) was regioregular and the molecular weight could be controlled by varying the catalyst concentration.

While Ni(dppe)Cl<sub>2</sub> and Ni(dppp)Cl<sub>2</sub> are the most common precatalysts used for CTP (Kumada and Negishi coupling),<sup>2</sup> palladium systems have recently been employed to broaden the scope of cross-coupling strategies available.<sup>5d,6</sup> The palladium-based CTP catalysts are bound to bulky, electron-rich phosphine ligands such as P<sup>t</sup>Bu<sub>3</sub> or RuPhos. The ligand scope was expanded

to  $\sigma$ -donating NHCs when **Pd-PEPPSI-IPr**<sup>7</sup> was used to initiate Kumada and Suzuki CTP of several aryl monomers.<sup>8</sup> The successful application of carbene-based catalysts in CTP as well as their widespread use in cross-coupling,<sup>9</sup> led us to explore Pd-NHCs in a Stille chain-growth process of the benchmark material, P3HT.<sup>10</sup>

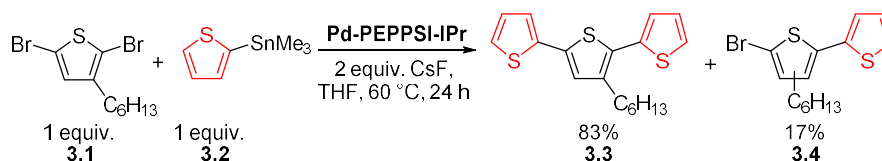
**Scheme 3.1. Synthesis of poly(3-hexylthiophene) using a Pd-NHC catalyst.**



**3.2 Results and Discussion**

Mechanistically, chain-growth polycondensation proceeds through a repeating oxidative addition (OA), transmetalation and reductive elimination (RE) sequence. The RE in each catalytic cycle is followed by formation of a metal-polymer  $\pi$ -complex, resulting in intramolecular OA at the polymer chain-end. Model compound reactions can be used to provide evidence of an intramolecular OA event.<sup>1a,11</sup> Herein, a model compound experiment was conducted by combining one equivalent of compounds **3.1** and **3.2** in THF at 60 °C with 2 mol % of **Pd-PEPPSI-IPr** and CsF as an additive (Scheme 3.2). After 24 h, **3.2** was nearly completely consumed and terthiophene **3.3** and bithiophene **3.4** were formed in a 83:17 ratio (Supporting Information). Preferential double substitution (e.g. **3.3**) is indicative of intramolecular OA and suggests Pd-PEPPSI is a suitable catalyst for Stille CTP of thiophene.

**Scheme 3.2. Investigation of preferential double substitution using the PEPPSI catalyst system. The percent yields listed for 3.3 and 3.4 are reported with respect to compound 3.2.**



The polymerization of **SnHTBr** (Scheme 3.1) was explored using similar conditions to the model reaction. Monomer consumption proceeded smoothly at 40 °C and was nearly complete within 120 min using 2 mol % catalyst. The reaction mixture was quenched (90% conversion – **P3HT<sub>50</sub>**) using 6 M methanolic HCl solution and the precipitated polymer was washed with cold methanol, hexanes and acetone to remove any remaining monomer and short oligomers. A series of polymerizations were conducted to ensure molecular weight control could be obtained by altering the [monomer]/[catalyst] ratio (Table 3.1 and Figure 3.1). All polymerizations were stopped between 70 – 90% monomer conversion to prevent any chain termination events since McNeil and coworkers have observed catalyst stability issues once the monomer is fully consumed.<sup>8a</sup>

**Table 3.1. Comparison of P3HT samples prepared by adjusting [monomer]/[catalyst] ratio.**

Sample <sup>a</sup>	Time (min)	Conv. <sup>b</sup> (%)	$M_n$ (GPC) <sup>c</sup>	$\bar{D}$	$M_n$ (NMR) <sup>d</sup>
<b>P3HT<sub>25</sub></b>	80	73	7000	1.14	5100
<b>P3HT<sub>33</sub></b>	110	89	9500	1.18	6600
<b>P3HT<sub>50</sub></b>	120	90	14000	1.24	8600
<b>P3HT<sub>100</sub></b>	125	84	23800	1.30	14200
<b>P3HT<sub>200</sub></b>	140	81	45600	1.43	27300
<b>P3HT<sub>400</sub></b>	150	74	73300	1.53	45000

<sup>a</sup>Subscripted sample numbers correspond to the [monomer]/[catalyst] ratio used in the polymerization. <sup>b</sup>Conversion was determined by GC-MS using nonadecane as the internal standard, yields are provided in the supporting information. <sup>c</sup>GPC was recorded at 40 °C in chloroform versus polystyrene standards. <sup>d</sup> $M_n$  was calculated based on end-group analysis using <sup>1</sup>H NMR spectroscopy.

Gel permeation chromatography (GPC) of the **P3HT<sub>50</sub>** relative to polystyrene in chloroform indicated a unimodal distribution ( $M_n = 14,000$ ) with a fairly narrow dispersity ( $\bar{D} = 1.24$ ). This narrow dispersity is indicative of a chain-growth mechanism and when degrees of polymerization (DP) above 100 were targeted, higher molecular weight distributions (1.4-1.5) were obtained (Table 3.1). A termination process is likely occurring as the polymerization proceeds to higher molecular weights.

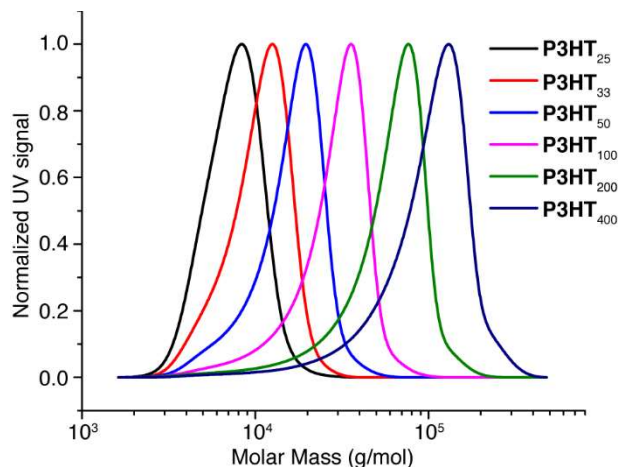


**Figure 3.1.** GPC traces of P3HT samples obtained by varying the [monomer]/[catalyst] ratio.

To confirm that the catalyst does not leave the growing polymer chain, a separate experiment was conducted using 4 mol % catalyst. An aliquot was removed from the reaction mixture at 55% conversion, quenched and washed with cold solvents (methanol, diethyl ether, hexanes and acetone). Analysis using MALDI-TOF mass spectrometry revealed the primary distribution of end-groups to be H/Br (Figure 3.2), which is consistent with a chain-growth process and the previously reported Kumada CTP.<sup>8a</sup>

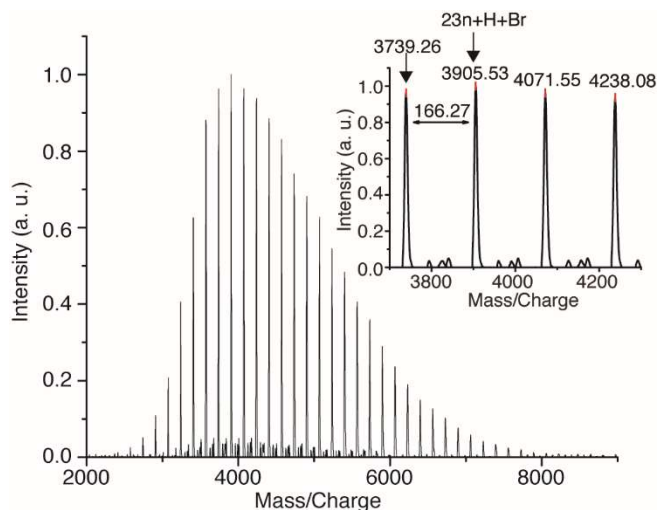


**Figure 3.2.** MALDI-TOF mass spectrum of SnHTBr polymerization using 4 mol % catalyst.

The <sup>1</sup>H NMR spectra obtained for the different samples of P3HT (Table 3.1) were compared to previous reports<sup>12</sup> and end-group assignments were confirmed using 2D correlation

NMR experiments (long-range COSY, HSQC and HMBC). The NMR analysis revealed several important features of the polymerization including highly regioregular (head to tail - HT) enchainment of the thiophene monomer (HT-HT triads in Figure 3.3).<sup>12c</sup> A tail to tail regioerror is present within the polymer chain (TT-HT triad) which arises from precatalyst initiation similar to the Grignard metathesis reaction.<sup>12b</sup> A head to head regioerror is not present in the backbone since neither the HT-HH nor the TT-HH triad is observed.

Interestingly, the TT defect from precatalyst initiation is primarily located within the polymer backbone rather than at the chain-end. The methylene signal of a Br terminated TT end-group should appear as a triplet at 2.54 ppm but this signal is almost unobservable in our <sup>1</sup>H NMR spectrum. Instead, HT end-groups produce two triplets corresponding to the methylene signals observed at 2.62 and 2.57 ppm (Signals **B** and **D** in Figure 3.3).<sup>12d</sup> This result confirms that chain-growth is not proceeding unidirectionally and the Pd-NHC catalyst is capable of “ring-walking” similar to the nickel systems.<sup>13</sup> Both signal **A** (6.90 ppm) and signal **C** (6.83 ppm) correspond to the protons of a regioregular HT end-group. All assigned signals agree with previous reports for P3HT.<sup>12a,12d,13</sup> End-group analysis was aided by a high-resolution F2 proton-coupled HSQC experiment. The <sup>1</sup>J<sub>C,H</sub> for the HT C-H proton within the polymer backbone is 164 Hz while the <sup>1</sup>J<sub>C,H</sub> observed for signal **A** is significantly larger (183 Hz). The other terminal thiophene ring has a slightly larger <sup>1</sup>J<sub>C,H</sub> (signal **C**, 167 Hz) as compared to the regioregular HT unit due to the nearby bromine atom. The <sup>1</sup>H NMR analysis is clearly indicative of ring-walking and to our knowledge, this has not been observed previously in Pd CTP processes.

With the end-group assignments, <sup>1</sup>H NMR spectra of P3HT samples were used to determine *M<sub>n</sub>* (Table 3.1), since GPC versus polystyrene overestimates molecular weight.<sup>14</sup> Integration of signal **A** was compared to the integration of the HT-HT triad to obtain the DP and *M<sub>n</sub>*.

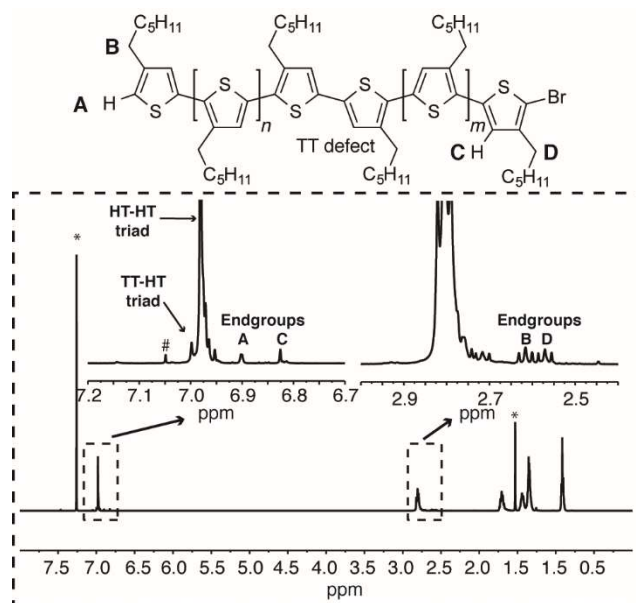


**Figure 3.3.**  $^1\text{H}$  NMR Spectrum of P3HT<sub>33</sub>. Insets highlight the end-groups of the polymer chain.

\* represents the solvent signal ( $\text{CHCl}_3$  at 7.26 ppm) and  $\text{H}_2\text{O}$  (1.53 ppm). The # sign indicates a  $^{13}\text{C}$  satellite of the  $\text{CHCl}_3$  solvent.

To confirm the chain-growth nature of the polymerization, a  $M_n$  versus monomer conversion plot was obtained. A polymerization reaction was conducted with 2 mol % of the **Pd-PEPPSI-IPr** catalyst and aliquots were removed from the reaction mixture and analyzed using GC-MS and GPC. The molecular weights increased linearly with conversion and the dispersity remained low throughout the reaction (Figure 3.4, Table 3.3 and Table 3.4).

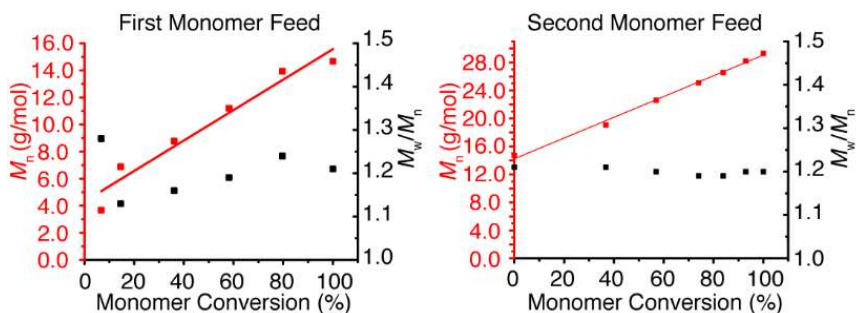


**Figure 3.4.** Left - Plot of  $M_n$  versus conversion for polymerization of SnHTBr using 2 mol % Pd-PEPPSI-IPr. Right – after refeeding the SnHTBr monomer.

To determine if the catalyst remains active, a second equivalent of **SnHTBr** was quickly added to the reaction mixture after complete consumption of the first monomer feed. The reaction mixture was sampled and the polymerization continued, strongly supporting a chain-growth process (Figure 3.4). The final polymer obtained was nearly twice the molecular weight of the material from the first feed.

Transmission low-angle and wide-angle (LAXS and WAXS) X-ray scattering patterns of Soxhlet extracted **P3HT**<sub>33</sub> and **P3HT**<sub>400</sub> revealed a familiar set of Bragg peaks observed for partially crystalline P3HT (Figure 3.5 – a and b).<sup>15</sup> The (n00) reflections originate from the layered structure of *rr*-P3HT with the spacing dictated by the non-interdigitated arrangement of alkyl side chains ( $d = 16.05 \pm .05$ , crystal form I).<sup>16</sup> The (020) peak ( $d = 3.62 \pm .02$ ) is due to  $\pi$ - $\pi$  stacking between P3HT backbones.<sup>16</sup> Tapping mode AFM images of ultra-thin films of the same samples cast onto silicon wafers (Figure 3.5 – c and d) exhibit nanofibrillar structures. These structures correspond to  $\pi$ -stacked P3HT chains with the stacking plane perpendicular to the substrate, and *rr*-P3HT chains perpendicular to the long axis of the fibril.<sup>15</sup> For **P3HT**<sub>33</sub>, the average lateral spacing between the fibrils was equal to  $\sim 19$  nm while for **P3HT**<sub>400</sub>, the average width of the fibrils was equal to  $\sim 33$  nm. The dependence of fibril width on polymer length up to a saturation limit (DP  $\sim 50$ ), has been observed previously.<sup>15</sup>

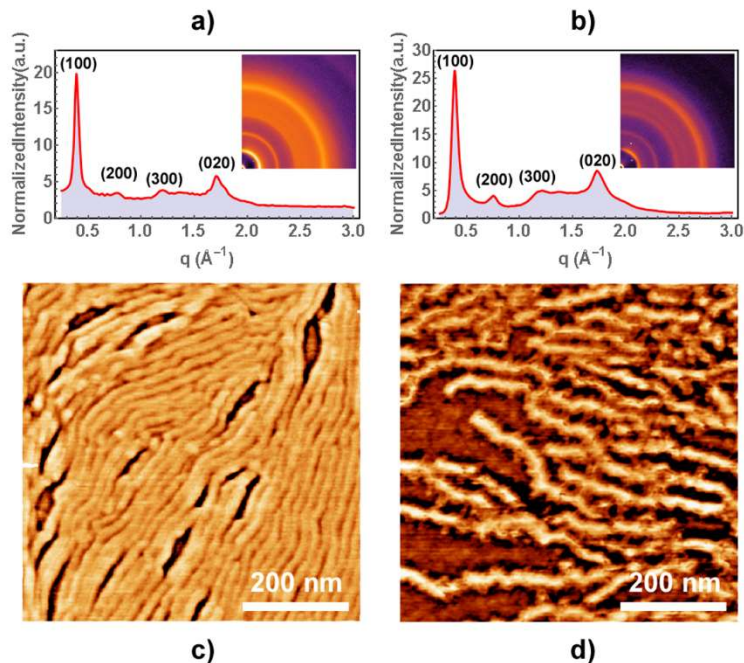


**Figure 3.5.** a) and b) Azimuthally-averaged profiles of X-ray scattering patterns (insets) showing lamellar and  $\pi$ -stacking crystalline order peaks. c) and d) Tapping-mode AFM phase images of extended nanofibrillar structures corresponding to  $\pi$ -stacked P3HT chains. Images in a) and c) were obtained for **P3HT**<sub>33</sub> and images in b) and d) were obtained for **P3HT**<sub>400</sub>.

### 3.3 Conclusions

In conclusion, we have demonstrated an effective system for Stille catalyst-transfer polycondensation of thiophene using a Pd-NHC catalyst. The polymerization proceeds in a chain-growth manner with  $M_n$  increasing linearly with conversion. The poly(3-hexylthiophene) molecular weights can be controlled and chain-end functionality is preserved (H/Br). The Pd catalyst has been shown to “ring-walk” based on the observed polymer microstructure. A similar methodology has also been explored for monomers other than thiophene. However, the limited monomer scope and complicated purification procedures using Stille CTP along with the toxicity concern regarding tin byproducts made us choose alternative protocols, which is discussed in Chapter 4.

### 3.4 Experimental

**Materials and Methods.** All reactions and manipulations of air or water sensitive compounds were carried out under dry nitrogen using an mBraun glovebox or standard Schlenk techniques. Tetrahydrofuran was purchased from Fisher Scientific, degassed with argon, and dried using a jcmeyer solvent system prior to use. All other solvents were purchased from Fisher Scientific and used as received. **Pd-PEPPSI-IPr** and nonadecane were obtained from Sigma Aldrich. Cesium fluoride was obtained from Matrix Scientific.  $\text{CDCl}_3$  was purchased from Cambridge Isotope Laboratories (CIL) and used as received. 2,5-Dibromo-3-hexylthiophene,<sup>17</sup> 2-trimethylstannylthiophene<sup>18</sup> and 2-bromo-3-hexyl-5-trimethylstannylthiophene<sup>19</sup> were prepared according to literature procedures. A stock solution of **Pd-PEPPSI-IPr** was prepared by dissolution of 0.100 g of catalyst in 20 mL of THF. This solution was used for all polymerization experiments and stored at  $-40\text{ }^\circ\text{C}$  in the glovebox.

**NMR analysis.** All NMR experiments were collected at 300 K on a two-channel Bruker Avance<sup>TM</sup> III NMR instrument operating at 500.13 MHz for  $^1\text{H}$  and 125.76 MHz for  $^{13}\text{C}$ , equipped with a room temperature Broad Band Inverse (BBI) probe with z-only pulse field gradient accessory. 1D  $^1\text{H}$ , 1D  $^{13}\text{C}$ , long-range COSY (cosylrqr), edited-HSQC (hsqcedetgpcisp2.2) and echo/antiecho-HMBC with triple low-pass filter to remove one-bond correlations (hmbcetgpl3nd) are standard experiments from the Bruker pulseprogram library in TopSpin 3.1. The F2 proton-coupled HSQC was performed using the recently published Perfect-HSQC pulse program,<sup>20</sup> kindly provided by Dr. Teodor Parella (<http://sermn.uab.cat/2014/10/perfect-hsqc-experiments-pure-in-phase-spectra/>). Both the regular and the F2 coupled HSQC experiments were collected with a digital resolution in F1 ( $^{13}\text{C}$ ) of 2.9 Hz/point. This resolution is almost equivalent to a 1D  $^{13}\text{C}$  NMR spectrum. The HMBC was optimized for 8 Hz long-range proton-coupling ( $^nJ_{\text{CH}}$ ). 1D  $^1\text{H}$  NMR spectra are referenced to residual protio solvent (7.26 for  $\text{CHCl}_3$ ). For each P3HT spectrum obtained, a  $30^\circ$  magnetization

tip angle and 10 second recycling delay time were used to ensure accurate integration of all protons for end-group analysis.

**MALDI-TOF MS.** MALDI-TOF mass spectrometry was performed in linear mode on an Applied Biosystems Voyager DE-STR time-of-flight (TOF) instrument using dithranol as the matrix. Higher molecular weight polymer samples (**P3HT<sub>100</sub>**, **P3HT<sub>200</sub>** and **P3HT<sub>400</sub>**) were difficult to analyze since larger P3HT chains have a lower propensity to be ionized.

**Gel-Permeation Chromatography.** GPC measurements were performed on a Waters 2690 separations module apparatus and a Waters 2487 dual  $\lambda$  absorbance detector with chloroform as the eluent (flow rate 1 mL/min, 40 °C,  $\lambda = 254$  nm) and two SDV columns (Porosity 1000 and 100000 Å; Polymer Standard Services). An 11-point calibration based on polystyrene standards (Poly(styrene) ReadyCal Kit, Polymer Standard Services) was applied for determination of molecular weights. All polymer aliquots subjected to GPC were prepared by quenching ~0.2 mL of the polymer solution with ~2.0 mL of 6 M methanolic HCl. The precipitate was filtered and washed with cold solvents (methanol, diethyl ether, hexanes, and acetone) to remove any monomer and low molecular weight oligomers. The resultant polymer was dissolved in 1~2 mL of chloroform, filtered through a 0.22  $\mu$ m PTFE syringe filter and analyzed.

**GC-MS analysis.** GC-MS analysis was performed on a Hewlett-Packard Agilent 6890-5973 GC-MS workstation. The GC column was a Hewlett-Packard fused silica capillary column cross-linked with 5% phenylmethylsiloxane. Helium was used as the carrier gas. The following conditions were used for all GC-MS analyses: injector temperature, 250 °C; initial temperature, 70 °C; temperature ramp, 10 °C/min; final temperature, 280 °C. All polymer aliquots subjected to GC-MS were prepared by quenching ~0.1 mL of the polymer solution with ~1.0 mL of acidic methanol (HCl:methanol, 1:200 v/v). This was diluted with 4 mL of diethyl ether in a 20 mL scintillation vial and 0.1 mL of this resultant solution, filtered through a 0.22  $\mu$ m PTFE syringe filter into a 2 mL vial and diethyl ether was added to fill the vial. Due to destannylation of the

monomer in acidic methanol, the monomer conversion was calculated by integration of the nonadecane internal standard to 2-bromo-3-hexylthiophene.

**Wide-Angle X-ray Scattering (WAXS).** Data was collected using a Rigaku (Woodlands, TX) RUH3R microfocus rotating Cu anode ( $\lambda = 1.54 \text{ \AA}$ ) at 40 kV accelerating voltage and 100 mA current, equipped with Xenocs (Sassenage, France) FOX2D focusing collimation optics with a beam width of 1 mm. Scattering patterns were collected with a Rigaku Mercury CCD two-dimensional detector with  $1024 \times 1024$  pixel array (0.068 mm/pixel). The sample to detector distance S (83.8 mm) was calibrated using a silver behenate powder in the same geometry as the P3HT samples.

**Atomic Force Microscopy.** Samples were prepared from 0.01 mg/mL solutions of **P3HT**<sub>33</sub> and **P3HT**<sub>400</sub> in dry chloroform (Intelligent Technologies PureSolv MD5) on  $2 \times 2$  cm silicon wafers with native oxide. The wafers were cleaned by spraying with fresh acetone and isopropanol and dried under a jet of filtered, dry nitrogen, followed by UV/Ozone treatment at 120 °C for 45 minutes (Novascan PSD-UVT). The as-treated wafers were placed in a petri dish with dry chloroform, completely covered with a minimum amount of solution, and allowed to dry slowly in the chloroform-saturated atmosphere. The as-obtained films were imaged with a Bruker Dimension V hybrid AFM in tapping mode.

### Model Compound Reaction



In a N<sub>2</sub> filled glovebox, a 20 mL vial was charged with 2,5-dibromo-3-hexylthiophene (1.0 equiv, 0.25 g, 0.77 mmol), 2-trimethylstannylthiophene (1.0 equiv, 0.189 g, 0.77 mmol), CsF (2.0 equiv, 0.233 g, 1.5 mmol), **Pd-PEPPSI-IPr** (2 mol %, 0.0104 g, 0.015 mmol), nonadecane as the internal standard (1.0 equiv, 0.206 g, 0.77 mmol) and 7.7 mL of THF. After 30 seconds of stirring inside the glovebox, an aliquot was withdrawn from the solution and subjected to GC-MS to determine the initial ratios of starting material to the internal standard. The vial was removed

from the glovebox and immersed in an oil bath at 60 °C. After 24 hours, the reaction was cooled to room temperature. A second aliquot was removed and GC-MS was performed to determine the relative ratio of 3'-hexyl-2,2':5',2"-terthiophene and the two bithiophene isomers, as well as to confirm the consumption of 2-trimethylstannylthiophene.

**General polymerization procedure.** In a N<sub>2</sub> filled glovebox, a 40 mL scintillation vial equipped with a Teflon screw cap was charged with a calculated amount of **Pd-PEPPSI-IPr** stock solution (5 mg/mL), CsF (2.0 equiv, 0.185 g, 1.22 mmol), nonadecane (1.0 equiv, 0.163 g, 0.61 mmol) as the internal standard and THF was added to bring the final solution to 10 mL. The vial was removed from the glovebox and immersed in an oil bath at 40 °C. 2-Bromo-3-hexyl-5-trimethylstannylthiophene (1.0 equiv, 0.25 g, 0.61 mmol) in 4 mL of THF was injected into the solution to start the polymerization. After 30 s of stirring, an aliquot was withdrawn from the solution and subjected to GC-MS to determine the initial ratio of monomer to the internal standard. After a period of time, a final aliquot was withdrawn to determine the monomer conversion and the polymerization was quenched using 6 M methanolic HCl solution. The precipitate was suction filtered then washed with cold methanol, hexanes and acetone to remove the unreacted monomer and oligomers. The final polymer was dried *in vacuo* and characterized using GPC, <sup>1</sup>H NMR spectroscopy, and MALDI-TOF mass spectrometry (P3HT 25, 33, and 50). <sup>1</sup>H NMR spectra and GPC traces of the six polymer samples (**P3HT**<sub>25</sub> – **P3HT**<sub>400</sub>) are shown below and relevant data is summarized in Table 3.2.

**Table 3.2. Detailed comparison of P3HT samples prepared by adjusting [monomer]/[catalyst] ratio.**

Sample	[M]/ [Cat]	Time (min)	Conversion <sup>a</sup> (%)	$M_n^b$ (GPC)	$\bar{D}$	$M_n^c$ (NMR)	Yield <sup>d</sup> (%)
<b>P3HT</b> <sub>25</sub>	25	80	73	7000	1.14	5100	42.5
<b>P3HT</b> <sub>33</sub>	33	110	89	9500	1.18	6600	52.7
<b>P3HT</b> <sub>50</sub>	50	120	90	14000	1.24	8600	62.3
<b>P3HT</b> <sub>100</sub>	100	125	84	23800	1.30	14200	63.8
<b>P3HT</b> <sub>200</sub>	200	140	81	45600	1.43	27300	60.9
<b>P3HT</b> <sub>400</sub>	400	150	74	73300	1.53	45000	62.5

<sup>a</sup>Conversion was determined by GC-MS using nonadecane as the internal standard. <sup>b</sup>GPC was completed at 40 °C in chloroform versus polystyrene standards. <sup>c</sup> $M_n$  was calculated based on end-group analysis using <sup>1</sup>H NMR spectroscopy where  $M_n = [(\text{Integration of HT-HT and TT-HT triads signal} + 2 \text{ end groups}) \times 166.284] + 1.0078 + 79.904$ . <sup>d</sup>Isolated yields.

### Procedure of sequential monomer addition experiment

In a N<sub>2</sub> filled glovebox, a 40 mL scintillation vial equipped with a Teflon screw cap was charged with 1.69 mL of **Pd-PEPPSI-IPr** stock solution (5 mg/mL, 2 mol %), CsF (4.0 equiv, 0.37 g, 2.44 mmol) and nonadecane (1.0 equiv, 0.163 g, 0.61 mmol) as the internal standard. THF was added to bring the final solution to 10 mL. The vial was removed from the glovebox and immersed in an oil bath at 40 °C. 2-Bromo-3-hexyl-5-trimethylstannylthiophene (1.0 equiv, 0.25 g, 0.61 mmol) in 4 mL of THF was injected into the solution to start the polymerization. After 30 s of stirring, an aliquot was withdrawn from the solution and subjected to GC-MS to determine the initial ratio of monomer to the internal standard. Several aliquots (~0.3 mL) were withdrawn after 25, 40, 55, 75, 100 and 130 min to determine the monomer conversion (GC-MS) and polymer molecular weight (GPC). After 130 min, a second monomer feed (1.0 equiv, 0.25 g, 0.61 mmol) in 1.68 mL of THF was added to the solution and an aliquot was withdrawn immediately and analyzed by GC-MS to determine the second initial ratio of monomer to the internal standard. After 15, 30, 45, 60, 85 and 110 min, another series of aliquots (~0.3 mL) were withdrawn and analyzed using GC-MS and GPC. All data is summarized in Tables 3.3 and 3.4.

**Table 3.3. Data used to construct monomer conversion versus  $M_n$  from first monomer feed.**

Monomer Conversion (%)	$M_n$	$D$
6.74	3670	1.28
14.55	6879	1.13
36.12	8778	1.16
58.18	11200	1.19
79.62	13938	1.24
100	14674	1.21

**Table 3.4. Data used to construct monomer conversion versus  $M_n$  from second monomer feed.**

Monomer Conversion (%)	$M_n$	$D$
0	14674	1.21
36.72	19076	1.21
56.91	22606	1.20
73.97	25081	1.19
83.87	26573	1.19
92.92	28224	1.20
100	29277	1.20

### 3.5 References

- (1) (a) Sheina, E. E.; Liu, J.; Iovu, M. C.; Laird, D. W.; McCullough, R. D. *Macromolecules* **2004**, *37*, 3526-3528. (b) Yokoyama, A.; Miyakoshi, R.; Yokozawa, T. *Macromolecules* **2004**, *37*, 1169-1171. (c) Miyakoshi, R.; Yokoyama, A.; Yokozawa, T. *Macromol. Rapid Commun.* **2004**, *25*, 1663-1666.
- (2) (a) Bryan, Z. J.; McNeil, A. J. *Macromolecules* **2013**, *46*, 8395-8405. (b) Yokozawa, T.; Nanashima, Y.; Kohno, H.; Suzuki, R.; Nojima, M.; Ohta, Y. *Pure Appl. Chem.* **2013**, *85*, 573-587. (c) Ohta, Y.; Yokozawa, T. *Adv. Polym. Sci.* **2013**, *262*, 191-238. (d) Okamoto, K.; Luscombe, C. K. *Polym. Chem.* **2011**, *2*, 2424-2434. (e) Yokozawa, T.; Yokoyama, A. *Chem. Rev.* **2009**, *109*, 5595-5619.
- (3) Carsten, B.; He, F.; Son, H. J.; Xu, T.; Yu, L. *Chem. Rev.* **2011**, *111*, 1493-1528.
- (4) Kang, S.; Ono, R. J.; Bielawski, C. W. *J. Am. Chem. Soc.* **2013**, *135*, 4984-4987.
- (5) (a) Yokozawa, T.; Nanashima, Y.; Ohta, Y. *ACS Macro Lett.* **2012**, *1*, 862-866. (b) Elmalem, E.; Kiriy, A.; Huck, W. T. S. *Macromolecules* **2011**, *44*, 9057-9061. (c) Tkachov, R.; Komber, H.; Rauch, S.; Lederer, A.; Oertel, U.; Häußler, L.; Voit, B.; Kiriy, A. *Macromolecules* **2014**, *47*, 4994-5001. (d) Tkachov, R.; Karpov, Y.; Senkovskyy, V.; Raguzin, I.; Zessin, J.; Lederer, A.; Stamm, M.; Voit, B.; Beryozkina, T.; Bakulev, V.; Zhao, W.; Facchetti, A.; Kiriy, A. *Macromolecules* **2014**, *47*, 3845-3851.
- (6) (a) Tkachov, R.; Senkovskyy, V.; Beryozkina, T.; Boyko, K.; Bakulev, V.; Lederer, A.; Sahre, K.; Voit, B.; Kiriy, A. *Angew. Chem., Int. Ed.* **2014**, *53*, 2402-2407. (b) Grisorio, R.; Mastrorilli, P.; Suranna, G. P. *Polym. Chem.* **2014**, *5*, 4304-4310. (c) Zhang, H.-H.; Xing, C.-H.; Hu, Q.-S. *J. Am. Chem. Soc.* **2012**, *134*, 13156-13159. (d) Huddleston, N. E.; Sontag, S. K.; Bilbrey, J. A.; Sheppard, G. R.; Locklin, J. *Macromol. Rapid Commun.* **2012**, *33*, 2115-2120. (e) Hohl, B.; Bertschi, L.; Zhang, X.; Schlüter, A. D.; Sakamoto, J. *Macromolecules* **2012**, *45*, 5418-5426. (f) Sakamoto, J.; Rehahn, M.; Wegner, G.; Schlüter, A. D. *Macromol. Rapid Commun.* **2009**, *30*, 653-687. (g) Yokoyama, A.; Suzuki, H.; Kubota, Y.; Ohuchi, K.; Higashimura, H.; Yokozawa, T.

- J. Am. Chem. Soc.* **2007**, *129*, 7236-7237. (h) Verswyvel, M.; Steverlynck, J.; Mohamed, S. H.; Trabelsi, M.; Champagne, B.; Koeckelberghs, G. *Macromolecules* **2014**, *47*, 4668-4675. (i) Yokozawa, T.; Suzuki, R.; Nojima, M.; Ohta, Y.; Yokoyama, A. *Macromol. Rapid Commun.* **2011**, *32*, 801-806.
- (7) O'Brien, C. J.; Kantchev, E. A. B.; Valente, C.; Hadei, N.; Chass, G. A.; Lough, A.; Hopkinson, A. C.; Organ, M. G. *Chem. - Eur. J.* **2006**, *12*, 4743-4748.
- (8) (a) Bryan, Z. J.; Smith, M. L.; McNeil, A. J. *Macromol. Rapid Commun.* **2012**, *33*, 842-847. (b) Sui, A.; Shi, X.; Tian, H.; Geng, Y.; Wang, F. *Polym. Chem.* **2014**, *5*, 7072-7080.
- (9) Hopkinson, M. N.; Richter, C.; Schedler, M.; Glorius, F. *Nature* **2014**, *510*, 485-496.
- (10) Sista, P.; Luscombe, C. K. *Adv. Polym. Sci.* **2014**, DOI: 10.1007/12\_2014\_278.
- (11) (a) Larrosa, I.; Somoza, C.; Banquy, A.; Goldup, S. M. *Org. Lett.* **2011**, *13*, 146-149. (b) Weber, S. K.; Galbrecht, F.; Scherf, U. *Org. Lett.* **2006**, *8*, 4039-4041.
- (12) (a) Kohn, P.; Huettner, S.; Komber, H.; Senkovskyy, V.; Tkachov, R.; Kiriy, A.; Friend, R. H.; Steiner, U.; Huck, W. T. S.; Sommer, J.-U.; Sommer, M. *J. Am. Chem. Soc.* **2012**, *134*, 4790-4805. (b) Iovu, M. C.; Sheina, E. E.; Gil, R. R.; McCullough, R. D. *Macromolecules* **2005**, *38*, 8649-8656. (c) Barbarella, G.; Bongini, A.; Zambianchi, M. *Macromolecules* **1994**, *27*, 3039-3045. (d) Verswyvel, M.; Monnaie, F.; Koeckelberghs, G. *Macromolecules* **2011**, *44*, 9489-9498.
- (13) Tkachov, R.; Senkovskyy, V.; Komber, H.; Sommer, J.-U.; Kiriy, A. *J. Am. Chem. Soc.* **2010**, *132*, 7803-7810.
- (14) (a) Liu, J.; Loewe, R. S.; McCullough, R. D. *Macromolecules* **1999**, *32*, 5777-5785. (b) Wong, M.; Hollinger, J.; Kozycz, L. M.; McCormick, T. M.; Lu, Y.; Burns, D. C.; Seferos, D. S. *ACS Macro Lett.* **2012**, *1*, 1266-1269.
- (15) Zhang, R.; Li, B.; Iovu, M. C.; Jeffries-EL, M.; Sauv e, G.; Cooper, J.; Jia, S.; Tristram-Nagle, S.; Smilgies, D. M.; Lambeth, D. N.; McCullough, R. D.; Kowalewski, T. *J. Am. Chem. Soc.* **2006**, *128*, 3480-3481.

- (16) McCullough, R. D.; Tristram-Nagle, S.; Williams, S. P.; Lowe, R. D.; Jayaraman, M. *J. Am. Chem. Soc.* **1993**, *115*, 4910-4911.
- (17) Locke, J. R.; McNeil, A. J. *Macromolecules* **2010**, *43*, 8709-8710.
- (18) Rossi, R.; Carpita, A.; Ciofalo, M.; Lippolis, V. *Tetrahedron* **1991**, *47*, 8443-8460.
- (19) Burkhart, B.; Khlyabich, P. P.; Cakir Canak, T.; LaJoie, T. W.; Thompson, B. C. *Macromolecules* **2011**, *44*, 1242-1246.
- (20) Castañar, L.; Sistaré, E.; Virgili, A.; Williamson, R. T.; Parella, T.; *Magn. Reson. Chem.* **2015**, *53*, 115-119.

## CHAPTER 4

### Nickel-Catalyzed Suzuki Polycondensation for Controlled Synthesis of Ester-Functionalized Conjugated Polymers

#### 4.1 Introduction

Rational design of catalysts and monomers has been crucial in the development of precision polymerization protocols; and this can afford materials with control over size, topology, and functionality.<sup>1</sup> Catalyst-transfer polycondensation (CTP) in particular, is used to prepare well-defined  $\pi$ -conjugated polymer materials.<sup>2</sup> However, the highly reactive monomers typically employed in CTP (e.g, organomagnesium or organozinc reagents) often limit the selection of solubilizing substituents tethered to the aromatic ring (Figure 4.1). The substituents appended to any  $\pi$ -conjugated backbone not only impart solubility, but are also crucial for tuning the chemical and physical properties of the desired polymer.<sup>3</sup> The combination of side chain engineering with controlled polymerization will afford a wide range of new  $\pi$ -conjugated architectures where electronic structure and physical properties can be manipulated along with shape, size and solid-state organization.

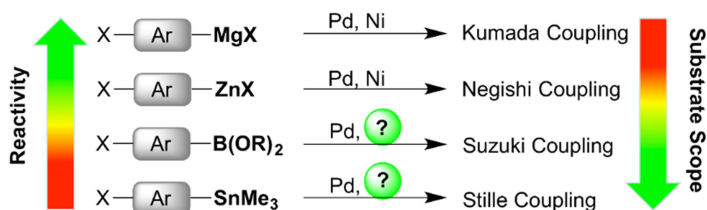


**Figure 4.1.** Cross-coupling methods used in catalyst-transfer polycondensation.

Beyond Kumada and Negishi cross-coupling, Stille and Suzuki-Miyaura cross-coupling reactions have also attracted attention to prepare conjugated polymers with controlled molecular weights and narrow molecular weight distributions.<sup>4</sup> The lower nucleophilicity of the SnMe<sub>3</sub> and B(OR)<sub>2</sub> transmetalating agents (Figure 4.1) make these methods well-suited to enhance the substrate scope of CTP. Controlled polycondensations with these transmetalating agents are generally achieved using a Pd catalyst paired with a bulky  $\sigma$ -donating phosphine ligand (P<sup>t</sup>Bu<sub>3</sub>) or

an *N*-heterocyclic carbene (NHC).<sup>5</sup> However, there is an interest to explore Ni catalysts for Stille and Suzuki CTP due to the lower cost as compared to Pd, and the facile oxidative addition observed with a diverse range of pseudo-halides or non-activated halides.<sup>6</sup> Additionally, the chain-growth mechanism for conjugated polymers is proposed to occur via a catalyst polymer  $\pi$ -complex to facilitate intramolecular oxidative addition at the polymer chain-end. The stronger Ni binding interaction as compared to Pd may be important for achieving enhanced control in chain-growth polymerizations.<sup>7</sup>

Ni-catalyzed Suzuki cross-coupling to form biaryl compounds has been reported with relatively mild reaction conditions and moderate catalyst loadings.<sup>6c</sup> This led us to investigate the possibility of Suzuki CTP with  $\pi$ -accepting ester groups as the side chain substituent. We chose the ester moiety since it can increase the ambient stability of polythiophene,<sup>8</sup> and can also be exploited in post-polymerization modification.<sup>9</sup>

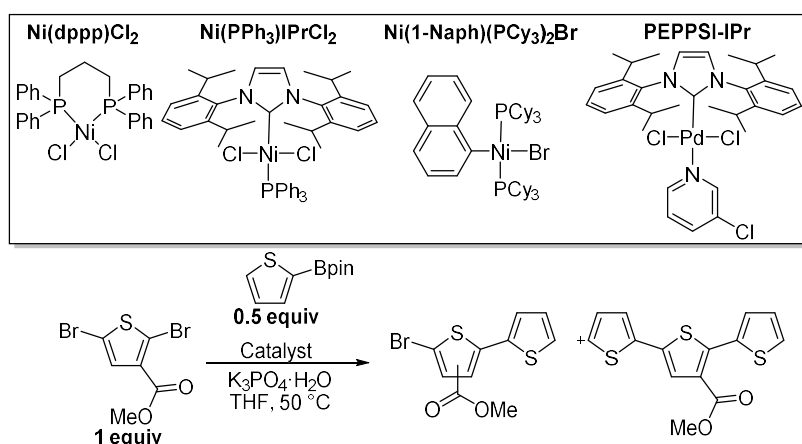
To our knowledge, CTP with  $\pi$ -accepting groups in conjugation with the monomer is unknown, though protection-deprotection strategies have been employed to synthesize similar polymers.<sup>10</sup> We used model compound studies to determine if hexyl thiophene-3-carboxylate was a suitable monomer for polycondensation. These experiments were then used as a guide for polymerization of the ester-functionalized thiophene. Finally, alternating and block copolymers of hexyl thiophene-3-carboxylate and 3-hexylthiophene were synthesized and characterized.

## 4.2 Results and Discussion

We first explored three nickel catalysts to couple methyl-2,5-dibromothiophene-3-carboxylate and thiophene-2-boronic acid pinacol ester (ThBpin). Ni(PPh<sub>3</sub>)IPrCl<sub>2</sub> and Ni(dppp)Cl<sub>2</sub> were selected since both have been successful in Kumada CTP,<sup>11</sup> while Ni(1-Naph)(PCy<sub>3</sub>)<sub>2</sub>Br has been successfully used in Suzuki cross-coupling to form biaryl compounds.<sup>12</sup> Only half an equivalent of the ThBpin was used to explore whether intramolecular oxidative addition is favored and if terthiophene formation is preferred. Similar studies have been used previously to provide indirect evidence for metal  $\pi$ -complex formation with the substrate.<sup>11b</sup>

The catalysts were screened initially at moderate loadings (5 mol %) and all reactions were conducted for 24 h. All three nickel catalysts: Ni(PPh<sub>3</sub>)IPrCl<sub>2</sub>, Ni(1-Naph)(PCy<sub>3</sub>)<sub>2</sub>Br and Ni(dppp)Cl<sub>2</sub> afforded the terthiophene with greater than 90% selectivity and high conversion (Table 4.1, entries 1, 3 and 5). This suggested the nickel systems have potential in Suzuki CTP with  $\pi$ -accepting groups. When lower catalyst loadings (1 mol %) were explored, Ni(PPh<sub>3</sub>)IPrCl<sub>2</sub> and Ni(dppp)Cl<sub>2</sub> retained good selectivity (Figure 4.7), though complete consumption of the ThBpin was not observed with Ni(dppp)Cl<sub>2</sub> (Table 4.1, entry 6). By contrast, a marked decrease in conversion and selectivity was observed with 1 mol % Ni(1-Naph)(PCy<sub>3</sub>)<sub>2</sub>Br (Table 4.1, entry 4). Similar catalyst loading limitations with this type of catalyst have been noted previously<sup>12b</sup> and suggest potential complications in polymerization.

**Table 4.1. Model Compound Reactions with Methyl 2,5-Dibromothiophene-3-carboxylate**



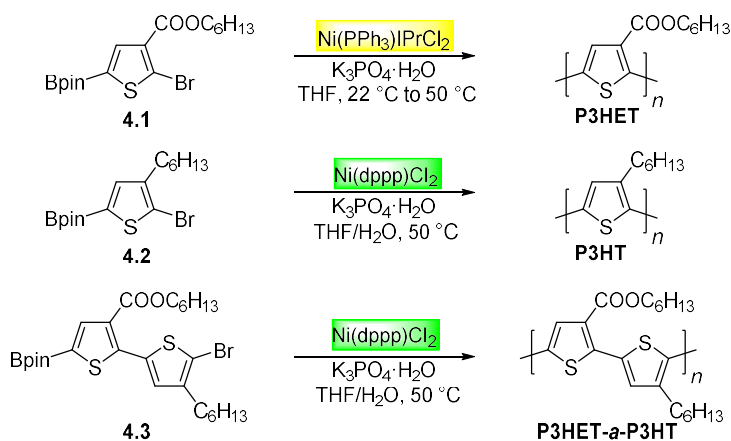
Entry	Catalyst (mol %) <sup>a</sup>	% Conv. GC-MS <sup>b</sup>	% Terthiophene GC-MS (NMR) <sup>c</sup>
1	Ni(PPh <sub>3</sub> )IPrCl <sub>2</sub> (5)	99	99 (99)
2	Ni(PPh <sub>3</sub> )IPrCl <sub>2</sub> (1)	99	99 (99)
3	Ni(1-Naph)(PCy <sub>3</sub> ) <sub>2</sub> Br (5)	99	94 (97)
4	Ni(1-Naph)(PCy <sub>3</sub> ) <sub>2</sub> Br (1)	72	44 (72)
5	Ni(dppp)Cl <sub>2</sub> (5)	99	95 (96)
6	Ni(dppp)Cl <sub>2</sub> (1)	82	97 (95)
7	PEPPSI-IPr (5)	99	52 (72)
8	PEPPSI-IPr (1)	99	64 (78)

<sup>a</sup>Relative to ThBpin. <sup>b</sup>Conversion of ThBpin was determined by GC-MS using trimethoxybenzene as the internal standard. <sup>c</sup>Relative ratio of products determined via GC-MS and <sup>1</sup>H NMR spectroscopy.

A Pd-NHC precatalyst (PEPPSI-IPr), was also explored in these model compound studies (Table 4.1, entries 7 and 8) for comparison with Ni(PPh<sub>3</sub>)IPrCl<sub>2</sub>. PEPPSI-IPr produced good conversion at either 5 or 1 mol % loading, but selectivity for the terthiophene product was lower than that observed with Ni(PPh<sub>3</sub>)IPrCl<sub>2</sub>. This type of comparison though informative, should be used with caution since the other ligands (3-chloropyridine for Pd and PPh<sub>3</sub> for Ni) may not be innocent in the catalytic cycle.<sup>13</sup> To further probe the limits of the Ni-NHC catalyst,<sup>14</sup> two separate experiments were conducted: one at 65 °C and one with a larger deficiency of the ThBpin (5:1 ratio, carboxylate:ThBpin). Greater than 90% selectivity for the terthiophene was still observed in both cases, suggesting this catalyst is highly suited for exploration in CTP with the ester-functionalized thiophene.

Poly(hexylthiophene-3-carboxylate) referred to as poly(3-hexylesterthiophene) (P3HET) has been prepared previously.<sup>15</sup> However, to our knowledge, progress on the controlled synthesis of this polymer has not been reported.<sup>16</sup> Additionally, most reports of these materials have not proceeded to higher molecular weights until recently, when a direct arylation protocol was employed.<sup>15a</sup> The Suzuki monomer (**4.1**) used in this study was prepared using a three-step synthesis starting from 3-thiophenecarboxylic acid (Scheme 4.2). Borylation of the thiophene ring with pinacolborane was achieved using an iridium-catalyzed C-H borylation reaction.<sup>17</sup>

#### Scheme 4.1. Polymers Prepared using Nickel-Catalyzed Suzuki CTP



Polymerization of monomer **4.1** proceeded smoothly in THF with Ni(PPh<sub>3</sub>)IPrCl<sub>2</sub> and K<sub>3</sub>PO<sub>4</sub>·H<sub>2</sub>O (Scheme 4.1). A previous report from Yokozawa and coworkers on Pd-catalyzed Suzuki CTP indicated that added water was essential in promoting the controlled synthesis of poly(3-hexylthiophene) (P3HT).<sup>18</sup> Interestingly, the water from the K<sub>3</sub>PO<sub>4</sub>·H<sub>2</sub>O is sufficient to promote the controlled reaction for monomer **4.1**. When additional water is added to the polymerization reaction, low conversion and lower molecular weight materials are obtained which we suspect is due to competitive protodeborylation. Stability issues of 2-heterocyclic boronic acids are known,<sup>19</sup> particularly those containing electron withdrawing groups.<sup>20</sup> We noted some small variations in reaction rate and dispersity (1.2-1.3) between monomer batches and we suspect this discrepancy is linked to trace water in the monomer. Molecular weights can be modulated according to catalyst loading (Table 4.2, entries 1-3) though in the GPC traces, we sometimes observe a small shoulder which is approximately double the molecular weight of the primary distribution. We suspect this shoulder is a consequence of disproportionation.<sup>2b,2c</sup> A polymer sample was also analyzed using MALDI-TOF mass spectrometry to explore the end group fidelity of the P3HET polymer. Mass spectrometry confirmed the primary distribution is H/Br (Figure 4.2) with a smaller H/H distribution also present.

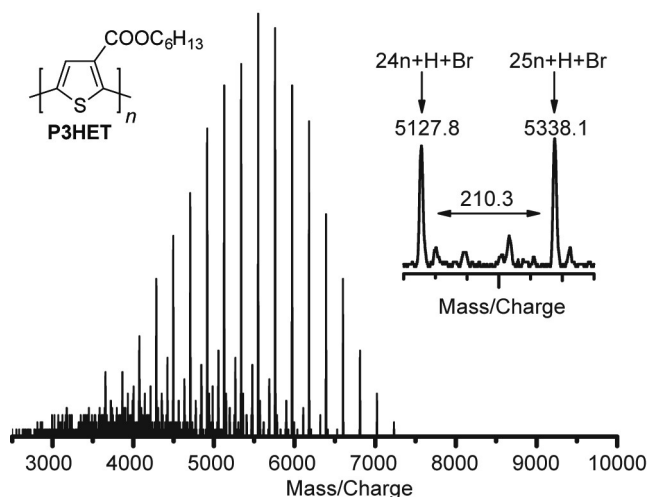


**Figure 4.2.** MALDI-TOF mass spectrum of P3HET prepared using Ni(PPh<sub>3</sub>)IPrCl<sub>2</sub>.

The efficiency of Ni(1-Naph)(PCy<sub>3</sub>)<sub>2</sub>Br was also evaluated, and low dispersity polymers were obtained using 5 mol % of the catalyst (Table 4.2, entry 4). The <sup>1</sup>H NMR spectrum of the final polymer exhibited the expected signals for the naphthyl end group. However, a broadened distribution was obtained when the catalyst loading was lowered to 2 mol %, indicative of early termination or chain transfer (Table 4.2, entry 5). This observation correlates well with the model compound studies in Table 4.1 and with the prior report.<sup>12b</sup> Polymerization of **4.1** with PEPPSI-IPr and Ni(dppp)Cl<sub>2</sub> (Table 4.2, entries 6 and 7) resulted in relatively slow polymerization reactions and higher dispersities. The use of additional water with these two catalysts improved the dispersity of the final polymer, but produced macromolecules with lower molecular weights and low conversion, which again, is likely due to protodeborylation.

We also explored this protocol to polymerize a 3-hexylthiophene monomer (**2**, Scheme 4.1). When employing Ni(PPh<sub>3</sub>)IPrCl<sub>2</sub> and K<sub>3</sub>PO<sub>4</sub>·H<sub>2</sub>O, the reaction was dramatically different than the polymerization of monomer **4.1** and produced low molecular weight P3HT with higher dispersity. The addition of water drastically increased both the reaction rate and molecular weight while narrowing the dispersity (Table 4.2, entry 8), which is consistent with the previous report.<sup>18</sup> The differences between monomer **4.1** and **4.2** are striking. The water from the K<sub>3</sub>PO<sub>4</sub>·H<sub>2</sub>O seems to be sufficient for promoting the reaction of the ester-functionalized monomer with good control. However, with the alkyl side group, additional water is needed to achieve the desired chain-growth behavior (Table 4.3). It is plausible that the ester group in monomer **4.1** stabilizes the Ni(Ar)X intermediate via chelation, which may alter the polymerization behavior of **4.1** as compared to **4.2**.<sup>21</sup>

The added water also revealed a significant sensitivity of Ni(PPh<sub>3</sub>)IPrCl<sub>2</sub> to the reaction conditions. The final molecular weight of P3HT was much greater than expected (Table 4.2, entry 8), likely from conversion of some precatalyst to Ni(OH)<sub>2</sub>.<sup>21-22</sup> In all experiments where water is added to Ni(PPh<sub>3</sub>)IPrCl<sub>2</sub>, polymers with higher than expected molecular weights were obtained,

though controlled behavior was still observed. Recent reports have highlighted the sensitivity of Ni-NHC catalysts to water,<sup>22</sup> and this will impact Suzuki CTP reactions using this system.

To probe the combination of Ni(dppp)Cl<sub>2</sub> with monomer **4.2**, we conducted two experiments: with and without additional water. Without water, the polymerization of **4.2** proceeded slowly, similar to the experiment using the Ni-NHC catalyst. However, additional water with Ni(dppp)Cl<sub>2</sub> produced P3HT with excellent control over molecular weight and dispersity (Table 4.2, entry 9).

**Table 4.2. Polymerization Studies for Monomers 4.1, 4.2, and 4.3**

Entry	M	Cat. (mol %)	Yield (%)	<i>M<sub>n</sub></i> (GPC) <sup>a</sup>	<i>Đ</i>
1	<b>4.1</b>	Ni(PPh <sub>3</sub> )IPrCl <sub>2</sub> (5)	53	7600	1.19
2	<b>4.1</b>	Ni(PPh <sub>3</sub> )IPrCl <sub>2</sub> (2)	75	16400	1.25
3	<b>4.1</b>	Ni(PPh <sub>3</sub> )IPrCl <sub>2</sub> (1)	79	30600	1.30
4	<b>4.1</b>	Ni(1-Naph) (PCy <sub>3</sub> ) <sub>2</sub> Br (5)	58	4500	1.14
5	<b>4.1</b>	Ni(1-Naph) (PCy <sub>3</sub> ) <sub>2</sub> Br (2)	69	10500	1.60
6	<b>4.1</b>	PEPPSI-IPr (2)	20	5500	1.28
7	<b>4.1</b>	Ni(dppp)Cl <sub>2</sub> (2)	69	13600	1.55
8 <sup>b</sup>	<b>4.2</b>	Ni(PPh <sub>3</sub> )IPrCl <sub>2</sub> (2)	71	74400	1.30
9 <sup>b</sup>	<b>4.2</b>	Ni(dppp)Cl <sub>2</sub> (2)	59	18600	1.08
10	<b>4.3</b>	Ni(PPh <sub>3</sub> )IPrCl <sub>2</sub> (2)	67	27700	1.63
11 <sup>b</sup>	<b>4.3</b>	Ni(dppp)Cl <sub>2</sub> (2)	59	36500	1.13
12 <sup>b</sup>	<b>4.3</b>	Ni(dppp)Cl <sub>2</sub> (1)	52	49000	1.48

<sup>a</sup>GPC traces were recorded at 40 °C versus polystyrene standards using THF as the eluent. <sup>b</sup>0.1 mL of H<sub>2</sub>O was added.

We also evaluated how quickly these precatalysts are reduced under the polymerization conditions. A separate experiment was conducted with ThBPin, K<sub>3</sub>PO<sub>4</sub> and the catalyst precursor. Upon addition of water, these reactions were monitored using GC-MS since reduction of the precatalyst should be accompanied with the formation of bithiophene. For both Ni(PPh<sub>3</sub>)IPrCl<sub>2</sub> and Ni(dppp)Cl<sub>2</sub>, bithiophene was observed within 2 minutes of water addition. Complete reduction was not quantified, but these experiments confirm that the formation of Ni(0) is relatively facile under the polymerization conditions employed. These results are also consistent with the report from Percec and co-workers which indicated fast reduction of Ni(II) under similar

conditions.<sup>12a</sup> When Pd-PEPPSI-IPr was explored, reduction to the active Pd(0) seemed to be slower, though more studies are needed to examine this in detail.

An alternating copolymer consisting of P3HET and P3HT was also synthesized (Scheme 4.1). This type of material is related to donor-acceptor copolymers, a common target for organic electronic devices. Precision synthesis of donor-acceptor materials with tunable molecular weight and narrow distributions has been realized only recently,<sup>23</sup> but the scope of acceptor moieties is limited. Benzotriazole has been explored due to excellent compatibility with Grignard reagents,<sup>23a,23b</sup> and benzothiadiazole containing polymers have also been polymerized using Suzuki CTP.<sup>23d</sup> However,  $\pi$ -accepting functional groups which are often present in donor-acceptors,<sup>24</sup> are incompatible with Grignard reagents, though diimide monomers have attracted attention with Zn<sup>23c,23e</sup> and Sn<sup>25</sup> as the transmetallating agent.

An alternating copolymer consisting of P3HET and P3HT was prepared using Suzuki CTP with Ni(dppp)Cl<sub>2</sub> as the precatalyst (Table 4.2, entries 11 and 12). The preparation of monomer **4.3** was shown in Scheme 4.3. Results suggest a controlled polymerization and, in the presence of additional water, high molecular weight P3HET-*a*-P3HT polymers were obtained with relatively short reaction times (1-2 h). Ni(PPh<sub>3</sub>)IPrCl<sub>2</sub> performed quite poorly without added water and proceeded in an uncontrolled fashion (entry 10). Employing additional water produced a GPC trace with a bimodal distribution (Table 4.4).

Finally, a block copolymer of P3HET and P3HT was prepared. Both Ni(PPh<sub>3</sub>)IPrCl<sub>2</sub> and Ni(dppp)Cl<sub>2</sub> can generate diblock architectures regardless of the order of monomer addition, though high molecular weights cannot always be generated. Water was a complicating factor since it is needed for controlled P3HT synthesis but can promote protodeborylation of the more electron-deficient **4.1** and moreover, the Ni-NHC catalyst is sensitive to water. P3HT can be prepared using 4 mol % Ni(PPh<sub>3</sub>)IPrCl<sub>2</sub> and 0.1 mL of water ( $M_n = 21100$ ,  $D = 1.14$ ) after which, addition of monomer **4.1** to the reaction mixture afforded the desired block copolymer in a controlled manner (P3HT-*b*-P3HET,  $M_n = 29500$ ,  $D = 1.28$ , Figure 4.3).

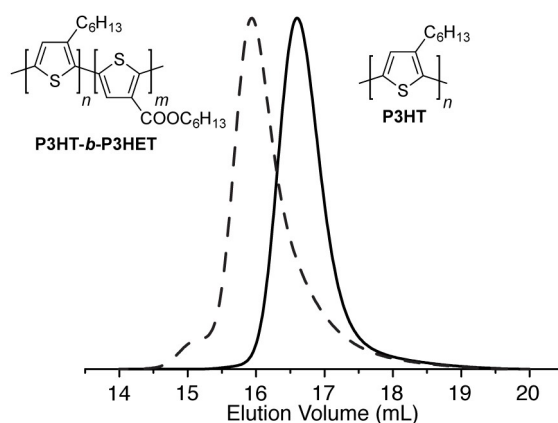


**Figure 4.3.** GPC chromatograms for the P3HT homopolymer and P3HT-*b*-P3HET copolymer synthesized using Ni(PPh<sub>3</sub>)IPrCl<sub>2</sub>.

The optical properties of P3HET, P3HT, P3HET-*a*-P3HT and P3HT-*b*-P3HET were probed both in solution and in the solid-state (Figure 4.4). P3HET is significantly blue-shifted as compared to P3HT, suggesting the ester side chain may be causing a more twisted polymer backbone as compared to the linear alkyl chain.

The absorption profile of P3HT-*b*-P3HET ( $\lambda_{\text{max}} = 445 \text{ nm}$ ) is quite close to that of P3HT ( $\lambda_{\text{max}} = 453 \text{ nm}$ ) in solution and also in the solid state (P3HT-*b*-P3HET,  $\lambda_{\text{max}} = 550 \text{ nm}$ ). The absorption profile of P3HET-*a*-P3HT ( $\lambda_{\text{max}} = 452 \text{ nm}$ ) is also nearly identical to P3HT ( $\lambda_{\text{max}} = 453 \text{ nm}$ ) in solution. However, P3HET-*a*-P3HT ( $\lambda_{\text{max}} = 627 \text{ nm}$ ,  $E_g^{\text{opt}} = 1.85 \text{ eV}$ ) is red-shifted compared to both homopolymers in the solid-state as the vibronic band becomes the dominant absorption in this spectrum.

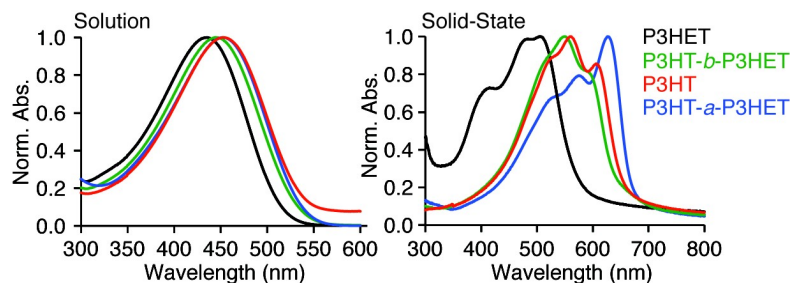


**Figure 4.4.** Solution (CHCl<sub>3</sub>) and solid-state UV-vis spectra for all polymers with P3HT included for reference.

End group analysis of P3HET and P3HET-*a*-P3HT was completed using 2D NMR spectroscopy. For P3HET, a tail-to-tail (TT) defect from precatalyst initiation ( $H_A$ , Figure 4.5) is present in the spectrum along with signals that result from the H/Br polymer end groups ( $H_B$ ,  $H_C$  and  $H_D$ , Figure 4.5). The H terminated thiophene end group ( $H_C$ , Figure 4.5) appears at 8.17 ppm and is correlated with a signal at 7.81 ppm ( $H_D$ , Figure 4.5). The signal attributed to the tail-to-tail (TT) defect appears at 7.60 ppm ( $H_A$ ) and the Br terminated chain-end produced one  $^1\text{H}$  NMR signal ( $H_B$ , Figure 4.5 at 7.68 ppm). Additionally, integration of the chain-end signals and the TT defect approximately produced a 2:1:1 ratio ( $H_A:H_B:H_C$ ) indicating good control over the end groups. This is consistent with the analysis by MALDI-TOF mass spectrometry (Figure 4.2).

Signal  $H_B$  did not show the expected correlations in the HMBC spectrum and to confirm its identity, an experiment was carried out where the polymer was reacted with  $\text{Ni}(\text{COD})_2$  followed by reaction with acid to selectively functionalize the C-Br bond. The signal attributed to  $H_B$  nearly disappeared after the reaction, and provided good evidence for the assignment (Figure 4.6).

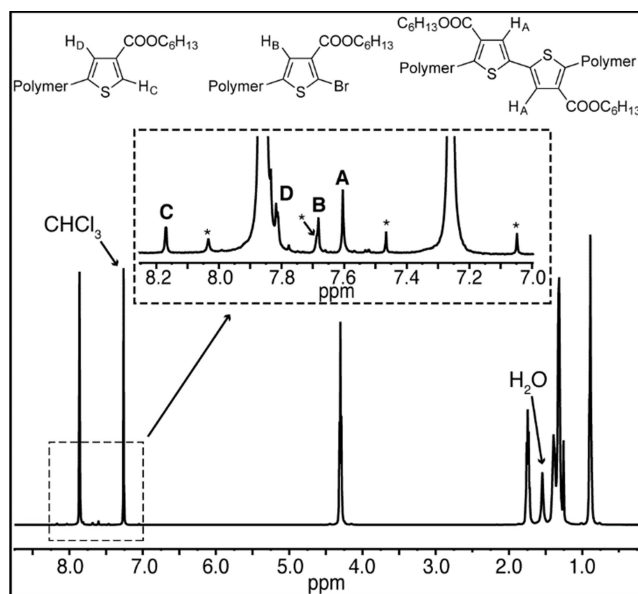


**Figure 4.5.**  $^1\text{H}$  NMR spectrum and end group analysis of P3HET. The star symbols (\*) correspond to  $^{13}\text{C}$  satellites for the aromatic signal of the polymer and the solvent.

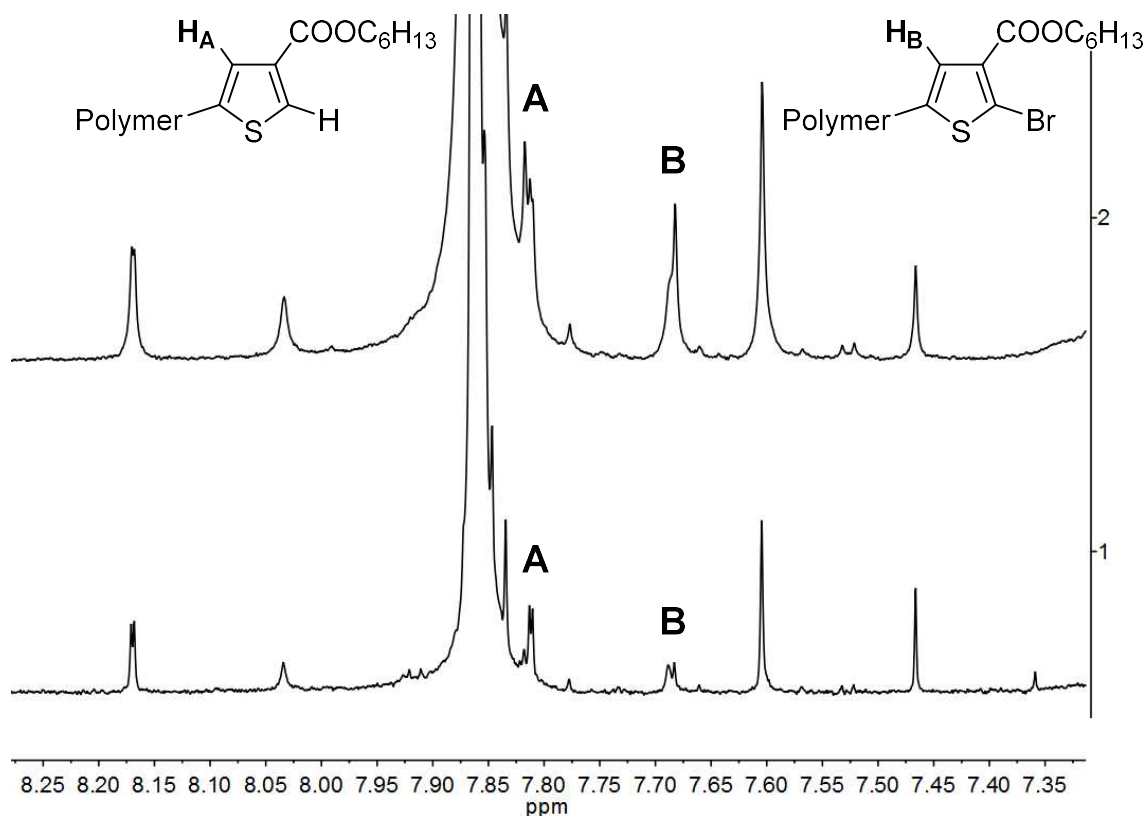


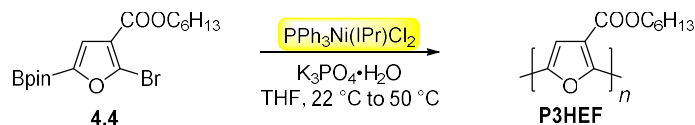
**Figure 4.6.** Top – <sup>1</sup>H NMR Spectrum of P3HET. Bottom – P3HET treated with Ni(COD)<sub>2</sub> and HCl illustrating the loss of the Br-terminated end group.

2D NMR spectroscopy was also used to confirm the highly alternating nature of P3HET-*a*-P3HT. Similar to P3HET, the TT defect for P3HET-*a*-P3HT appears at 7.55 ppm. The H terminated end group at 7.01 ppm is correlated with another signal at 7.32 ppm and these signals correspond to a regioregular 3-hexylthiophene chain-end. The Br terminated chain-end produced one signal in the <sup>1</sup>H NMR spectrum at 7.17 ppm, again corresponding to a regioregular 3-hexylthiophene.

To investigate the suitability of this protocol for other heterocycles, an ester-stabilized furan monomer (**4.4**) was synthesized and polymerized under similar conditions yielding samples with controlled molecular weight and dispersity (Table 4.3). The resultant polymer was found to be extremely soluble in typical ‘good’ solvents (chloroform or THF) and moderately soluble in hexanes and diethyl ether. Moreover, storage in solution and solid-state under ambient conditions

led to no discernable degradation, though further photostability tests should be conducted to fully elucidate this matter.

**Table 4.3. Synthesis of P3HEF.**



Catalyst	% Cat.	$M_n$ (GPC)	$\bar{D}$	Yield (%)
Ni(PPh <sub>3</sub> ) <sub>2</sub> IPrCl <sub>2</sub>	2	6700	1.10	55
Ni(PPh <sub>3</sub> ) <sub>2</sub> IPrCl <sub>2</sub>	1	9200	1.26	48

<sup>a</sup>GPC traces were recorded at 40 °C versus polystyrene standards using THF as the eluent.

The end group fidelity was investigated using matrix-assisted laser desorption ionization time-of-flight (MALDI-TOF) mass spectrometry (Figure 4.7). The difference between adjacent peaks showed excellent agreement with the molecular weight of repeating unit. Moreover, the primary distribution of the end groups is H/Br, indicating a highly controlled CTP process.

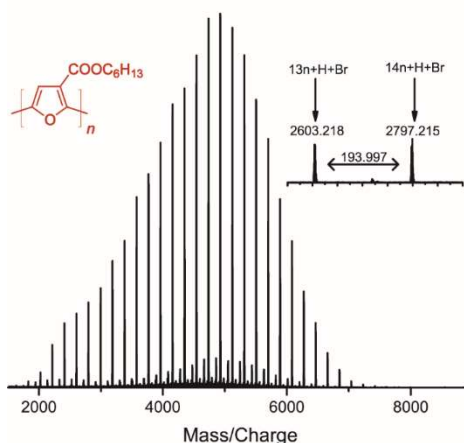


**Figure 4.7.** MALDI-TOF spectrum for low molecular weight P3HEF.

### 4.3 Conclusions

In summary, we have demonstrated the first example of a Suzuki catalyst-transfer polycondensation (CTP) using Ni precatalysts and explored this protocol with ester-functionalized monomers. The ester-functionalized polythiophene could be obtained with molecular weight control, and block copolymers were synthesized with 3-hexylthiophene.

Furthermore, the controlled synthesis of an alternating polymer is highly valuable and this Suzuki CTP protocol will be used to explore more sophisticated donor-acceptor polymers. Expanding this protocol to other monomers such as furan with an ester group was also successful. The crucial role of water in the Suzuki CTP process is currently under investigation.

#### 4.4 Experimental

**Materials and Methods.** All reactions and manipulations of air and water sensitive compounds were carried out under a dry nitrogen atmosphere using an mBraun glovebox or standard Schlenk techniques. All compounds were purchased from commercial sources and used as received. 2,5-Dibromothiophene-3-carboxylic acid<sup>26</sup>, 2-(4-hexylthiophen-2-yl)-4,4,5,5-tetramethyl-1,3,2-dioxaborolane<sup>27</sup> and monomer **4.2**<sup>28</sup> were synthesized according to literature procedures. All reaction solvents (tetrahydrofuran, dichloromethane, hexanes) were degassed with argon and dried prior to use. All solvents and chemicals used for extraction and column chromatography were used as received. Polymer samples were precipitated with 6 M methanolic HCl and washed with both methanol and acetone for GPC, NMR, and UV-vis analysis. Monomer conversion in polymerization experiments was typically monitored by GC-MS comparing the protodeborylated monomer to an internal standard. Since deborylation was not always quantitative (mixtures of monomer and protodeborylated monomer) and since it can occur either as a side reaction or also during GC analysis, it was simply used as a rough estimate for monomer conversion.

**NMR analysis.** All NMR experiments were collected at 300 K on a two-channel Bruker Avance III NMR instrument equipped with a Broad Band Inverse (BBI) probe, operating at 500 MHz for <sup>1</sup>H (126 MHz for <sup>13</sup>C). <sup>1</sup>H NMR spectra are referenced to residual protio solvent (7.26 for CHCl<sub>3</sub>, 5.32 for CHDCl<sub>2</sub>, and 7.16 for C<sub>6</sub>D<sub>5</sub>H) and <sup>13</sup>C NMR spectra are referenced to the solvent signal (δ 77.23 for CDCl<sub>3</sub>, 54.00 for CD<sub>2</sub>Cl<sub>2</sub> and 128.39 for C<sub>6</sub>D<sub>6</sub>). The F2 proton-coupled HSQC was performed using the recently published Perfect-HSQC pulse program.<sup>29</sup> The HMBC experiments were optimized for 4 and 8 Hz long-range proton-coupling (<sup>n</sup>J<sub>CH</sub>).

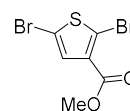
**Mass Spectrometry.** High Resolution Electron Impact Mass Spectrometry (HRMS), Electrospray Mass Spectrometry (ESI-MS) and MALDI-TOF Mass Spectrometry were performed in the School of Chemical Sciences Mass Spectrometry Laboratory at the University of Illinois, Urbana-Champaign.

**GC-MS Analysis.** GC-MS analysis was performed on a Hewlett-Packard Agilent 6890-5973 GC-MS workstation. The GC column was a Hewlett-Packard fused silica capillary column crosslinked with 5% phenylmethylsiloxane. Helium was used as the carrier gas. The following conditions were used for all GC-MS analyses: injector temperature, 250 °C; initial temperature, 70 °C; temperature ramp, 10 °C/min; final temperature, 280 °C. Polymer aliquots were typically subjected to GC-MS analysis to provide rough estimates of monomer conversion by comparing the protodeborylated monomer to an internal standard. Since deborylation was not always quantitative and since it can occur either as a side reaction or also during GC analysis, conversion values were not reported in the main article or in the supporting information. Polymer aliquots were prepared by quenching ~0.2 mL of the polymer solution with ~1.0 mL of methanol in a 20 mL scintillation vial. This was diluted with ~1.0 mL of diethyl ether and ~0.1 mL of this resultant solution was filtered through a 0.22 µm PTFE syringe filter into a 2 mL vial and diethyl ether was added to fill the vial.

**UV-vis Spectroscopy.** UV-vis spectra of polymers were recorded on a Varian Cary 5000 spectrophotometer. Solution measurements were conducted in CHCl<sub>3</sub> at 0.01 mg/mL concentration. Thin film samples were prepared from a spin-coating process. 22 × 22 mm glass cover slips were cleaned by spraying with fresh acetone, isopropanol and dried under a jet of filtered, dry nitrogen. Polymer solutions (5 mg/mL) in dry toluene were heated to 80 °C in amber glass vials for 10 min, filtered through a 0.22 µm PTFE syringe filter using a glass syringe, and re-heated for 5 min prior to spin-casting from hot solutions. The spin-coating conditions consisted of three cycles, a 400 RPM spreading cycle for 5 s, a 1000 RPM main cycle for 30 s and a 2000 RPM wicking cycle for 15 s. The films were annealed at 150 °C for 1 h under N<sub>2</sub>.

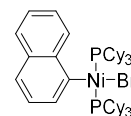
**Gel-Permeation Chromatography.** GPC measurements were performed on a Waters Instrument equipped with a 717 plus autosampler, a Waters 2414 refractive index (RI) detector and two SDV columns (Porosity 1000 and 100000 Å; Polymer Standard Services) with THF as the eluent (flow rate 1 mL/min, 40 °C). A 10-point calibration based on polystyrene standards (Polystyrene, ReadyCal Kit, Polymer Standard Services) was applied for determination of molecular weights. All polymer aliquots subjected to GPC analysis were prepared by quenching ~0.2 mL of the polymer solution with ~2.0 mL of 6 M methanolic HCl. The precipitate was filtered and washed with methanol and acetone to remove any monomer and low molecular weight oligomers. The resultant polymer was dissolved in ~1 mL of THF, filtered through a 0.22 µm PTFE syringe filter and analyzed.

*methyl-2,5-dibromothiophene-3-carboxylate.* An oven-dried 250 mL Schlenk flask was charged with 2,5-dibromothiophene-3-carboxylic acid (4.56 g, 15.9 mmol), 15 mL of thionyl chloride and catalytic dimethylformamide (~0.05 mL). The solution was heated to 40 °C and stirred overnight. Excess thionyl chloride was removed *in vacuo* and the residue was triturated with diethyl ether to afford an off-white solid that was used without further purification. An oven-dried 100 mL Schlenk flask was charged with a portion of the crude acid chloride (3.04 g, 10.0 mmol) and 25 mL of dichloromethane. The flask was cooled to 0 °C using an ice bath, then methanol (0.8 mL, 19.8 mmol) and triethylamine (2.78 mL, 19.9 mmol) were added to the flask. The mixture was stirred at room temperature for 2 h and, an aliquot was removed and analyzed using GC-MS to confirm formation of the product. The reaction mixture was then transferred to a separatory funnel and 1 M HCl solution (30 mL) was added. The organic layer was separated and the aqueous layer was extracted twice more with dichloromethane (2 × 30 mL). The combined organic extracts were washed with a saturated NaHCO<sub>3</sub> solution (10 mL), dried over MgSO<sub>4</sub> and concentrated to yield an off-white solid. The compound was purified on a short path of silica, eluting with hexanes:ethyl acetate (5:1), affording the title compound as a white crystalline solid (2.72 g, 91%). <sup>1</sup>H NMR (500 MHz, CDCl<sub>3</sub>) δ 7.34 (s, 1H), 3.86 (s, 3H).

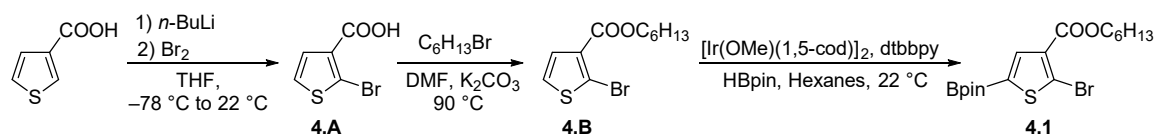


$^{13}\text{C}$  NMR (126 MHz,  $\text{CDCl}_3$ )  $\delta$  161.4, 131.9, 131.8, 119.5, 111.6, 52.3. HRMS (ESI-TOF) ( $m/z$ ):  $[\text{M} + \text{H}]^+$  calculated for  $\text{C}_6\text{H}_5\text{Br}_2\text{O}_2\text{S}$ , 298.8377; found, 298.8382.

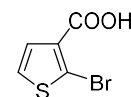
*Ni(1-Naph)(PCy<sub>3</sub>)<sub>2</sub>Br*. This compound was prepared according to a modified literature procedure.<sup>30</sup> In a  $\text{N}_2$  filled glove box, a 20 mL scintillation vial was charged with  $\text{Ni}(\text{COD})_2$  (0.10 g, 0.36 mmol), tricyclohexylphosphine (0.30 g, 1.07 mmol), and THF (1.5 mL). The solution was stirred at room temperature for 30 min, turning deep red, at which time, 1-bromonaphthalene (0.075 g, 0.36 mmol) was added to the reaction mixture. The mixture was stirred overnight and a yellow precipitate formed. The precipitate was collected using vacuum filtration and washed with hexanes ( $5 \times 5$  mL). The yellow solid was transferred to a scintillation vial and dried *in vacuo* (0.16 g, 54%).  $^{31}\text{P}\{^1\text{H}\}$  NMR (202 MHz,  $\text{C}_6\text{D}_6$ )  $\delta$  11.6.  $^1\text{H}$  NMR (500 MHz,  $\text{C}_6\text{D}_6$ )  $\delta$  10.68 (d,  $J = 8.3$  Hz, 1H), 7.71 (d,  $J = 6.7$  Hz, 1H), 7.62 (br t,  $J = 6.8$  Hz, 1H), 7.53 (d,  $J = 8.2$  Hz, 1H), 7.32 (br t,  $J = 9.3$  Hz, 2H), 7.14 (d,  $J = 7.5$  Hz, 1H), 2.75 – 0.35 (m, 66H). Note: the signal at 7.14 ppm overlaps with the solvent signal.  $^{13}\text{C}$  NMR (126 MHz,  $\text{C}_6\text{D}_6$ )  $\delta$  157.2 (t,  $J_{\text{PC}} = 32.7$  Hz), 142.9, 137.7 (t,  $J_{\text{PC}} = 3.7$  Hz), 135.4, 133.5 (t,  $J_{\text{PC}} = 2.6$  Hz), 128.8 (d,  $J_{\text{PC}} = 26.1$  Hz), 125.6, 125.2 (t,  $J_{\text{PC}} = 2.7$  Hz), 123.6, 122.6 (t,  $J_{\text{PC}} = 2.3$  Hz), 34.8 (t,  $J_{\text{PC}} = 8.5$  Hz), 31.2, 30.7, 28.7 (t,  $J_{\text{PC}} = 5.4$  Hz), 28.4 (t,  $J_{\text{PC}} = 4.3$  Hz), 27.4. HR-EIMS ( $m/z$ ):  $[\text{M} - \text{Br}]^+$  calculated for  $\text{C}_{46}\text{H}_{73}\text{P}_2\text{Ni}$ , 745.4541; found, 745.4533.



#### Scheme 4.2. Synthesis of Monomer 4.1.

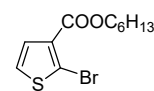


*2-bromothiophene-3-carboxylic acid (4.A)*. An oven-dried 500 mL Schlenk flask was charged with thiophene-3-carboxylic acid (15.9 g, 124 mmol) and 300 mL of THF. The solution was cooled to  $-78$  °C using a dry-ice acetone bath and 2.5 M *n*-butyllithium in hexanes (100 mL, 250 mmol) was added via cannula over a 20 min period. During the addition, a white precipitate formed. The reaction mixture was stirred for 30 min at  $-78$  °C and then,

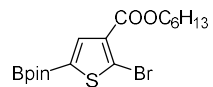


bromine (6.67 mL, 130 mmol) was added dropwise by syringe. The flask was not removed from the cold bath to ensure the reaction vessel returned to room temperature slowly overnight. A small amount of 1 M HCl solution (5 – 10 mL) was added to quench the reaction mixture and then, the mixture was concentrated to approximately 50 mL. The remaining solution was transferred to a separatory funnel, diluted with 150 mL of 1 M HCl solution and, extracted with ethyl acetate (3 × 150 mL). The combined organic extracts were washed with brine, dried over MgSO<sub>4</sub> and concentrated to afford an off-white solid. The compound was recrystallized twice using a water:ethanol mixture (4:1) to furnish the title compound as faint yellow needles (16.53 g, 64%). The <sup>1</sup>H and <sup>13</sup>C NMR spectra were compared to a previous report.<sup>31</sup>

*hexyl 2-bromothiophene-3-carboxylate (4.B)*. An oven-dried 100 mL Schlenk flask was charged with 2-bromothiophene-3-carboxylic acid (**A**) (6.00 g, 29.0 mmol), K<sub>2</sub>CO<sub>3</sub> (12.0 g, 86.8 mmol) and 40 mL of dimethylformamide. 1-Bromohexane (9.60 g, 58.2 mmol) was subsequently added by syringe. The flask was immersed in an oil bath at 90 °C and the solution was stirred for 12 h under a N<sub>2</sub> atmosphere. The reaction mixture was cooled to room temperature, diluted with 50 mL of water and transferred to a 500 mL separatory funnel. The aqueous layer was extracted with diethyl ether (3 × 100 mL) and the combined organic extracts were washed with water (50 mL) and brine (50 mL), then dried over Na<sub>2</sub>SO<sub>4</sub> and concentrated using rotary evaporation. The crude product was purified using column chromatography on silica gel eluting with hexanes:ethyl acetate (50:1) to afford the final product as a clear liquid (6.06 g, 72%). The *R<sub>f</sub>* of the product is ~0.7 in hexanes:ethyl acetate = 9:1. <sup>1</sup>H NMR (500 MHz, CDCl<sub>3</sub>) δ 7.37 (d, *J* = 5.8 Hz, 1H), 7.21 (d, *J* = 5.8 Hz, 1H), 4.28 (t, *J* = 6.7 Hz, 2H), 1.79 – 1.70 (m, 2H), 1.49 – 1.40 (m, 2H), 1.38 – 1.28 (m, 4H), 0.94 – 0.85 (m, 3H). <sup>13</sup>C NMR (126 MHz, CDCl<sub>3</sub>) δ 162.3, 131.6, 129.7, 126.0, 119.8, 65.4, 31.6, 28.8, 25.9, 22.8, 14.2. HRMS (ESI-TOF) (*m/z*): [M + H]<sup>+</sup> calculated for C<sub>11</sub>H<sub>16</sub>O<sub>2</sub>SBr, 291.0054; found, 291.0062.

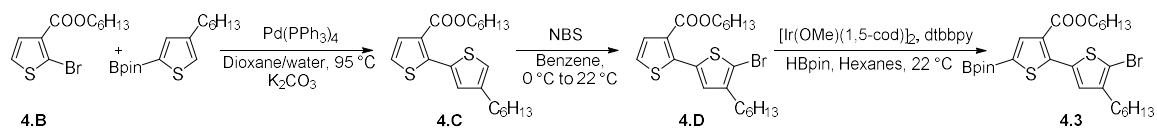


hexyl 2-bromo-5-(4,4,5,5-tetramethyl-1,3,2-dioxaborolan-2-yl)thiophene-3-carboxylate (**4.1**). In a N<sub>2</sub> filled glovebox, a 40 mL scintillation vial was

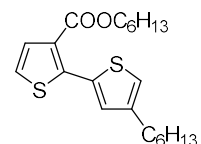


charged with pinacolborane (HBpin) (1.16 g, 9.06 mmol), di- $\mu$ -methoxobis(1,5-cyclooctadiene)diiridium (0.045 g, 0.068 mmol) and 3 mL of dry hexanes. To this stirring mixture, 4,4'-Bis(di-*t*-butyl)-2,2'-bipyridine (dtbbpy) (0.036 g, 0.13 mmol) in 3 mL of hexanes was added in portions and the mixture was stirred for 15 min. The color of the reaction mixture went from yellow to dark brown during that period. Compound **4.B** (1.32 g, 4.53 mmol) was then dissolved in 4 mL of hexanes and added to the mixture slowly (H<sub>2</sub> gas evolves in this step). The solution was kept in the glovebox and stirred overnight. The crude mixture was then removed from the glovebox, loaded directly onto silica gel, and eluted with hexanes:dichloromethane (1:1). The *R<sub>f</sub>* of the product is ~0.4 in hexanes:dichloromethane = 1:1. The final product was collected as a clear oil and slowly solidified after drying *in vacuo* to afford an off-white powder (1.40 g, 74%). <sup>1</sup>H NMR (500 MHz, CDCl<sub>3</sub>)  $\delta$  7.85 (s, 1H), 4.27 (t, *J* = 6.7 Hz, 2H), 1.77 – 1.70 (m, 2H), 1.47 – 1.39 (m, 2H), 1.37 – 1.28 (m, 16H), 0.93 – 0.87 (m, 3H). <sup>13</sup>C NMR (126 MHz, CDCl<sub>3</sub>)  $\delta$  162.2, 139.2, 132.7, 126.3, 84.9, 65.4, 31.7, 28.8, 25.9, 25.0, 22.8, 14.2. Note: one aromatic signal is missing in the <sup>13</sup>C NMR spectrum due to quadrupolar relaxation. HR-EIMS (*m/z*): [M]<sup>+</sup> calculated for C<sub>17</sub>H<sub>26</sub>O<sub>4</sub>BrSB, 416.0828; found, 416.0832.

#### Scheme 4.3. Synthesis of Monomer 4.3.



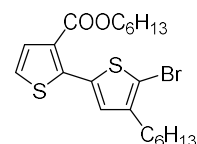
hexyl 4'-hexyl-[2,2'-bithiophene]-3-carboxylate (**4.C**). In a N<sub>2</sub> filled glovebox, a 20 mL scintillation vial was charged with compound **4.B** (0.50 g, 1.72 mmol), 2-(4-hexylthiophen-2-yl)-4,4,5,5-tetramethyl-1,3,2-dioxaborolane



(0.51 g, 1.73 mmol), Pd(PPh<sub>3</sub>)<sub>4</sub> (0.10 g, 0.087 mmol), K<sub>2</sub>CO<sub>3</sub> (0.71 g, 5.14 mmol) and 10 mL of dioxane. The vial was removed from the glovebox and 2 mL of water was added into the vial by

syringe. The vial was then immersed in an oil bath at 95 °C and the solution was stirred for 12 h before cooling to room temperature. The mixture was transferred to a separatory funnel, diluted with 100 mL of diethyl ether and washed with water and brine. The organic layer was dried using Na<sub>2</sub>SO<sub>4</sub>, and concentrated using rotary evaporation. The crude material was purified using column chromatography on silica gel, eluting with hexanes:dichloromethane (3:1) to afford the final product as a clear oil (0.58 g, 89%). The *R<sub>f</sub>* of the product is ~0.6 in hexanes:dichloromethane = 1:1. <sup>1</sup>H NMR (500 MHz, CD<sub>2</sub>Cl<sub>2</sub>) δ 7.45 (d, *J* = 5.5 Hz, 1H), 7.26 (d, *J* = 1.4 Hz, 1H), 7.20 (d, *J* = 5.4 Hz, 1H), 7.01 (q, *J* = 1.1 Hz, 1H), 4.20 (t, *J* = 6.7 Hz, 2H), 2.61 (t, *J* = 7.7 Hz, 2H), 1.70 – 1.59 (m, 4H), 1.41 – 1.25 (m, 12H), 0.94 – 0.84 (m, 6H). <sup>13</sup>C NMR (126 MHz, CD<sub>2</sub>Cl<sub>2</sub>) δ 163.7, 144.1, 143.6, 134.0, 131.1, 130.9, 128.7, 124.4, 122.8, 65.5, 32.3, 32.1, 31.1, 31.0, 29.6, 29.2, 26.3, 23.22 and 23.15 (2 overlapping signals), 14.44 and 14.37 (2 overlapping signals). HRMS (ESI-TOF) (*m/z*): [M + H]<sup>+</sup> calculated for C<sub>21</sub>H<sub>31</sub>O<sub>2</sub>S<sub>2</sub>, 379.1765; found, 379.1772.

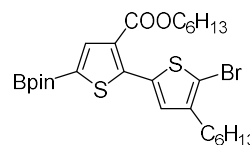
*hexyl 5'-bromo-4'-hexyl-[2,2'-bithiophene]-3-carboxylate (4.D)*. Compound **4.C** (0.58 g, 1.53 mmol) was dissolved in 100 mL of benzene and the solution was cooled to 0 °C. N-Bromosuccinimide (0.30 g, 1.69 mmol) was then added



to the reaction mixture in portions while maintaining a temperature of 0 °C. The reaction mixture was slowly warmed to room temperature and stirred overnight. The mixture was quenched with 50 mL of a saturated NaHCO<sub>3</sub> solution and the entire contents of the flask were transferred to a separatory funnel. The aqueous layer was extracted with diethyl ether (3 × 50 mL) and the combined organic extracts were washed with a saturated NaHCO<sub>3</sub> solution and brine. The extracts were then dried over Na<sub>2</sub>SO<sub>4</sub> and concentrated using rotary evaporation. The crude product was purified using column chromatography on silica gel, eluting with hexanes:dichloromethane (15:1) to afford the final product as a clear oil (0.45 g, 64%). The *R<sub>f</sub>* of the product is ~0.4 in hexanes:dichloromethane = 7:3. <sup>1</sup>H NMR (500 MHz, CDCl<sub>3</sub>) δ 7.46 (d, *J* = 5.4 Hz, 1H), 7.17 (d, *J* = 5.4 Hz, 1H), 7.11 (s, 1H), 4.24 (t, *J* = 6.7 Hz, 2H), 2.56 (t, *J* = 7.7 Hz,

2H), 1.73 – 1.64 (m, 2H), 1.64 – 1.56 (m, 2H), 1.41 – 1.24 (m, 12H), 0.94 – 0.84 (m, 6H).  $^{13}\text{C}$  NMR (126 MHz,  $\text{CDCl}_3$ )  $\delta$  163.4, 142.8, 142.2, 133.6, 130.7, 130.1, 128.2, 124.0, 112.1, 65.3, 31.8, 31.7, 29.9, 29.8, 29.2, 28.8, 25.9, 22.82 and 22.78 (2 overlapping signals), 14.3, 14.2. HRMS (ESI-TOF) ( $m/z$ ):  $[\text{M} + \text{H}]^+$  calculated for  $\text{C}_{21}\text{H}_{30}\text{O}_2\text{S}_2\text{Br}$ , 457.0871; found, 457.0869.

hexyl 5'-bromo-4'-hexyl-5-(4,4,5,5-tetramethyl-1,3,2-dioxaborolan-2-yl)-[2,2'-bithiophene]-3-carboxylate (**4.3**). In a  $\text{N}_2$  filled glovebox, a 40 mL



scintillation vial was charged with pinacolborane (HBPin) (0.50 g, 3.9

mmol), Di- $\mu$ -methoxybis(1,5-cyclooctadiene)diiridium (0.033 g, 0.050 mmol) and 2 mL of dry hexanes. To this stirring mixture, 4,4'-Bis(di-*t*-butyl)-2,2'-bipyridine (dtbbpy) (0.026 g, 0.097 mmol) in 2 mL of hexanes was added in portions and the mixture was stirred for 15 min. The color of the reaction mixture went from yellow to dark brown during that period. Compound **4.D**

(1.50 g, 3.28 mmol) was then dissolved in 4 mL of hexanes and added to the reaction mixture slowly ( $\text{H}_2$  gas evolves in this step). The solution was kept in the glovebox and stirred overnight.

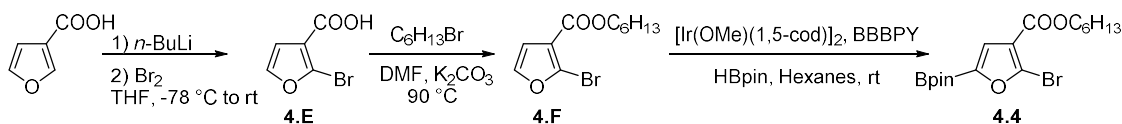
The crude mixture was then removed from the glovebox, loaded directly onto silica gel, and eluted with gradient solvent conditions (hexanes:dichloromethane = 1:1, followed by dichloromethane). The  $R_f$  of the product is  $\sim 0.5$  in hexanes:dichloromethane = 1:1. The final

product was collected as a green oil and, upon drying, slowly solidified to a light-green solid (1.41 g, 74%).  $^1\text{H}$  NMR (500 MHz,  $\text{CDCl}_3$ )  $\delta$  7.95 (s, 1H), 7.22 (s, 1H), 4.24 (t,  $J = 6.8$  Hz, 2H), 2.55 (t,  $J = 7.7$  Hz, 2H), 1.75 – 1.64 (m, 2H), 1.64 – 1.53 (m, 2H), 1.43 – 1.20 (m, 24H), 0.95 –

0.83 (m, 6H).  $^{13}\text{C}$  NMR (126 MHz,  $\text{CDCl}_3$ )  $\delta$  163.4, 149.0, 142.3, 140.6, 133.6, 130.4, 128.7, 113.0, 84.8, 65.3, 31.8, 31.7, 29.8, 29.7, 29.1, 28.9, 25.9, 25.0, 22.79 and 22.76 (2 overlapping

signals), 14.3, 14.2. Note: one aromatic signal is missing in the  $^{13}\text{C}$  NMR spectrum due to quadrupolar relaxation. HRMS (ESI-TOF) ( $m/z$ ):  $[\text{M} + \text{H}]^+$  calculated for  $\text{C}_{27}\text{H}_{41}\text{O}_4\text{S}_2\text{BrB}$ , 583.1723; found, 583.1719.

#### Scheme 4.4. Synthesis of Monomer 4.4

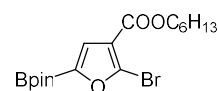


*2-bromofuran-3-carboxylic acid (4.E)*. An oven-dried 250 mL Schlenk flask was charged with furan-3-carboxylic acid (5.60 g, 50 mmol) and 150 mL THF. The solution was cooled to -78 °C using a dry-ice acetone bath and 2.5 M *n*-BuLi solution (42 mL, 105 mmol) was added using a syringe over 20 minutes. During the addition, a white precipitate formed. The solution was stirred for 2 hours at the same temperature at which point, bromine (2.82 mL, 55 mmol) was added dropwise using a syringe. The flask was not removed from the cold bath to ensure the reaction vessel returned to room temperature slowly overnight. The reaction was quenched by adding 1M HCl solution (60 mL) and most THF was removed *in vacuo*. The remaining solution was transferred to a separatory funnel and extracted with ethyl acetate (3 x 75 mL). The combined organic fractions were washed with brine, dried over magnesium sulfate and concentrated to reveal a brown solid. The solid was dissolved by adding an aqueous NaOH solution (c.a. 50 mL) and then transferred to a separatory funnel again. The aqueous layer was washed with diethyl ether (3 x 50 mL) and then transferred to a 125 mL Erlenmeyer flask and cooled to 0 °C. Concentrated HCl (37 % w/w) was added until pH < 1. The precipitate was collected via vacuum filtration and washed with cold water to reveal a light brown solid that was used directly (6.94 g, 73%). <sup>1</sup>H NMR (500 MHz, CDCl<sub>3</sub>) δ 11.80 (br s, 1H), 7.47 (d, *J* = 2.1 Hz, 1H), 6.82 (d, *J* = 2.1 Hz, 1H). <sup>13</sup>C NMR (126 MHz, CDCl<sub>3</sub>) δ 167.5, 144.8, 130.9, 117.0, 113.2. HR-EIMS (*m/z*): [M]<sup>+</sup> calculated for C<sub>5</sub>H<sub>3</sub>BrO<sub>3</sub>, 189.9265; found, 189.9267.

*hexyl 2-bromofuran-3-carboxylate (4.F)*. An oven-dried 100 mL Schlenk flask was charged with 2-bromofuran-3-carboxylic acid (4.E) (3 g, 0.016 mol), K<sub>2</sub>CO<sub>3</sub> (6.55 g, 0.047 mol) and 40 mL of DMF. 1-Bromohexane (5.21 g, 0.032 mol) was then added via a syringe. The flask was immersed in an oil bath at 90 °C and the solution was stirred for 12 h

under a N<sub>2</sub> atmosphere before cooling to room temperature. The solution was diluted with 50 mL of water and transferred to a 500 mL separatory funnel. The aqueous layer was extracted with diethyl ether (100 × 3 times) and the combined organic layer was washed with water, brine, dried over Na<sub>2</sub>SO<sub>4</sub> and concentrated using rotary evaporation. The final product was purified by using column chromatography on silica gel (hexanes: dichloromethane = 20: 3) to afford the final product as a clear liquid (1.75 g, 40%). The *R<sub>f</sub>* of the product is ~0.5 in hexanes: dichloromethane = 1: 1. <sup>1</sup>H NMR (500 MHz, CDCl<sub>3</sub>) δ 7.41 (d, *J* = 2.1 Hz, 1H), 6.75 (d, *J* = 2.1 Hz, 1H), 4.25 (t, *J* = 6.7 Hz, 2H), 1.75 – 1.67 (m, 2H), 1.47 – 1.36 (m, 2H), 1.31 (h, *J* = 3.5 Hz, 4H), 0.93 – 0.83 (m, 3H). <sup>13</sup>C NMR (126 MHz, CDCl<sub>3</sub>) δ 162.1, 144.4, 128.9, 117.8, 113.0, 65.2, 31.6, 28.7, 25.8, 22.7, 14.1. HRMS (ESI-TOF) (*m/z*): [M + H]<sup>+</sup> calculated for C<sub>11</sub>H<sub>16</sub>O<sub>3</sub>Br, 275.0283; found, 275.0294.

*hexyl 2-bromo-5-(4,4,5,5-tetramethyl-1,3,2-dioxaborolan-2-yl)furan-3-*



*carboxylate (4.4)*. In a N<sub>2</sub> filled glovebox, a 40 mL of scintillation vial was charged with 4,4,5,5-tetramethyl-1,3,2-dioxaborolane (HBpin) (1.16 g, 0.009 mol), (1,5-cyclooctadiene)(methoxy)iridium(I) dimer (0.045g, 0.068 mmol) and 3 mL of dry hexanes. To this stirring mixture, 4,4'-di-*tert*-butyl-2,2'-dipyridyl (dtbbpy) (0.037g, 0.138 mmol) in 3 mL of hexanes was added in portions and stirred for 15 mins (the mixture color changed from yellow to dark brown). Compound **4.F** (1.25 g, 0.005 mol) was then dissolved in 4 mL of hexane and added into the reaction mixture slowly (H<sub>2</sub> gas evolution). The solution was stirred overnight inside the glovebox. The crude mixture was finally removed from the glovebox, directly loaded onto the silica gel and eluted with dichloromethane. The *R<sub>f</sub>* of the product is ~0.2 in hexanes: dichloromethane = 1: 1. The final product was collected as a clear liquid and dried *in vacuo* (1.35 g, 74%). <sup>1</sup>H NMR (500 MHz, CDCl<sub>3</sub>) δ 7.37 (s, 1H), 4.25 (t, *J* = 6.6 Hz, 2H), 1.74 – 1.66 (m, 2H), 1.46 – 1.38 (m, 2H), 1.34 (s, 12H), 1.33 – 1.29 (m, 4H), 0.92 – 0.87 (m, 3H). <sup>13</sup>C NMR (126 MHz, CDCl<sub>3</sub>) δ 162.0, 134.0, 125.7, 118.4, 85.1, 77.4, 65.2, 31.7, 28.8, 25.9, 24.9, 22.8, 14.2

Note: one aromatic signal is missing in the  $^{13}\text{C}$  NMR spectrum due to quadrupolar relaxation.

HR-EIMS ( $m/z$ ):  $[\text{M}]^+$  calculated for  $\text{C}_{17}\text{H}_{26}\text{O}_5\text{BrB}$ , 400.1056; found, 400.1059.

### Model Compound Studies

*Representative procedure.* In a  $\text{N}_2$  filled glove box, a 20 mL scintillation vial was charged with the dihalogenated thiophene (0.50 mmol), 4,4,5,5-tetramethyl-2-(thiophen-2-yl)-1,3,2-dioxaborolane (ThBPIn) (0.053 g, 0.25 mmol),  $\text{K}_3\text{PO}_4 \cdot \text{H}_2\text{O}$  (0.14 g, 0.61 mmol) and either 1,3,5-trimethoxybenzene (0.042 g, 0.25 mmol) or nonadecane (0.067 g, 0.25 mmol) as an internal standard. Finally, the catalyst (mol % relative to ThBPIn) was added along with 3 mL of THF. The vial was sealed, and removed from the glovebox and an aliquot was analyzed using GC-MS ( $t = 0$  h). The vial was then placed in an oil bath at  $50\text{ }^\circ\text{C}$  and stirred for 24 h. An aliquot (0.1 mL) was then removed and subjected to GC-MS analysis while another aliquot (0.3 mL) was concentrated, dissolved in  $\text{CDCl}_3$ , filtered through a  $0.22\text{ }\mu\text{m}$  PTFE filter, and analyzed using  $^1\text{H}$  NMR spectroscopy. For the  $^1\text{H}$  NMR spectra, the methyl [2,2':5',2''-terthiophene]-3'-carboxylate was isolated from one of the reaction mixtures for comparison.  $^1\text{H}$  NMR (300 MHz,  $\text{CDCl}_3$ )  $\delta$  7.53 (s, 1H), 7.49 (dd,  $J = 3.7, 1.2$  Hz, 1H), 7.42 (dd,  $J = 5.1, 1.2$  Hz, 1H), 7.27 (dd,  $J = 5.3, 1.2$  Hz, 1H), 7.20 (dd,  $J = 3.6, 1.2$  Hz, 1H), 7.06 (ddd,  $J = 11.9, 5.1, 3.7$  Hz, 2H), 3.85 (s, 3H). Note: the signal at 7.27 ppm overlapped with the solvent signal. Integration of the methyl carboxylate signal was used to determine the ratio of terthiophene:bithiophene. For the monosubstituted bithiophene product, two regioisomers are possible, but we did not identify the regioisomer formed.

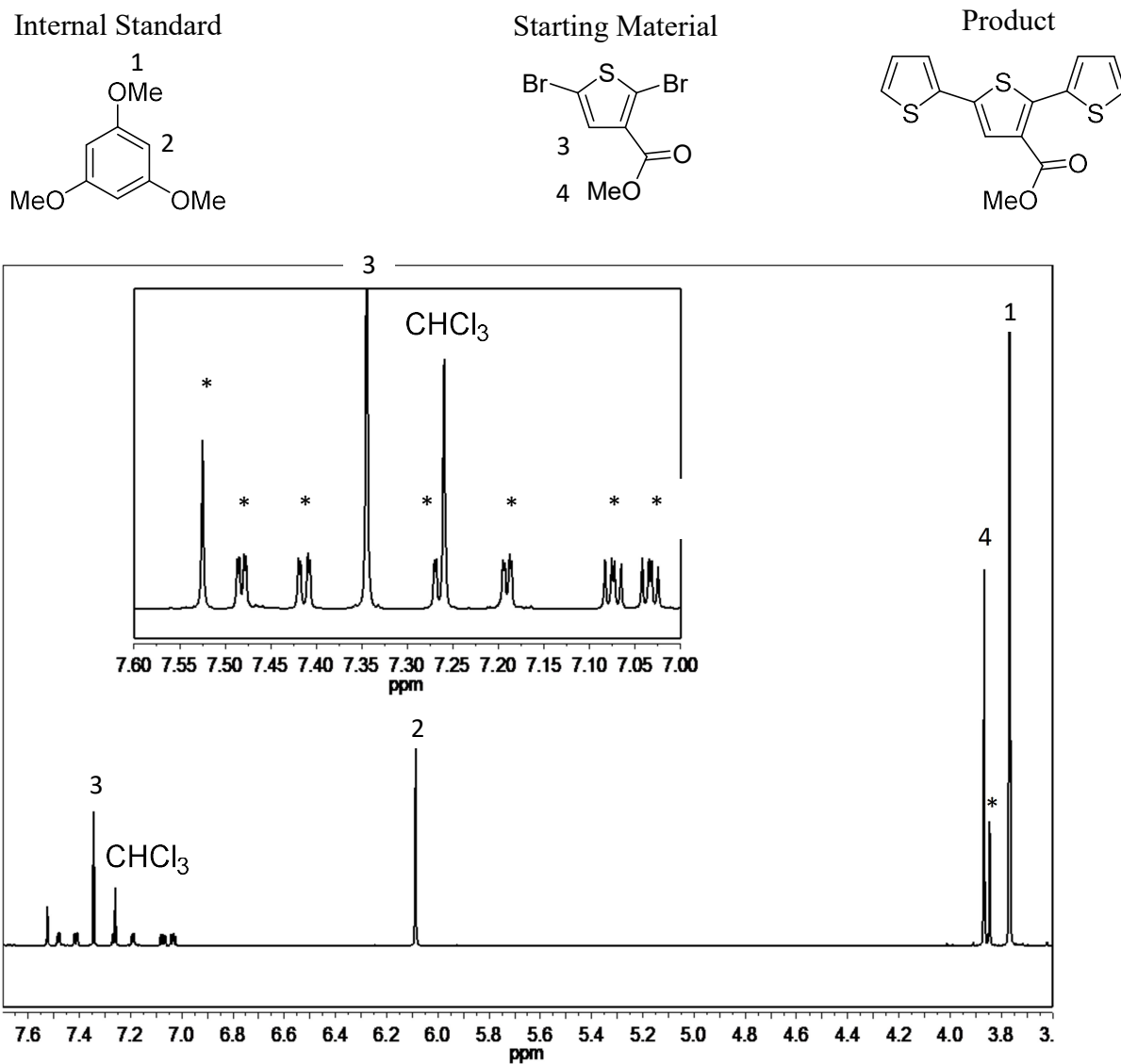
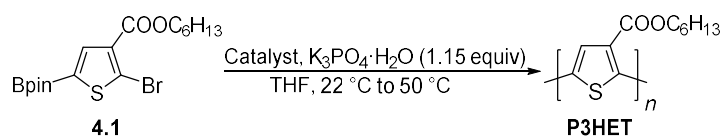
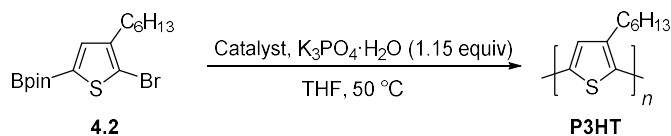


**Figure 4.8.** Representative crude  $^1\text{H}$  NMR Spectrum (500 MHz,  $\text{CDCl}_3$ ) for model compound Suzuki-Miyaura coupling at 50 °C using methyl-2,5-dibromothiophene-3-carboxylate and  $\text{Ni}(\text{PPh}_3)\text{IPrCl}_2$  (1 mol %). The star symbols correspond to the terthiophene product.

## Polymerization Studies



*Representative procedure for P3HET synthesis.* In a N<sub>2</sub> filled glovebox, a 20 mL scintillation vial equipped with a Teflon screw cap was charged with a calculated amount of catalyst (mol % listed in Table 4.3), K<sub>3</sub>PO<sub>4</sub>·H<sub>2</sub>O (0.080 g, 0.35 mmol), nonadecane (0.080 g, 0.30 mmol) as the internal standard, and 5 mL of THF. The vial was capped, removed from the glovebox and the reaction mixture was stirred at room temperature under N<sub>2</sub>. Monomer **4.1** (0.13 g, 0.31 mmol) in 2 mL of THF was injected into the solution to initiate the polymerization. After 30 s of stirring, an aliquot (0.2 mL) was withdrawn from the solution, quenched with methanol (1 mL), diluted with diethyl ether (1 mL) and subjected to GC-MS analysis. The reaction mixture was stirred at room temperature for 30 min before being placed in an oil bath at 50 °C. A final aliquot (0.2 mL) was withdrawn to determine the monomer conversion and the polymerization was quenched using 6 M methanolic HCl solution. The precipitate was collected using vacuum filtration, then washed with methanol and acetone to remove any unreacted monomer and oligomers. The final polymer was collected as a red solid and dried *in vacuo*. <sup>1</sup>H NMR (500 MHz, CDCl<sub>3</sub>) δ 7.86 (br s, 1H), 4.30 (t, *J* = 6.8 Hz, 2H), 1.81 – 1.67 (m, 2H), 1.44 – 1.22 (m, 6H), 0.96 – 0.81 (m, 3H). <sup>13</sup>C NMR (126 MHz, CDCl<sub>3</sub>) δ 162.9, 143.1, 132.6, 132.4, 128.4, 65.6, 31.7, 28.9, 25.9, 22.8, 14.3.



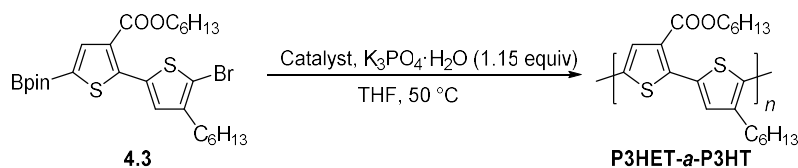
*Representative procedure for P3HT synthesis.* In a N<sub>2</sub> filled glove box, a 20 mL scintillation vial equipped with a Teflon screw cap was charged with a calculated amount of catalyst (mol % listed in Table 4.4), K<sub>3</sub>PO<sub>4</sub>·H<sub>2</sub>O (0.080 g, 0.35 mmol), nonadecane (0.080 g, 0.30 mmol) as the internal standard, and 5 mL of THF. The vial was sealed, removed from the glovebox and the reaction mixture was stirred at room temperature under N<sub>2</sub>. Monomer **4.2** (0.114 g, 0.31 mmol) in 2 mL of

THF was injected into the reaction mixture followed by degassed H<sub>2</sub>O then, the vial was immersed in an oil bath at 50 °C. The reaction mixture was sampled periodically and polymer aliquots were prepared by quenching ~0.2 mL of the polymer solution with ~2.0 mL of 6 M methanolic HCl. The precipitate was filtered and washed with methanol and acetone to remove any monomer and low molecular weight oligomers. The resultant polymer was dissolved in ~1 mL of THF with gentle heating, filtered through a 0.22 μm PTFE syringe filter, and analyzed using GPC (relative to polystyrene) with THF as the eluent.

**Table 4.4. Optimization of water content in P3HT synthesis from monomer 4.2.**

Catalyst	% Cat. (mol)	H <sub>2</sub> O (mL)	Time (min)	M <sub>n</sub> (GPC)	Đ
Ni(PPh <sub>3</sub> )IPrCl <sub>2</sub>	2	0	1200	6200	1.65
Ni(PPh <sub>3</sub> )IPrCl <sub>2</sub>	2	0.02	35	8100	1.54
Ni(PPh <sub>3</sub> )IPrCl <sub>2</sub>	2	0.05	35	8700	1.50
Ni(PPh <sub>3</sub> )IPrCl <sub>2</sub>	2	0.08	35	42100	1.37
Ni(PPh <sub>3</sub> )IPrCl <sub>2</sub>	2	0.10	15	61300	1.13
Ni(PPh <sub>3</sub> )IPrCl <sub>2</sub> <sup>a</sup>	2	0.10	45	74400	1.30
Ni(dppp)Cl <sub>2</sub>	2	0	1110	8200	1.54
Ni(dppp)Cl <sub>2</sub>	2	0.05	140	16000	1.15
Ni(dppp)Cl <sub>2</sub>	2	0.10	30	17100	1.09
Ni(dppp)Cl <sub>2</sub> <sup>b</sup>	2	0.10	60	18600	1.08

<sup>a</sup> Isolated yield = 71%. <sup>b</sup> Isolated yield = 59%.

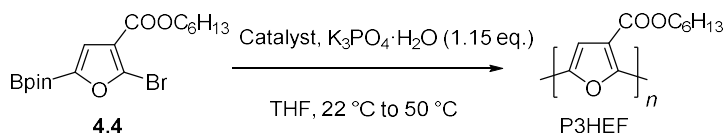


*Representative procedure for P3HET-a-P3HT synthesis.* In a N<sub>2</sub> filled glovebox, a 20 mL scintillation vial equipped with a Teflon screw cap was charged with a calculated amount of catalyst (listed in Table 4.5 below), K<sub>3</sub>PO<sub>4</sub>·H<sub>2</sub>O (0.080 g, 0.35 mmol) and 5 mL of THF. The vial was capped, removed from the glovebox and the reaction mixture was stirred at room temperature under N<sub>2</sub>. Monomer **4.3** (0.18 g, 0.31 mmol) in 2 mL of THF was injected into the reaction mixture followed by degassed H<sub>2</sub>O then, the vial was immersed in an oil bath at 50 °C. The reaction mixture was stirred for period of time and then, the polymerization was quenched using 6

M methanolic HCl solution. The precipitate was collected using vacuum filtration, then washed with methanol and acetone to remove any unreacted monomer and oligomers. The final polymer was collected as a purple solid and dried *in vacuo*.  $^1\text{H}$  NMR (500 MHz,  $\text{CDCl}_3$ )  $\delta$  7.54 (s, 1H), 7.38 (s, 1H), 4.30 (t,  $J = 6.7$  Hz, 2H), 2.80 (t,  $J = 7.9$  Hz, 2H), 1.81 – 1.57 (m, 4H), 1.49 – 1.27 (m, 12H), 0.97 – 0.83 (m, 6H).  $^{13}\text{C}$  NMR (126 MHz,  $\text{CDCl}_3$ )  $\delta$  163.3, 142.3, 140.9, 133.9, 132.5, 132.0, 129.1, 128.1, 65.5, 31.9, 31.7, 30.8, 29.6, 29.5, 28.9, 26.0, 22.9, 22.8, 14.34 and 14.26 (2 overlapping signals). Note: only 7 of the 8 possible signals from the thiophene rings are visible due to similarities between chemical environments.

**Table 4.5. Synthesis of P3HET-*a*-P3HT from monomer 4.3.**

Catalyst	% Cat. (mol)	$\text{H}_2\text{O}$ (mL)	Time (min)	$M_n$ (GPC)	$\bar{D}$	Yield (%)
Ni( $\text{PPh}_3$ ) $\text{IPrCl}_2$	2	0	210	27700	1.63	67
Ni( $\text{PPh}_3$ ) $\text{IPrCl}_2$	2	0.10	60	22600	6.08	52
Ni(dppp) $\text{Cl}_2$	2	0.10	60	36500	1.13	59
Ni(dppp) $\text{Cl}_2$	1	0.10	120	49000	1.48	52



*Representative procedure for P3HET synthesis.* In a  $\text{N}_2$  filled glovebox, a 20 mL scintillation vial equipped with a Teflon screw cap was charged with a calculated amount of Ni( $\text{PPh}_3$ ) $\text{IPrCl}_2$  catalyst,  $\text{K}_3\text{PO}_4 \cdot \text{H}_2\text{O}$  (0.08 g, 0.347 mmol), and 5 mL of THF. The vial was sealed, moved from the glovebox and stirred at room temperature. Monomer **4.4** (0.12 g, 0.31 mmol) in 2 mL of THF was injected into the solution to start the polymerization. The vial was allowed to stir at room temperature for 30 mins before being placed in an oil bath at 50 °C and stirred for a period of time. The polymerization was quenched using 6 M methanolic HCl solution. The precipitate was suction filtered then washed with cold methanol and acetone to remove the unreacted monomer and oligomers. The final polymer was dried *in vacuo* and characterized using GPC, MALDI-TOF mass spectrometry.

## 4.5 References

- (1) Müller, A. H. E.; Matyjaszewski, K. *Controlled and Living Polymerizations: From Mechanisms to Applications*; Wiley-VCH Verlag GmbH & Co. KGaA: Weinheim, Germany., 2009.
- (2) (a) Yokozawa, T.; Ohta, Y. *Chem. Rev.* **2016**, *116*, 1950-1968. (b) Grisorio, R.; Suranna, G. P. *Polym. Chem.* **2015**, *6*, 7781-7795. (c) Bryan, Z. J.; McNeil, A. J. *Macromolecules* **2013**, *46*, 8395-8405. (d) Okamoto, K.; Luscombe, C. K. *Polym. Chem.* **2011**, *2*, 2424-2434. (e) Kiriy, A.; Senkovskyy, V.; Sommer, M. **2011**, *32*, 1503-1517. (f) Yokozawa, T.; Yokoyama, A. *Chem. Rev.* **2009**, *109*, 5595-5619.
- (3) Mei, J.; Bao, Z. *Chem. Mater.* **2014**, *26*, 604-615.
- (4) (a) Zhang, H.-H.; Peng, W.; Dong, J.; Hu, Q.-S. *ACS Macro Lett.* **2016**, *5*, 656-660. (b) Zhang, H.-H.; Xing, C.-H.; Hu, Q.-S.; Hong, K. *Macromolecules* **2015**, *48*, 967-978. (c) Qiu, Y.; Mohin, J.; Tsai, C.-H.; Tristram-Nagle, S.; Gil, R. R.; Kowalewski, T.; Noonan, K. J. T. *Macromol. Rapid Commun.* **2015**, *36*, 840-844. (d) Grisorio, R.; Mastroilli, P.; Suranna, G. P. *Polym. Chem.* **2014**, *5*, 4304-4310. (e) Sui, A.; Shi, X.; Tian, H.; Geng, Y.; Wang, F. *Polym. Chem.* **2014**, *5*, 7072-7080. (f) Kang, S.; Ono, R. J.; Bielawski, C. W. *J. Am. Chem. Soc.* **2013**, *135*, 4984-4987. (g) Yokoyama, A.; Suzuki, H.; Kubota, Y.; Ohuchi, K.; Higashimura, H.; Yokozawa, T. *J. Am. Chem. Soc.* **2007**, *129*, 7236-7237.
- (5) Hopkinson, M. N.; Richter, C.; Schedler, M.; Glorius, F. *Nature* **2014**, *510*, 485-496.
- (6) (a) Prakasham, A. P.; Ghosh, P. *Inorg. Chim. Acta* **2015**, *431*, 61-100. (b) Tasker, S. Z.; Standley, E. A.; Jamison, T. F. *Nature* **2014**, *509*, 299-309. (c) Han, F.-S. *Chem. Soc. Rev.* **2013**, *42*, 5270-5298. (d) Rosen, B. M.; Quasdorf, K. W.; Wilson, D. A.; Zhang, N.; Resmerita, A.-M.; Garg, N. K.; Percec, V. *Chem. Rev.* **2011**, *111*, 1346-1416. (e) Hu, X. *Chem. Sci.* **2011**, *2*, 1867-1886. (f) Jana, R.; Pathak, T. P.; Sigman, M. S. *Chem. Rev.* **2011**, *111*, 1417-1492. (g) Phapale, V. B.; Cárdenas, D. J. *Chem. Soc. Rev.* **2009**, *38*, 1598-1607.

- (7) (a) Willot, P.; Koeckelberghs, G. *Macromolecules* **2014**, *47*, 8548-8555. (b) Bhatt, M. P.; Magurudeniya, H. D.; Sista, P.; Sheina, E. E.; Jeffries-EL, M.; Janesko, B. G.; McCullough, R. D.; Stefan, M. C. *J. Mater. Chem. A* **2013**, *1*, 12841-12849.
- (8) (a) Hu, X.; Shi, M.; Chen, J.; Zuo, L.; Fu, L.; Liu, Y.; Chen, H. *Macromol. Rapid Commun.* **2011**, *32*, 506-511. (b) Murphy, A. R.; Liu, J.; Luscombe, C.; Kavulak, D.; Fréchet, J. M. J.; Kline, R. J.; McGehee, M. D. *Chem. Mater.* **2005**, *17*, 4892-4899.
- (9) (a) Smith, Z. C.; Meyer, D. M.; Simon, M. G.; Staii, C.; Shukla, D.; Thomas III, S. W. *Macromolecules* **2015**, *48*, 959-966. (b) Liu, J.; Kadnikova, E. N.; Liu, Y.; McGehee, M. D.; Fréchet, J. M. J. *J. Am. Chem. Soc.* **2004**, *126*, 9486-9487.
- (10) (a) Bridges, C. R.; Guo, C.; Yan, H.; Miltenburg, M. B.; Li, P.; Li, Y.; Seferos, D. S. *Macromolecules* **2015**, *48*, 5587-5595. (b) Wang, C.; Kim, F. S.; Ren, G.; Xu, Y.; Pang, Y.; Jenekhe, S. A.; Jia, L. *J. Polym. Sci., Part A: Polym. Chem.* **2010**, *48*, 4681-4690.
- (11) (a) Tamba, S.; Shono, K.; Sugie, A.; Mori, A. *J. Am. Chem. Soc.* **2011**, *133*, 9700-9703. (b) Sheina, E. E.; Liu, J.; Iovu, M. C.; Laird, D. W.; McCullough, R. D. *Macromolecules* **2004**, *37*, 3526-3528. (c) Yokoyama, A.; Miyakoshi, R.; Yokozawa, T. *Macromolecules* **2004**, *37*, 1169-1171.
- (12) (a) Jezorek, R. L.; Zhang, N.; Leowanawat, P.; Bunner, M. H.; Gutsche, N.; Pesti, A. K. R.; Olsen, J. T.; Percec, V. *Org. Lett.* **2014**, *16*, 6326-6329. (b) Leowanawat, P.; Zhang, N.; Safi, M.; Hoffman, D. J.; Fryberger, M. C.; George, A.; Percec, V. *J. Org. Chem.* **2012**, *77*, 2885-2892.
- (13) (a) Chen, M.-T.; Vicic, D. A.; Turner, M. L.; Navarro, O. *Organometallics* **2011**, *30*, 5052-5056. (b) Nasielski, J.; Hadei, N.; Achonduh, G.; Kantchev, E. A. B.; O'Brien, C. J.; Lough, A.; Organ, M. G. *Chem.-Eur. J.* **2010**, *16*, 10844-10853. (c) Diebolt, O.; Jurčik, V.; Correa da Costa, R.; Braunstein, P.; Cavallo, L.; Nolan, S. P.; Slawin, A. M. Z.; Cazin, C. S. *J. Organometallics* **2010**, *29*, 1443-1450.
- (14) Bryan, Z. J.; Hall, A. O.; Zhao, C. T.; Chen, J.; McNeil, A. J. *ACS Macro Lett.* **2016**, *5*, 69-72.

- (15) (a) Gobalasingham, N. S.; Noh, S.; Thompson, B. C. *Polym. Chem.* **2016**, *7*, 1623-1631. (b) Zhou, C. Y.; Yan, L. T.; Zhang, L. N.; Ai, X. D.; Li, T. X.; Dai, C. A. *J. Macromol. Sci., Part A: Pure Appl. Chem.* **2012**, *49*, 293-297. (c) Amarasekara, A. S.; Pomerantz, M. *Synthesis* **2003**, 2255-2258. (d) Pomerantz, M.; Cheng, Y.; Kasim, R. K.; Elsenbaumer, R. L. *J. Mater. Chem.* **1999**, *9*, 2155-2163. (e) Pomerantz, M.; Cheng, Y.; Kasim, R. K.; Elsenbaumer, R. L. *Synth. Met.* **1997**, *85*, 1235-1236. (f) Pomerantz, M.; Yang, H.; Cheng, Y. *Macromolecules* **1995**, *28*, 5706-5708.
- (16) Thiophenes with an ester group in the side chain have been polymerized in a controlled manner using Kumada and Negishi CTP, though the ester was not in conjugation with the aromatic ring. See for example: (a) Kudret, S.; Van den Brande, N.; Defour, M.; Van Mele, B.; Lutsen, L.; Vanderzande, D.; Maes, W. *Polym. Chem.* **2014**, *5*, 1832-1837. (b) Suspène, C.; Miozzo, L.; Choi, J.; Girona, R.; Geffroy, B.; Tondelier, D.; Bonnassieux, Y.; Horowitz, G.; Yassar, A. *J. Mater. Chem.* **2012**, *22*, 4511-4518. (c) Ho, C.-C.; Liu, Y.-C.; Lin, S.-H.; Su, W.-F. *Macromolecules* **2012**, *45*, 813-820. (d) Vallat, P.; Lamps, J.-P.; Schosseler, F.; Rawiso, M.; Catala, J.-M. *Macromolecules* **2007**, *40*, 2600-2602.
- (17) Chotana, G. A.; Kallepalli, V. A.; Maleczka Jr., R. E.; Smith III, M. R. *Tetrahedron* **2008**, *64*, 6103-6114.
- (18) Kosaka, K.; Ohta, Y.; Yokozawa, T. *Macromol. Rapid Commun.* **2015**, *36*, 373-377.
- (19) Tyrrell, E.; Brookes, P. *Synthesis* **2003**, 469-483.
- (20) Brandão, M. A. F.; Braga de Oliveira, A.; Snieckus, V. *Tetrahedron Lett.* **1993**, *34*, 2437-2440.
- (21) Inada, K.; Miyaura, N. *Tetrahedron* **2000**, *56*, 8657-8660.
- (22) Astakhov, A. V.; Khazipov, O. V.; Degtyareva, E. S.; Khrustalev, V. N.; Chernyshev, V. M.; Ananikov, V. P. *Organometallics* **2015**, *34*, 5759-5766.
- (23) (a) Pollit, A. A.; Bridges, C. R.; Seferos, D. S. *Macromol. Rapid Commun.* **2015**, *36*, 65-70. (b) Todd, A. D.; Bielawski, C. W. *ACS Macro Lett.* **2015**, *4*, 1254-1258. (c) Tkachov, R.; Karpov,

- Y.; Senkovskyy, V.; Raguzin, I.; Zessin, J.; Lederer, A.; Stamm, M.; Voit, B.; Beryozkina, T.; Bakulev, V.; Zhao, W.; Facchetti, A.; Kiriya, A. *Macromolecules* **2014**, *47*, 3845-3851. (d) Elmalem, E.; Kiriya, A.; Huck, W. T. S. *Macromolecules* **2011**, *44*, 9057-9061. (e) Senkovskyy, V.; Tkachov, R.; Komber, H.; Sommer, M.; Heuken, M.; Voit, B.; Huck, W. T. S.; Kataev, V.; Petr, A.; Kiriya, A. *J. Am. Chem. Soc.* **2011**, *133*, 19966-19970.
- (24) Guo, X.; Baumgarten, M.; Müllen, K. *Prog. Polym. Sci.* **2013**, *38*, 1832-1908.
- (25) Goto, E.; Ando, S.; Ueda, M.; Higashihara, T. *ACS Macro Lett.* **2015**, *4*, 1004-1007.
- (26) Huo, L.; Chen, T. L.; Zhou, Y.; Hou, J.; Chen, H.-Y.; Yang, Y.; Li, Y. *Macromolecules* **2009**, *42*, 4377-4380.
- (27) Li, J.-C.; Lee, S.-H.; Hahn, Y.-B.; Kim, K.-J.; Zong, K.; Lee, Y.-S. *Synth. Met.* **2008**, *158*, 150-156.
- (28) (a) Yokozawa, T.; Suzuki, R.; Nojima, M.; Ohta, Y.; Yokoyama, A. *Macromol. Rapid Commun.* **2011**, *32*, 801-806. (b) Liversedge, I. A.; Higgins, S. J.; Giles, M.; Heeney, M.; McCulloch, I. *Tetrahedron Lett.* **2006**, *47*, 5143-5146.
- (29) Castañar, L.; Sistaré, E.; Virgili, A.; Williamson, R. T.; Parella, T. *Magn. Reson. Chem.* **2015**, *53*, 115-119.
- (30) Jezorek, R. L.; Zhang, N.; Leowanawat, P.; Bunner, M. H.; Gutsche, N.; Pesti, A. K. R.; Olsen, J. T.; Percec, V. *Org. Lett.* **2014**, *16*, 6326-6329.
- (31) Pomerantz, M.; Amarasekara, A. S.; Rasika Dias, H. V. *J. Org. Chem.* **2002**, *67*, 6931-6937.

## CHAPTER 5

### Synthesizing Electron-Rich and Electron-Deficient Conjugated Polymers by Direct Catalytic Cross-Coupling of Organolithium AB-Type Monomers

#### 5.1 Introduction

Organic  $\pi$ -conjugated polymers are very important components in a variety of optoelectronic devices such as organic light-emitting diode (OLED), organic photovoltaics (OPV), and thin-film transistors (OFET).<sup>1</sup> Conjugated polymers are commonly prepared using metal-catalyzed step-growth polymerizations (AA/BB-type route) with limited control over molecular weight and dispersity.

In the last decade, there is an interest in developing chain-growth polymerization methods to produce conjugated architectures with enhanced complexity.<sup>2</sup> Particularly, catalyst-transfer polycondensation (CTP) is among the most well-established methods in the controlled synthesis of well-defined conjugated polymers.<sup>2c</sup> Different named cross-coupling reactions such as Suzuki (organoboron), Kumada (organomagnesium) and Negishi (organozinc) have been widely applied in CTP. However, the direct application of highly reactive and versatile organolithium-based AB-type monomers in a chain-growth polymerization remains elusive. Organolithium-based monomers can be easily generated *in situ* by lithium-halogen exchange or deprotonation using cheap, commercially available alkyllithiums and subsequent polymerization generates a lithium halide and a alkyl halide as stoichiometric byproducts. By contrast, other organometallic monomers (Sn, B, Mg, Zn) are often produced using corresponding organolithium compounds as precursors (Figure 5.1). The direct use of organolithium monomers in polymerizations not only reduces these additional procedures but also eliminate the formation of toxic byproducts. Therefore, a facile, fast and universal chain-growth polymerization protocol using organolithium-based AB-type monomers is highly desirable.

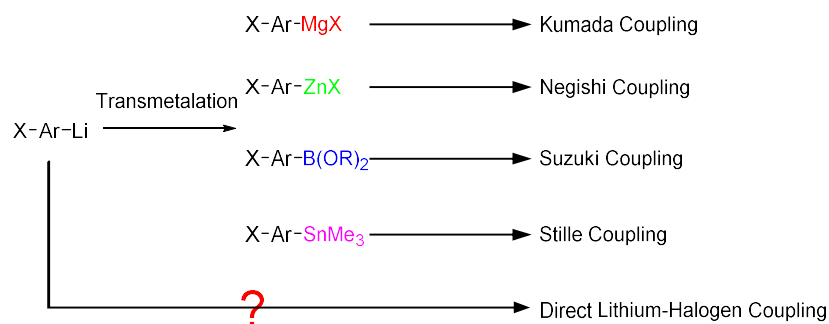


**Figure 5.1.** Summarized Cross-Coupling Reactions used in Chain-Growth Polymerizations.

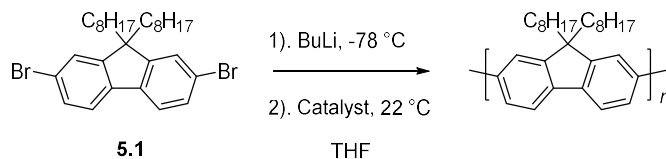
Previous studies using organolithium reagents as monomers have appeared in the literature and significant progress has been made by Mori's group in 2013.<sup>3</sup> However, the reported polymerization either proceeded in a step-growth fashion or was limited to electron-rich polymers. There is an interest to explore chain-growth polymerization for electron-deficient polymers and even donor-acceptor alternating copolymers. Therefore, we envision that this method should be widely applicable to afford functional conjugated polymers, not only restricted to those which are electron-rich.

## 5.2 Results and Discussion

We first tested the lithiation strategy by synthesizing polyfluorenes (a typical type of electron-rich polymers), since they are promising blue-emitting materials in OLED applications.<sup>4</sup> This polymer has been polymerized previously using organolithium-type monomers with  $Ni(dppp)Cl_2$  as the catalyst, however the molecular weight cannot be regulated by the catalyst/feed ratio, indicating a step-growth polymerization mechanism.<sup>3b</sup> The essence of transferring step-growth polymerizations into chain-growth polymerizations is the proper choice of catalysts used during the reaction. Recently, we and others have successfully demonstrated the feasibility of using carbene-supported palladium precatalysts in a chain-growth process.<sup>5</sup> With the success of using carbene-supported palladium precatalysts in small molecule couplings,<sup>6</sup> we decided to use PEPPSI-IPr to polymerize organolithium AB-type fluorene monomers.

Active monomers were generated by treating commercially available 9,9-dioctyl-2,7-dibromofluorene (**5.1**) with *n*-BuLi at  $-78\text{ }^{\circ}\text{C}$  in THF for an hour. Followed with the addition of PEPPSI-IPr, the polymerization rapidly took place at room temperature. Simple precipitation and washing with methanol and acetone removed the remaining excess monomer to afford polyfluorenes in high yield. Surprisingly, the dispersity was high indicating a step-growth process. Another reason may be the presence of a small percentage of dilithiated fluorene species generated upon addition of *n*-BuLi. The similar complication has been observed previously and was proven to be problematic.<sup>7</sup> To confirm this, monomer conversion experiments were conducted (Figure 5.14). Indeed, 89% monomers were formed along with 11% dilithiated fluorene byproducts. Nevertheless, molecular weight control can be realized by tuning the catalyst loading (entries 1-3, Table 5.1). By stark contrast, Kumada CTP using the same catalyst only afforded oligofluorenes.<sup>5c</sup> We also chose Ni(PPh<sub>3</sub>)IPrCl<sub>2</sub> to initiate the same polymerization since it has been used previously in similar small molecule reactions<sup>8</sup> and polymerizations.<sup>3a</sup> Interestingly, polymers obtained using Ni(PPh<sub>3</sub>)IPrCl<sub>2</sub> had comparable molecular weights and dispersities with those using PEPPSI-IPr. This may indicate some degrees of a chain-growth polymerization (entries 4-6, Table 5.1), though further experiments are needed to confirm this.

**Table 5.1. Polymerization Studies for Monomer 5.1.**

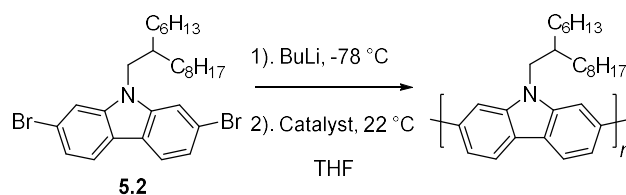


entry	Cat. (mol %)	$M_n^a$	$D^a$	Yield (%)
1	PEPPSI-IPr (8)	9800	1.73	85
2	PEPPSI-IPr (4)	13500	1.82	83
3	PEPPSI-IPr (2)	22800	1.82	85
4	Ni(PPh <sub>3</sub> )IPrCl <sub>2</sub> (8)	8900	1.74	94
5	Ni(PPh <sub>3</sub> )IPrCl <sub>2</sub> (4)	14000	2.04	93
6	Ni(PPh <sub>3</sub> )IPrCl <sub>2</sub> (2)	22300	1.77	83

<sup>a</sup>GPC traces were recorded at  $40\text{ }^{\circ}\text{C}$  versus polystyrene standards using THF as the eluent.

To further investigate the applicability of this protocol, another electron-rich monomer carbazole (**5.2**) was polymerized under similar conditions. Like polyfluorenes, polycarbazoles are well-known for their interesting optical and electrical properties.<sup>9</sup> Previous efforts on controlled synthesis of polycarbazoles only generated low molecular weight samples.<sup>10</sup> To our delight, both catalysts PEPPSI-IPr and Ni(PPh<sub>3</sub>)IPrCl<sub>2</sub> can produce desired polymers with similar molecular weights (Table 5.2). However, the dispersity was high suggesting a step-growth process.

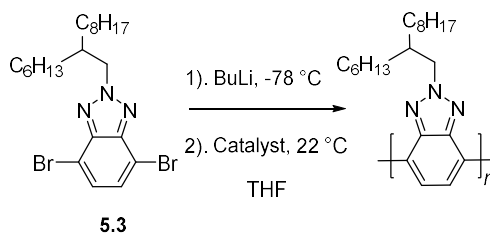
**Table 5.2. Polymerization Studies for Monomer 5.2.**



entry	Cat. (mol %)	$M_n^a$	$D^a$	Yield (%)
1	PEPPSI-IPr (2)	21200	1.99	71%
2	Ni(PPh <sub>3</sub> )IPrCl <sub>2</sub> (2)	20800	1.96	71%

<sup>a</sup>GPC traces were recorded at 40 °C versus polystyrene standards using THF as the eluent.

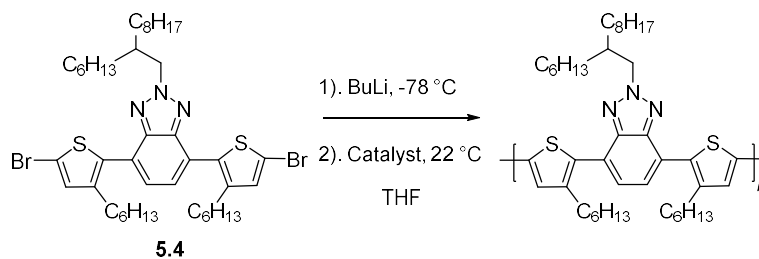
After the successful polymerization of electron-rich monomers, we sought to apply the same protocol to an electron-deficient benzotriazole monomer. This monomer has been previously polymerized in a controlled fashion where active monomers were produced by reacting with *n*-BuLi and subsequent transmetalation with MgCl<sub>2</sub>.<sup>11</sup> The dibromobenzotriazole monomer (**5.3**) was treated with *n*-BuLi at -78 °C for an hour and polymerized at room temperature. When PEPPSI-IPr was used as the catalyst, polymers with controlled molecular weights can be produced in high yields (entries 1-3, Table 5.3). By contrast, Ni(PPh<sub>3</sub>)IPrCl<sub>2</sub> failed to afford polybenzotriazoles with reasonable molecular weights. This is surprising considering both catalysts work for the fluorene monomer. It is conceivable that the benzotriazole monomer binds stronger with Ni catalyst than Pd, suppressing catalyst transfer process.<sup>12</sup> Further experiments using theoretical calculations are necessary to elucidate this.

**Table 5.3. Polymerization Studies for Monomer 5.3.**

entry	Cat. (mol %)	$M_n^a$	$D^a$	Yield (%)
1	PEPPSI-IPr (8)	5100	1.92	80
2	PEPPSI-IPr (4)	10100	1.81	90
3	PEPPSI-IPr (2)	14400	1.87	84
4	Ni(PPh <sub>3</sub> )IPrCl <sub>2</sub> (2)	Oligomer	-	-

<sup>a</sup>GPC traces were recorded at 40 °C versus polystyrene standards using THF as the eluent.

The presented method which was effective in polymerizing both electron-rich and electron-deficient monomers also led us to explore the synthesis of a donor-acceptor alternating copolymer. Donor-acceptor polymers serve as an important class of active materials in optoelectronic devices<sup>13</sup> and have been recently explored in chain-growth polymerizations.<sup>14</sup> We have designed, prepared a donor-acceptor monomer containing benzotriazole and thiophene (**4**) and subjected it to polymerization using PEPPSI-IPr. The targeted polymer was obtained with moderate molecular weight and dispersity (Table 5.4), demonstrating the broad scope of this protocol.

**Table 5.4. Polymerization Studies for Monomer 5.4.**

entry	Cat. (mol %)	$M_n^a$	$D^a$	Yield (%)
1	PEPPSI-IPr (2)	11000	1.57	66

<sup>a</sup>GPC traces were recorded at 40 °C versus polystyrene standards using THF as the eluent.

### 5.3 Conclusions

In conclusion, we have demonstrated an effective system for the synthesis of electron-rich and electron-deficient monomers through direct catalytic couplings of organolithium species. Polyfluorenes, polycarbazoles and polybenzotriazoles can be obtained with control over molecular weights in high yields. We believe that the presented method should provide mechanistic insights of CTP regarding different cross-coupling reactions and eventually lead to precise conjugated frameworks containing both electron-rich and electron-deficient moieties.

### 5.4 Experimental

**Materials and Methods.** All reactions and manipulations of air or water sensitive compounds were carried out under dry nitrogen using an mBraun glovebox or standard Schlenk techniques unless otherwise stated. Tetrahydrofuran was purchased from commercial sources, degassed with argon, and dried prior to use. N-bromosuccinimide (NBS) was recrystallized from hot water prior to use. All other solvents and chemicals were used as received from commercial sources. Monomer **2**<sup>11</sup> and **3**<sup>15</sup> were prepared according to literature procedures.

Polymer samples were precipitated with 6 M methanolic HCl solution and washed with both methanol and acetone before GPC analysis.

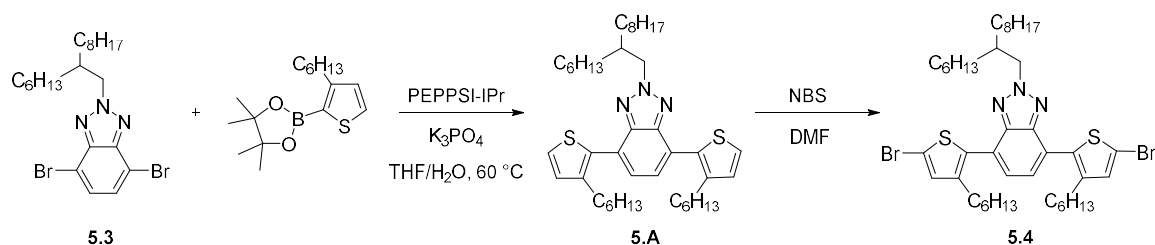
**NMR Analysis.** All NMR experiments were collected at 300 K on a two-channel Bruker Avance<sup>TM</sup> III NMR instrument equipped with a Broad Band Inverse (BBI) probe, operating at 500 MHz for <sup>1</sup>H (126 MHz for <sup>13</sup>C). <sup>1</sup>H NMR spectra are referenced to residual protio solvent (7.26 for CHCl<sub>3</sub>) and <sup>13</sup>C NMR spectra are referenced to the solvent signal ( $\delta$  77.23 for CDCl<sub>3</sub>).

**Mass Spectrometry.** High-resolution mass spectrometry experiments (electrospray and electron impact) were performed in the School of Chemical Sciences Mass Spectrometry Laboratory at the University of Illinois, Urbana-Champaign.

**Gel-Permeation Chromatography.** GPC measurements were performed on a Waters Instrument equipped with a 717 plus autosampler, a Waters 2414 refractive index (RI) detector and two SDV columns (Porosity 1000 and 100000 Å; Polymer Standard Services) with THF as the eluent (flow

rate 1 mL/min, 40 °C). A 10-point calibration based on polystyrene standards (Polystyrene, ReadyCal Kit, Polymer Standard Services) was applied for determination of molecular weights. The polymer sample was dissolved in ~1 mL of THF, filtered through a 0.22 µm PTFE syringe filter, and analyzed.

#### Scheme 5.1. Synthesis of Monomer 5.4.



*2-(2-hexyldecyl)-4,7-bis(3-hexylthiophen-2-yl)-2H-benzo[d][1,2,3]triazole (5.A)*. In a N<sub>2</sub> filled glovebox, a 20 mL vial was charged with 4,7-dibromo-2-(2-hexyldecyl)-2H-benzotriazole (**3**) (0.81 g, 1.62 mmol), 2-(3-hexylthiophen-2-yl)-4,4,5,5-tetramethyl-1,3,2-dioxaborolane (1 g, 3.40 mmol), K<sub>3</sub>PO<sub>4</sub> (1.37 g, 6.45 mmol), PEPPSI-IPr (0.022 g, 0.032 mmol) and 10 mL of THF. The vial was removed from the glovebox and 1 mL of water was added into the vial by syringe. The vial was then immersed in an oil bath at 60 °C and the solution was stirred for 12 h before cooling to room temperature. The mixture was transferred to a separatory funnel, diluted with 100 mL of diethyl ether and washed with 2 M HCl solution and brine. The organic layer was dried using Na<sub>2</sub>SO<sub>4</sub>, and concentrated using rotary evaporation. The crude material was purified using column chromatography on silica gel, eluting with hexanes:dichloromethane (4:1) to afford the final product as a clear yellow oil (0.60 g, 55%). The *R<sub>f</sub>* of the product is ~0.2 in hexanes:dichloromethane = 7:3. HRMS (ESI-TOF) (*m/z*): [M + H]<sup>+</sup> calculated for C<sub>42</sub>H<sub>66</sub>N<sub>3</sub>S<sub>2</sub>, 676.4698; found, 676.4675.

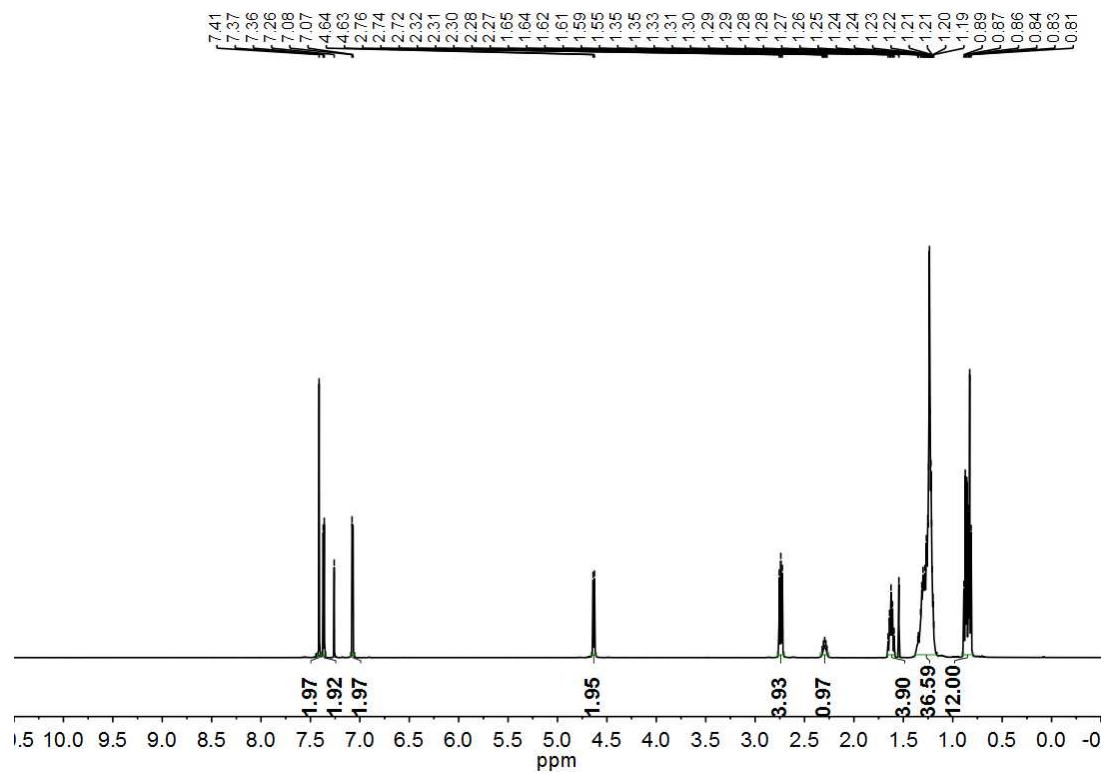


Figure 5.2. Compound 5.A  $^1\text{H}$  NMR Spectrum – 500 MHz,  $\text{CDCl}_3$ .

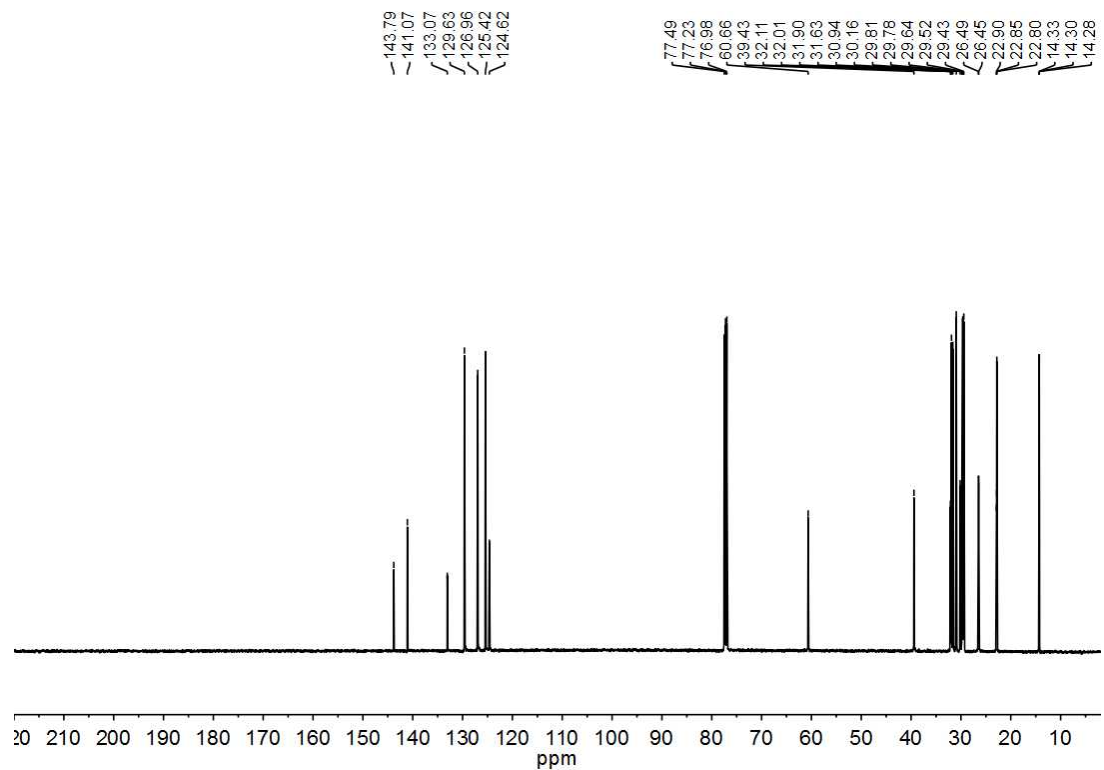
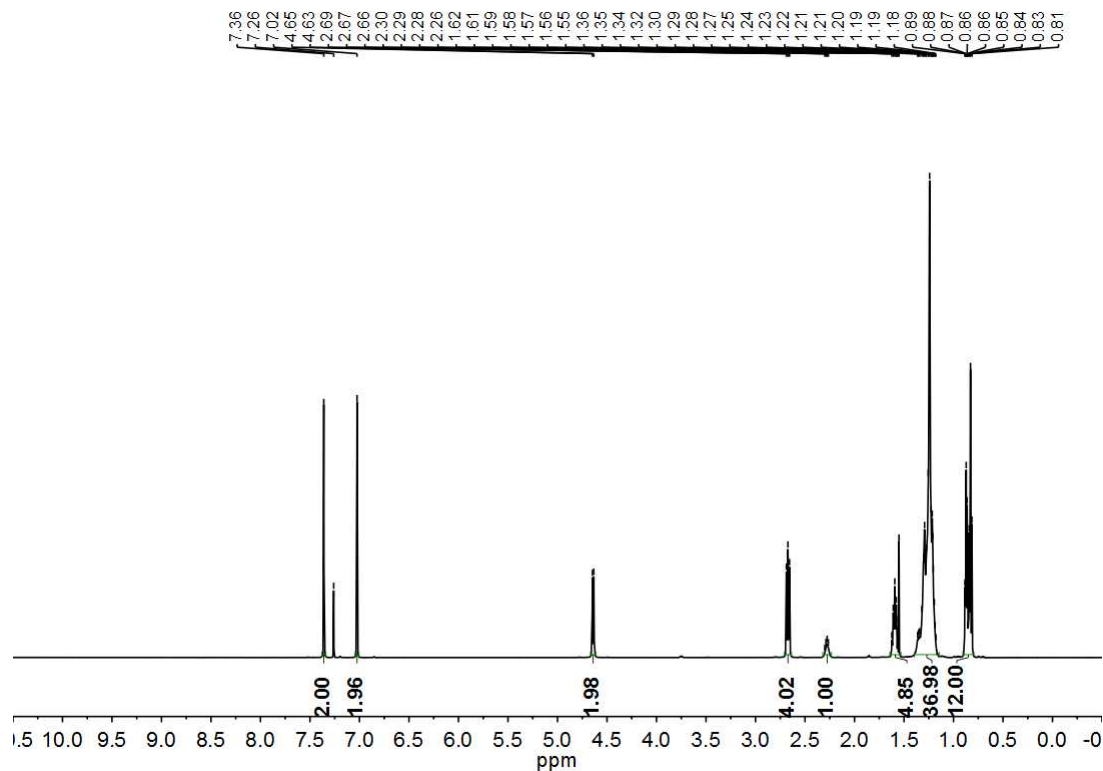
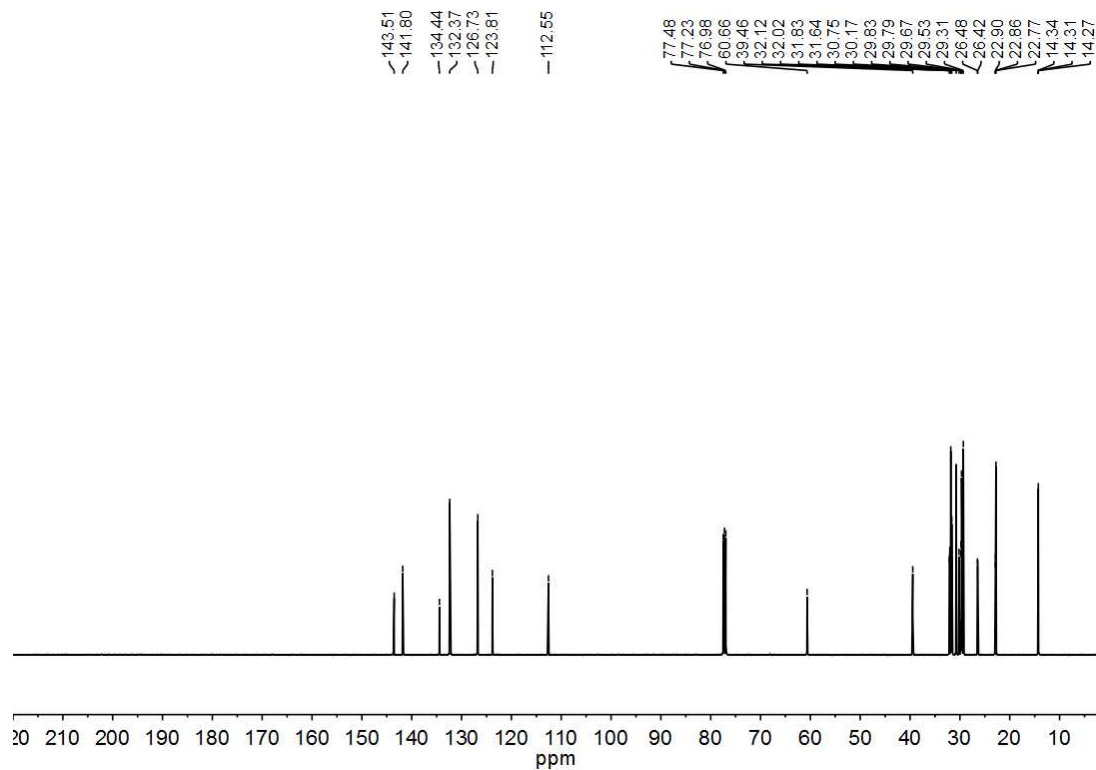


Figure 5.3. Compound 5.A  $^{13}\text{C}$  NMR Spectrum – 126 MHz,  $\text{CDCl}_3$ .

4,7-bis(5-bromo-3-hexylthiophen-2-yl)-2-(2-hexyldecyl)-2H-benzo[d][1,2,3]triazole (**5.4**). In a 50 mL round-bottom flask, compound **5.A** (0.60 g, 0.89 mmol) was dissolved in 10 mL of DMF. The flask was cooled to 0 °C using an ice-water bath. NBS (0.33 g, 0.19 mmol) was added into the solution in one portion and the reaction mixture was protected from ambient light. The mixture was slowly warmed to room temperature and stirred overnight. The reaction was quenched with saturated NaHCO<sub>3</sub> solution and transferred to a 500 mL of separatory funnel. The organic layer was separated and the aqueous layer was extracted two more times using diethyl ether (2 × 50 mL). The organic extracts were combined and washed with saturated NaHCO<sub>3</sub> solution, dried over Na<sub>2</sub>SO<sub>4</sub> and concentrated using rotary evaporation. The crude material was purified using column chromatography on silica gel, eluting with hexanes:dichloromethane (23:2) to afford the final product as a clear yellow oil (0.68 g, 92%). The *R<sub>f</sub>* of the product is ~0.7 in hexanes:dichloromethane = 7:3. HRMS (ESI-TOF) (*m/z*): [M + H]<sup>+</sup> calculated for C<sub>42</sub>H<sub>64</sub>Br<sub>2</sub>N<sub>3</sub>S<sub>2</sub>, 832.2908; found, 832.2947.



**Figure 5.4.** Compound **5.4** <sup>1</sup>H NMR Spectrum – 500 MHz, CDCl<sub>3</sub>.



**Figure 5.5.** Compound **5.4**  $^{13}\text{C}$  NMR Spectrum – 126 MHz,  $\text{CDCl}_3$ .

### General Polymerization Conditions

**Polyfluorenes.** The polymerization reaction was conducted under a  $\text{N}_2$  atmosphere. A 100 mL Schlenk flask was charged with compound **5.1** (0.5 g, 0.91 mmol) and 20 mL of THF. *n*-BuLi solution (2.5 M, 0.3 mL, 0.75 mmol) was slowly added to the reaction solution at  $-78\text{ }^\circ\text{C}$ . After stirring at  $-78\text{ }^\circ\text{C}$  for 1 h, a calculated amount of catalyst in 2 mL of THF was quickly added into the solution in one portion. The polymerization was stirred at room temperature for 1 h and subsequently quenched with 6 M methanolic HCl. 200 mL of methanol was then added to the polymer suspension. The final polymer was collected by filtration, dried in *vacuo*.

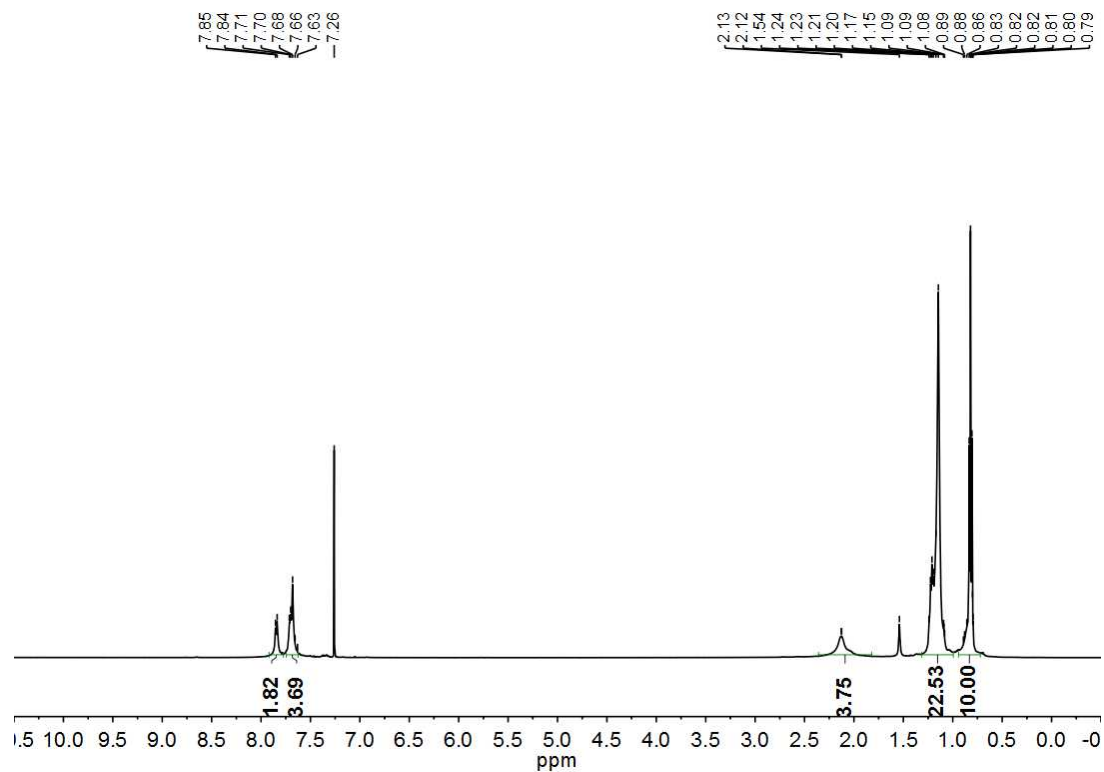


**Figure 5.6.** Polyfluorenes  $^1\text{H}$  NMR Spectrum – 500 MHz,  $\text{CDCl}_3$ .

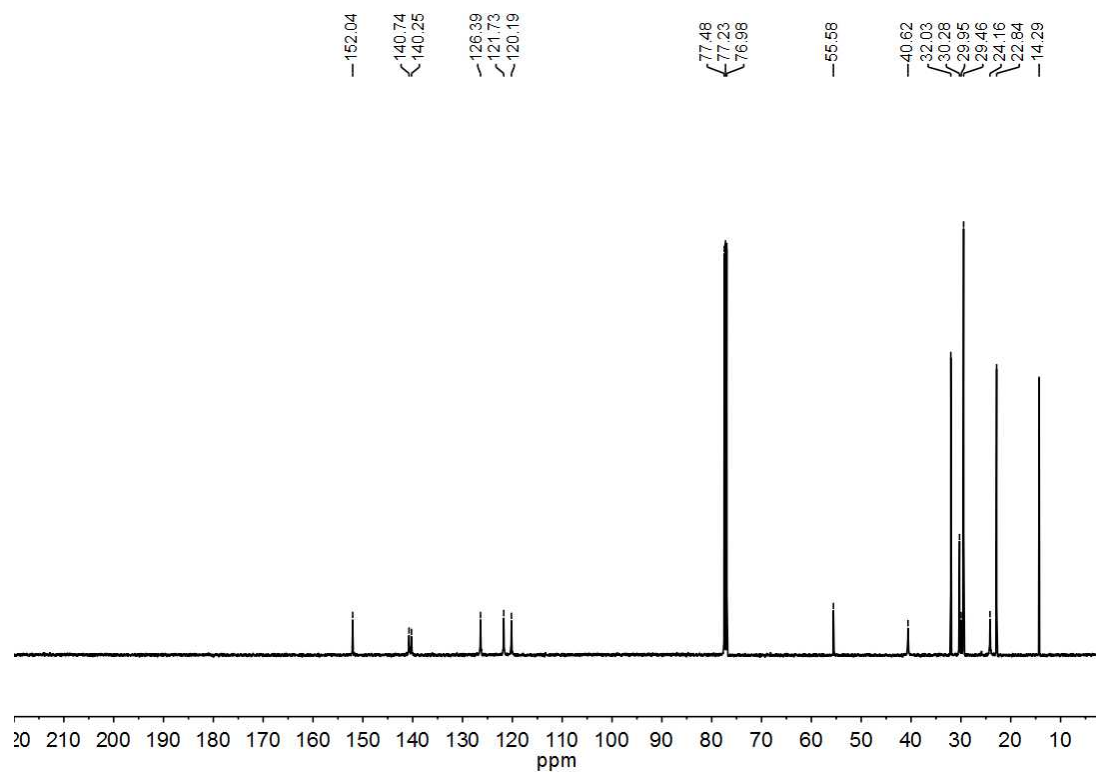


**Figure 5.7.** Polyfluorenes  $^{13}\text{C}$  NMR Spectrum – 126 MHz,  $\text{CDCl}_3$ .

**Polycarbazoles.** The polymerization reaction was conducted under a N<sub>2</sub> atmosphere. A 50 mL Schlenk flask was charged with compound **5.2** (0.25 g, 0.46 mmol) and 10 mL of THF. *n*-BuLi solution (2.5 M, 0.15 mL, 0.375 mmol) was slowly added to the reaction solution at -78 °C. After stirring at -78 °C for 1 h, a calculated amount of catalyst in 2 mL of THF was quickly added into the solution in one portion. The polymerization was stirred at room temperature for 1 h and subsequently quenched with 6 M methanolic HCl. 200 mL of methanol was then added to the polymer suspension. The final polymer was collected by filtration, dried in *vacuo*.

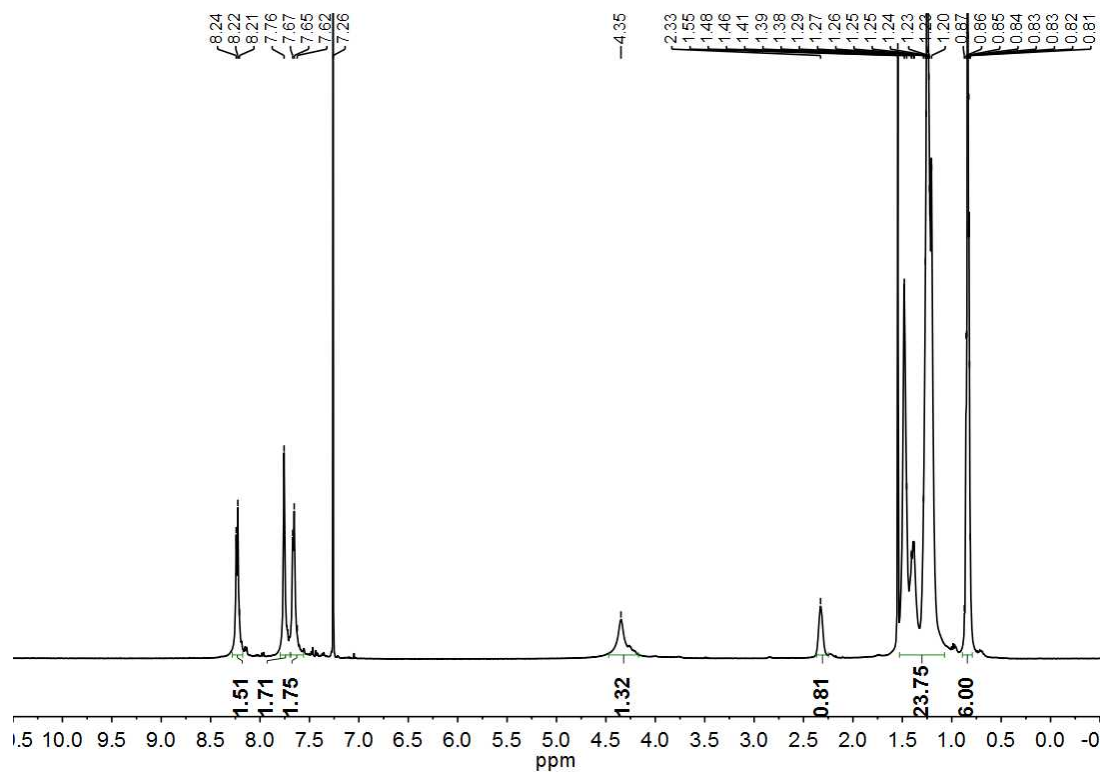


**Figure 5.8.** Polycarbazoles <sup>1</sup>H NMR Spectrum – 500 MHz, CDCl<sub>3</sub>.

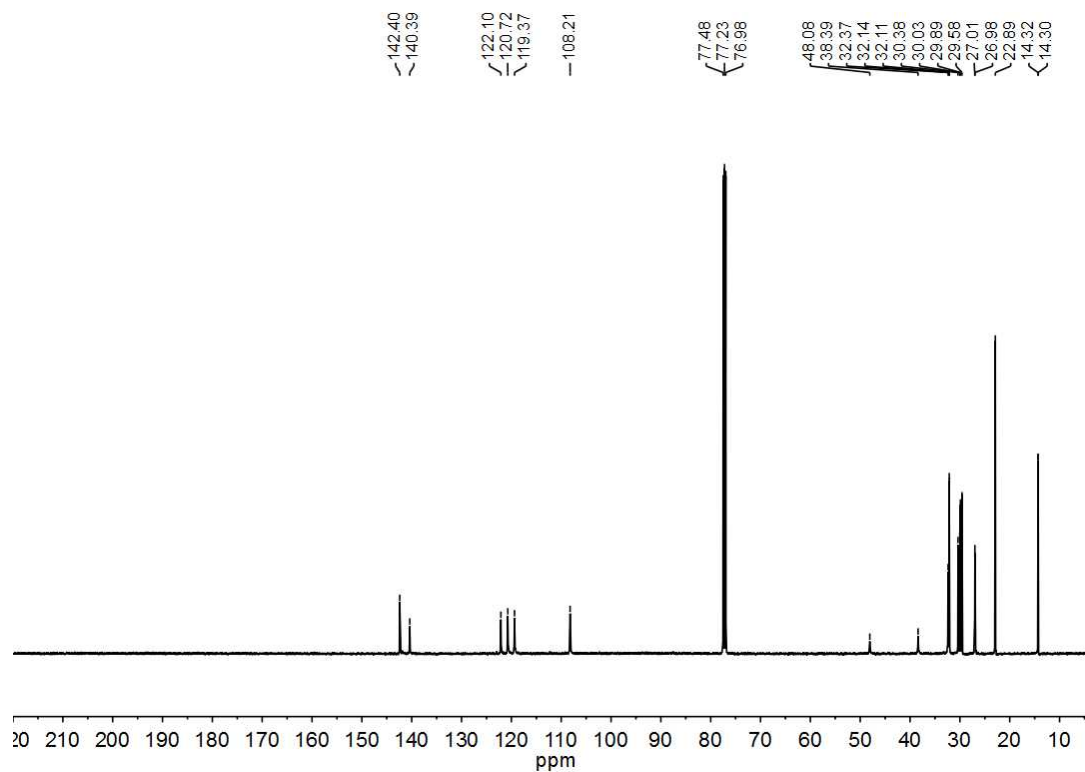


**Figure 5.9.** Polyfluorenes  $^{13}\text{C}$  NMR Spectrum – 126 MHz,  $\text{CDCl}_3$ .

**Polybenzotriazoles.** The polymerization reaction was conducted under a  $\text{N}_2$  atmosphere. A 50 mL Schlenk flask was charged with compound **5.3** (0.225 g, 0.46 mmol) and 10 mL of THF. *n*-BuLi solution (2.5 M, 0.15 mL, 0.375 mmol) was slowly added to the reaction solution at  $-78\text{ }^\circ\text{C}$ . After stirring at  $-78\text{ }^\circ\text{C}$  for 1 h, a calculated amount of catalyst in 2 mL of THF was quickly added into the solution in one portion. The polymerization was stirred at room temperature for 1 h and subsequently quenched with 6 M methanolic HCl. 200 mL of methanol was then added to the polymer suspension. The final polymer was collected by filtration, dried in *vacuo*.

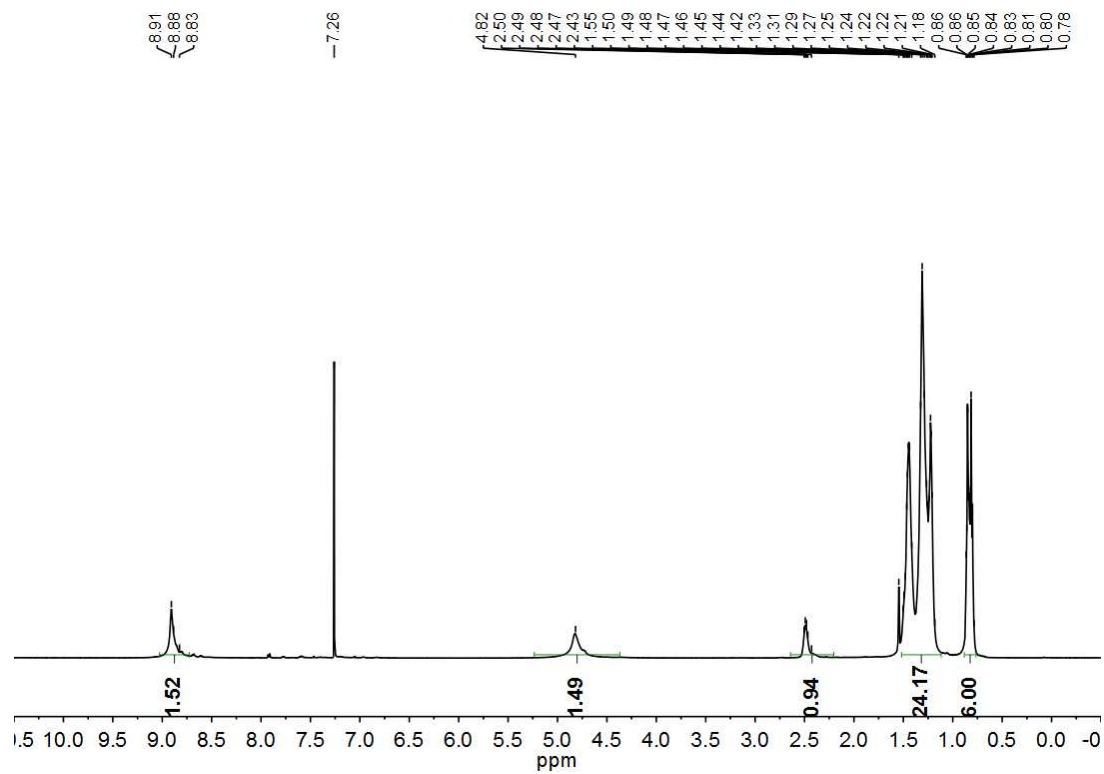


Figure 5.10. Polybenzotriazoles  $^1\text{H}$  NMR Spectrum – 500 MHz,  $\text{CDCl}_3$ .

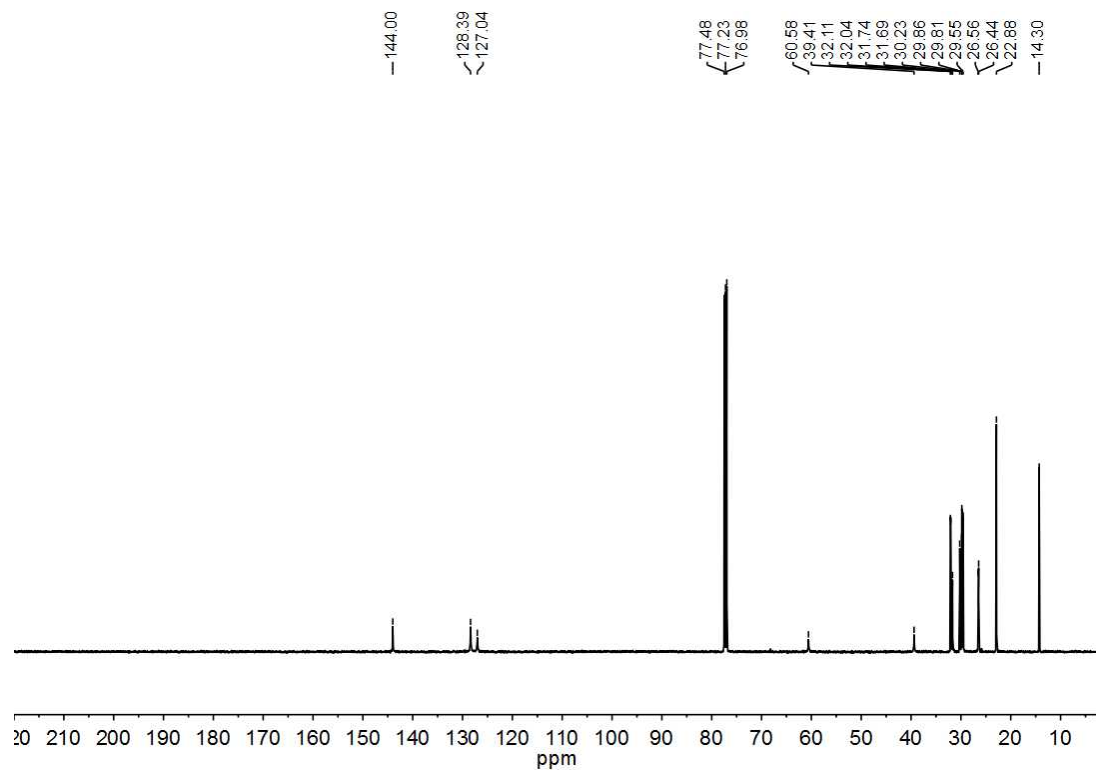
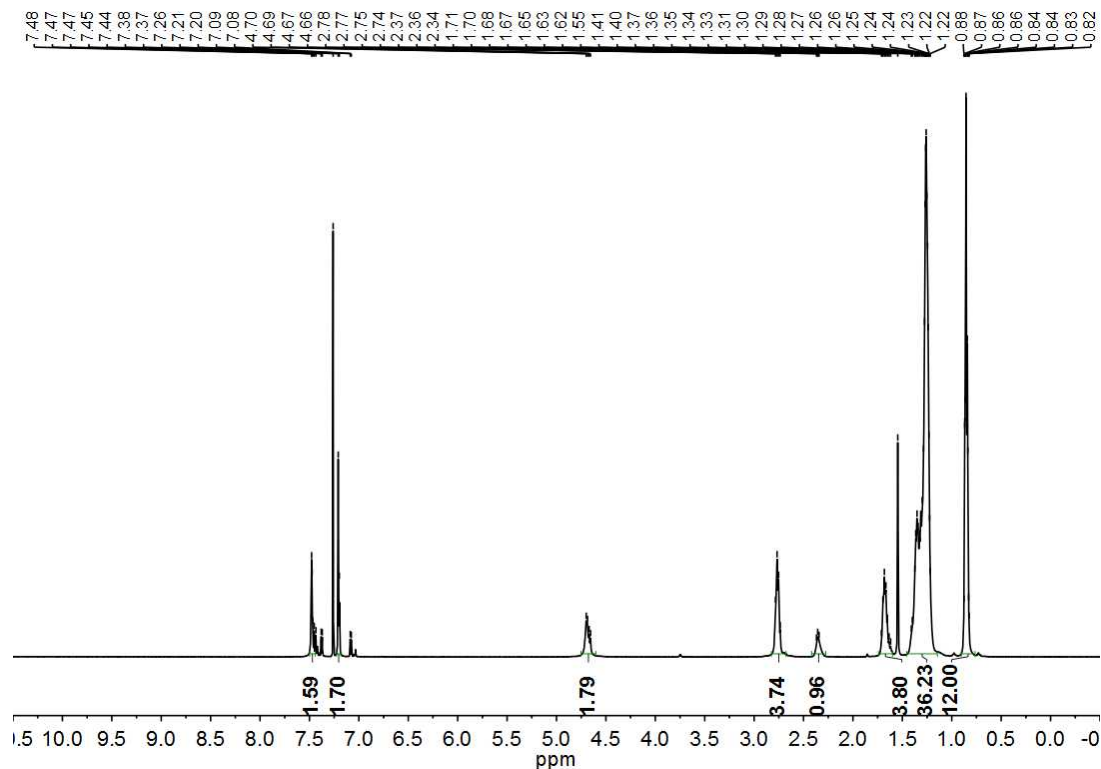
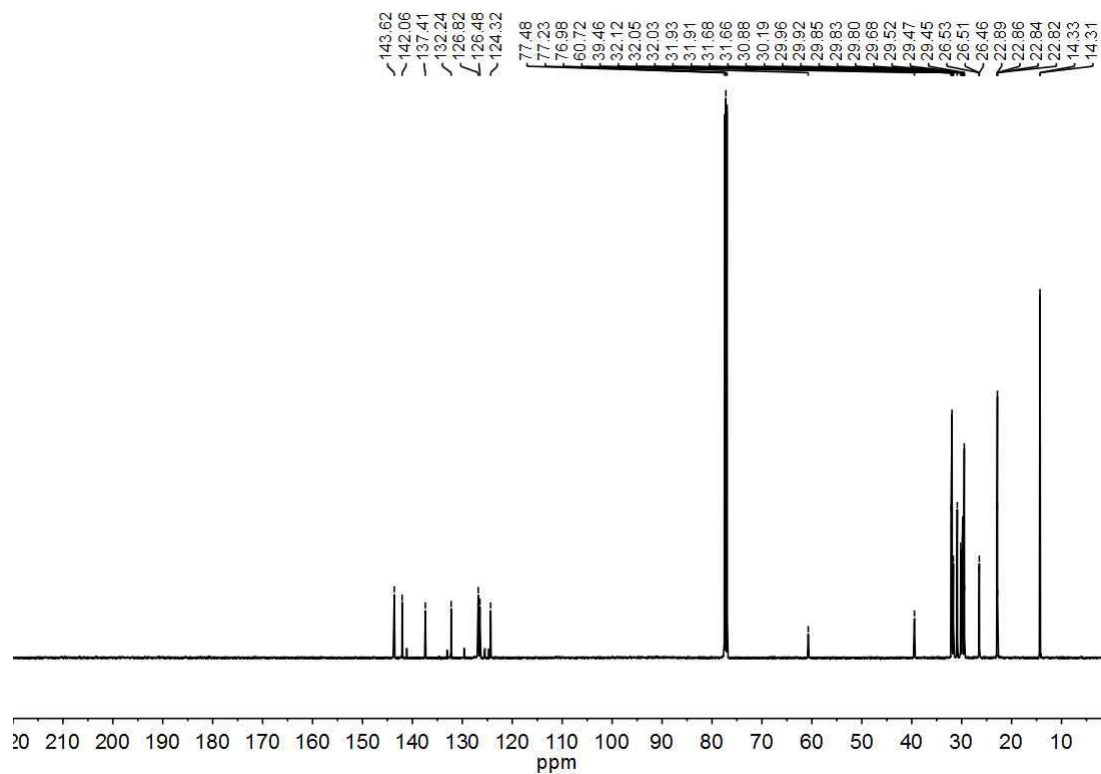


Figure 5.11. Polybenzotriazoles  $^{13}\text{C}$  NMR Spectrum – 126 MHz,  $\text{CDCl}_3$ .

**Polymerization of monomer 5.4.** The polymerization reaction was conducted under a N<sub>2</sub> atmosphere. A 50 mL Schlenk flask was charged with compound **5.4** (0.375 g, 0.46 mmol) and 10 mL of THF. *n*-BuLi solution (2.5 M, 0.15 mL, 0.375 mmol) was slowly added to the reaction solution at -78 °C. After stirring at -78 °C for 1 h, PEPPSI-IPr (5.1 mg, 2 mol %) in 2 mL of THF was quickly added into the solution in one portion. The polymerization was stirred at room temperature for 1 h and subsequently quenched with 6 M methanolic HCl. 200 mL of methanol was then added to the polymer suspension. The final polymer was collected by filtration, dried in *vacuo*.



**Figure 5.12.** Donor-acceptor copolymer <sup>1</sup>H NMR Spectrum – 500 MHz, CDCl<sub>3</sub>.



**Figure 5.13.** Donor-acceptor copolymer  $^{13}\text{C}$  NMR Spectrum – 126 MHz,  $\text{CDCl}_3$ .

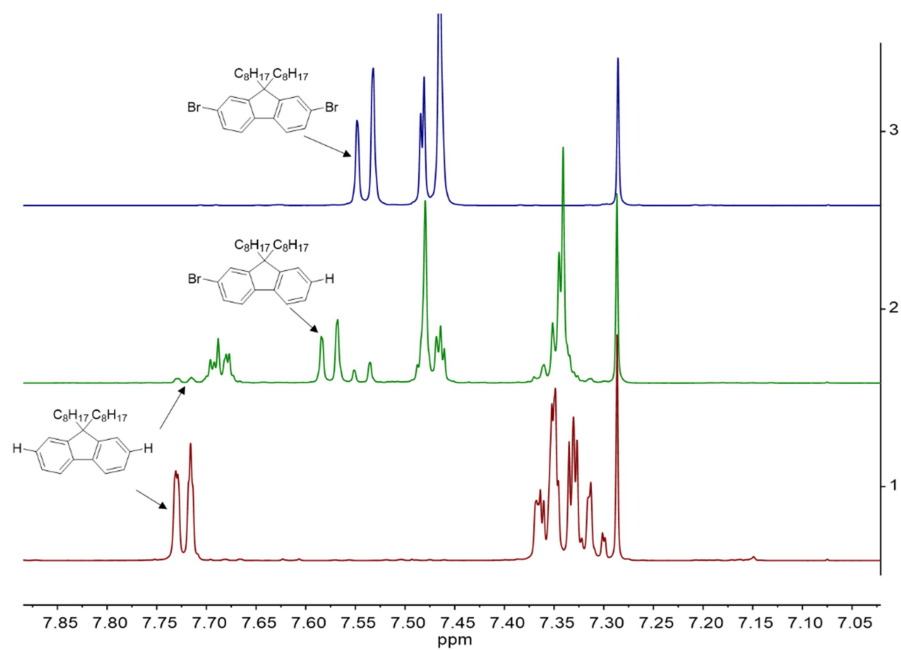


**Figure 5.14.** Crude  $^1\text{H}$  NMR Spectrum (500 MHz,  $\text{CDCl}_3$ ) for monomer conversion experiments. Top – reaction mixture before adding *n*-BuLi. Middle – reaction mixture after adding 1 equiv. of *n*-BuLi. Bottom – reaction mixture after adding 2 equiv. of *n*-BuLi for comparison.

## 5.5 References

- (1) Beaujuge, P. M.; Fréchet, J. M. J. *J. Am. Chem. Soc.* **2011**, *133*, 20009-20029.
- (2) (a) Yokozawa, T.; Ohta, Y. *Chem. Rev.* **2016**, *116*, 1950-1968. (b) Grisorio, R.; Suranna, G. P. *Polym. Chem.* **2015**, *6*, 7781-7795. (c) Bryan, Z. J.; McNeil, A. J. *Macromolecules* **2013**, *46*, 8395-8405.
- (3) (a) Fuji, K.; Tamba, S.; Shono, K.; Sugie, A.; Mori, A. *J. Am. Chem. Soc.* **2013**, *135*, 12208-12211. (b) Jhaveri, S. B.; Peterson, J. J.; Carter, K. R. *Macromolecules* **2008**, *41*, 8977-8979.
- (4) Scherf, U.; List, E. J. W. *Adv. Mater.* **2002**, *14*, 477-487.
- (5) (a) Qiu, Y.; Mohin, J.; Tsai, C.-H.; Tristram-Nagle, S.; Gil, R. R.; Kowalewski, T.; Noonan, K. J. T. *Macromol. Rapid Commun.* **2015**, *36*, 840-844. (b) Sui, A.; Shi, X.; Tian, H.; Geng, Y.; Wang, F. *Polym. Chem.* **2014**, *5*, 7072-7080. (c) Bryan, Z. J.; Smith, M. L.; McNeil, A. J. *Macromol. Rapid Commun.* **2012**, *33*, 842-847.
- (6) Hornillos, V.; Giannerini, M.; Vila, C.; Fañanás-Mastral, M.; Feringa, B. L. *Org. Lett.* **2013**, *15*, 5114-5117.
- (7) Tkachov, R.; Senkovskyy, V.; Beryozkina, T.; Boyko, K.; Bakulev, V.; Lederer, A.; Sahre, K.; Voit, B.; Kiriy, A. *Angew. Chem., Int. Ed.* **2014**, *53*, 2402-2407.
- (8) Heijnen, D.; Gualtierotti, J.-B.; Hornillos, V.; Feringa, B. L. *Chem. - Eur. J.* **2016**, *22*, 3991-3995.
- (9) Morin, J.-F.; Leclerc, M.; Adès, D.; Siove, A. *Macromol. Rapid Commun.* **2005**, *26*, 761-778.
- (10) (a) Wen, H.; Ge, Z.; Liu, Y.; Yokozawa, T.; Lu, L.; Ouyang, X.; Tan, Z. *Eur. Polym. J.* **2013**, *49*, 3740-3743. (b) Stefan, M. C.; Javier, A. E.; Osaka, I.; McCullough, R. D. *Macromolecules* **2009**, *42*, 30-32.
- (11) Bridges, C. R.; McCormick, T. M.; Gibson, G. L.; Hollinger, J.; Seferos, D. S. *J. Am. Chem. Soc.* **2013**, *135*, 13212-13219.
- (12) Willot, P.; Koeckelberghs, G. *Macromolecules* **2014**, *47*, 8548-8555.
- (13) Müllen, K.; Pisula, W. *J. Am. Chem. Soc.* **2015**, *137*, 9503-9505.

- (14) (a) Pollit, A. A.; Bridges, C. R.; Seferos, D. S. *Macromol. Rapid Commun.* **2015**, *36*, 65-70.  
(b) Todd, A. D.; Bielawski, C. W. *ACS Macro Lett.* **2015**, *4*, 1254-1258. (c) Tkachov, R.; Karpov, Y.; Senkovskyy, V.; Raguzin, I.; Zessin, J.; Lederer, A.; Stamm, M.; Voit, B.; Beryozkina, T.; Bakulev, V.; Zhao, W.; Facchetti, A.; Kiriy, A. *Macromolecules* **2014**, *47*, 3845-3851. (d) Elmalem, E.; Kiriy, A.; Huck, W. T. S. *Macromolecules* **2011**, *44*, 9057-9061. (e) Senkovskyy, V.; Tkachov, R.; Komber, H.; Sommer, M.; Heuken, M.; Voit, B.; Huck, W. T. S.; Kataev, V.; Petr, A.; Kiriy, A. *J. Am. Chem. Soc.* **2011**, *133*, 19966-19970.
- (15) Lemasson, F.; Berton, N.; Tittmann, J.; Hennrich, F.; Kappes, M. M.; Mayor, M. *Macromolecules* **2012**, *45*, 713-722.

## CHAPTER 6

### Conclusions and Outlook

#### 6.1 Conclusions

The previous chapters detailed some of our efforts in developing controlled methods for the synthesis of conjugated polymers by expanding the scope of catalysts, monomers, cross-coupling strategies and functional groups available. We have successfully expanded Kumada CTP protocol to another Group 16 heterocycle (furan) which is biorenewable and biodegradable. Limited photostability of these alkyl substituted polyfurans led us to explore furan containing polymers with an ester stabilized functional group. CTP protocols employing alternative cross-coupling reactions (Stille and Suzuki) with broader substrate scope have been developed. The ability to install functional groups at the side chain allows for the preparation of conjugated polymers with tunable structures and band gaps. Subsequent research in our group will include expansion to other functional groups and the synthesis of sequence defined conjugated polymers by varying side chain substituents and eventually polymerizing acceptor or donor-acceptor type conjugated monomers in a controlled manner.

Despite our recent effort in controlled synthesis of ester functionalized polythiophenes, functional groups that are amenable to CTP have remained limited. Donor-acceptor alternating copolymers or acceptor polymers often possess functional groups such as amide or imide (Figure 6.1).<sup>1</sup> Rylene diimides and thiophene diimides are among the most commonly used building blocks in donor-acceptor copolymers.<sup>1</sup> While naphthalene diimide based monomers have been previously polymerized in a chain-growth manner,<sup>2</sup> the controlled synthesis of thiophene diimides has not been realized.

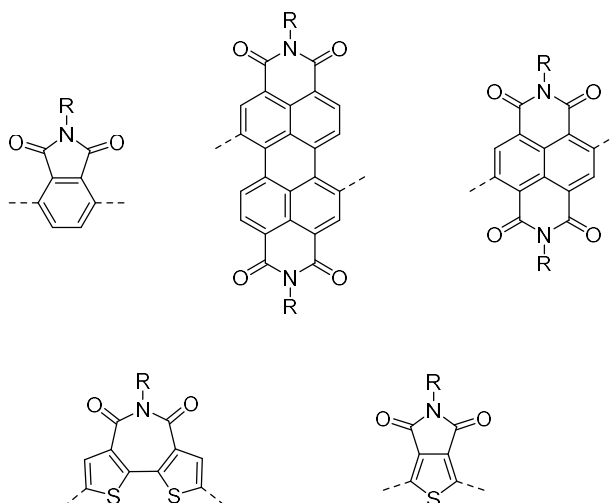


**Figure 6.1.** Selected Examples of Imide Containing Conjugated Building Blocks.

Serving as an entry point, we plan to investigate an amide functionalized thiophene monomer using our recently established Ni Suzuki CTP protocol. To further examine the scope of this methodology, cyano substituted thiophene monomers were also designed and subjected into polymerization. Similar cyano containing polythiophenes have been prepared previously via step-growth polycondensation and showed promising oxidative stability,<sup>3</sup> highlighting the benefit of this particular electron-withdrawing functional group. Different designs of dimeric and trimeric monomers will be proposed and polymerized to further explore the sequence effect on the property of resultant materials (Figure 6.2), since sequence control is one of the remaining frontiers in polymer synthesis.

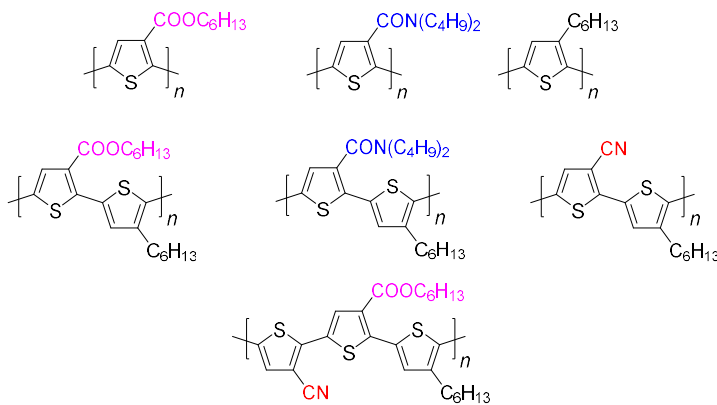


**Figure 6.2.** Functional Groups Expansion and Side Chain Sequence Defined Conjugated Polymers.

If these amide and cyano functionalized monomers can be successfully polymerized in a controlled fashion, we will apply the similar protocol to more complex conjugated frameworks involving electron-deficient polymers and donor-acceptor copolymers consisting of thiophene diimide (Figure 6.3).

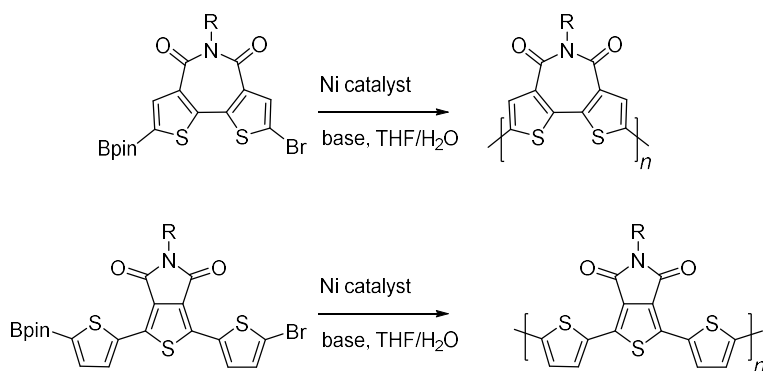


**Figure 6.3.** Proposed Controlled Synthesis of Imide Functionalized Conjugated Polymers.

We believe by controlling the composition, topology, and functionality of conjugated polymers, a wide range of functional materials based on conjugated polymers will emerge and lead to the next generation of organic electronics.

## 6.2 References

- (1) Guo, X.; Facchetti, A.; Marks, T. J. *Chem. Rev.* **2014**, *114*, 8943-9021.
- (2) Senkovskyy, V.; Tkachov, R.; Komber, H.; Sommer, M.; Heuken, M.; Voit, B.; Huck, W. T. S.; Kataev, V.; Petr, A.; Kiriy, A. *J. Am. Chem. Soc.* **2011**, *133*, 19966-19970.
- (3) (a) Rudenko, A. E.; Khlyabich, P. P.; Thompson, B. C. *ACS Macro Lett.* **2014**, *3*, 387-392. (b) Rudenko, A. E.; Khlyabich, P. P.; Thompson, B. C. *J. Polym. Sci., Part A: Polym. Chem.* **2016**, *54*, 1526-1536.